

The removal of phosphorous impurities and subsequent  
use of phosphogypsum in Portland Cement

by  
Elizabet Margaretha van der Merwe

submitted in partial fulfilment of the requirements for the degree

**The removal of phosphorous impurities and subsequent  
use of phosphogypsum in Portland Cement**

by

**Elizabet Margaretha van der Merwe**

submitted in partial fulfilment of the requirements for the degree

**Philosophiae Doctor**

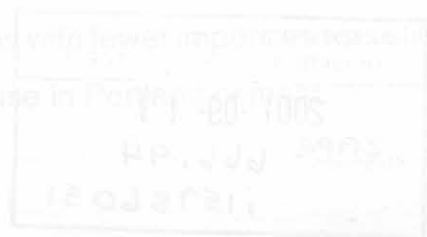
**Chemistry**

in the Faculty of Natural and Agricultural Sciences

University of Pretoria

Pretoria

July 2001



# **The removal of phosphorous impurities and subsequent use of phosphogypsum in Portland Cement**

by

**Elizabet Margaretha van der Merwe**

submitted in partial fulfilment of the requirements for the degree

**Philosophiae Doctor**

**Chemistry**

in the Faculty of Natural and Agricultural Sciences

Department of Chemistry

University of Pretoria

Pretoria

July 2001

**Supervisor: Professor C A Strydom**

## **Abstract**

Phosphogypsum is a by-product in the production of wet phosphoric acid, and most of the phosphogypsum produced in the world remains unutilized at present. The impurities included in phosphogypsum seriously restrict its industrial use as a set retarder in the cement industry. The aim of this study was to investigate different methods to remove the phosphorous impurities contained in South African phosphogypsum. The application of treated phosphogypsum samples to replace natural gypsum as a set retarder in Portland cement was subsequently studied.

It was indicated that sieving could be applied to reduce the amount of phosphorous impurities in some phosphogypsum particle size fractions. However, the amount of phosphorous impurities contained in the particle size fractions with fewer impurities was still above requirements, and were therefore unacceptable for use in Portland cement.



A method involving thermal treatment followed by washing with water and milk of lime proved not to remove the phosphorous impurities contained in the phosphogypsum crystal lattice, but was successful in removing some of the water-soluble impurities. Some improvement was shown in the performance of cement containing these treated phosphogypsum samples when compared to cement containing untreated phosphogypsum. However, this improvement proved to be unsatisfactory for the replacement of natural gypsum by these phosphogypsum samples in Portland cement.

The application of a method comprising the combination of thermal and sulphuric acid treatment proved to be successful in removing most of the harmful phosphorous impurities from the phosphogypsum crystal lattice. Subsequently, South African phosphogypsum treated by this suitable method could successfully replace natural gypsum in Portland cement.

This study attempts to readdress the worldwide problem of phosphogypsum waste utilization, and shows that its application as a set retarder in Portland cement is possible after exposure to an effective purification method.

## Samevatting

Fosfogips is 'n neweproduk in die vervaardiging van nat fosforsuur. Die oorgrote meerderheid fosfogips wat tans in die wêreld geproduseer word, word nie benut nie. Die onsuiverhede in fosfogips beperk die industriële gebruik daarvan as 'n set reguleerder in die sement industrie. Die doel van die studie was om verskillende metodes te ondersoek om die fosfor onsuiverhede uit Suid-Afrikaanse fosfogips te verwyder. Die toepassing van behandelde fosfogips om natuurlike gips as 'n set reguleerder in Portland sement te vervang, is daarna bestudeer.

Daar is aangetoon dat sifting gebruik kan word om die hoeveelheid fosfor onsuiverhede in sommige partikelgrootte fraksies te verminder. Die hoeveelheid fosfor onsuiverhede in die fraksies wat minder onsuiverhede bevat het was egter steeds hoog, en was onaanvaarbaar vir gebruik in Portland sement.

'n Metode wat termiese behandeling gevolg deur wassing met water en kalkwater insluit, kon nie die fosfor onsuiverhede uit die fosfogips kristalstruktuur verwyder nie, maar was suksesvol in die verwydering van sommige van die water-oplosbare onsuiverhede. 'n Verbetering in die werkverrigting van sement wat die behandelde fosfogips bevat is getoon in vergelyking met sement wat onbehandelde fosfogips bevat. Hierdie verbetering is egter nie bevredigend vir die vervanging van natuurlike gips deur hierdie fosfogips monsters in Portland sement nie.

Die toepassing van 'n metode bestaande uit die kombinasie van 'n termiese en swaelsuur behandelingsmetode was suksesvol in die verwydering van meeste van die ongewenste fosfor onsuiverhede uit die fosfogips kristalstruktuur. Suid Afrikaanse fosfogips wat met hierdie geskikte metode behandel is, kon natuurlike gips suksesvol in Portland sement vervang.

Hierdie studie poog om weer die wêreld-wye probleem van fosfogips afvalbenutting aan te spreek, en toon dat die aanwending van fosfogips as 'n set reguleerder in Portland sement moontlik is na blootstelling aan 'n effektiewe suiweringsmetode.

# Acknowledgements

I would like to express my gratitude to the following people, companies and institutions for their contribution to this study:

- My supervisor, Professor C Strydom, for her guidance, advice, financial support, and for sharing her expertise in the field of study
- Dr Linda Jacobs for her most valuable input, enthusiasm and encouragement throughout this project
- The University of Pretoria, Cement Industry of South Africa and the NRF for financial support
- The personnel at the Chemistry Department at the University of South Africa for creating the opportunity for me to conduct this study, and for their continuous assistance and encouragement
- ISCOR for XRF analyses of the samples
- PPC Technical services for conducting the cement tests
- Linda Prinsloo for her assistance on the FT-IR analyses
- Adelé Botha and Liana Swanepoel in the research group at the University of Pretoria for their advice, support with some experiments and useful discussions
- My parents, family and friends for their support and encouragement throughout my studies
- A special thanks to my husband, Tommie, for his participation in scientific discussions regarding this study, continuous emotional support, patience and understanding



# Contents

<b>Abstract</b> .....	<b>i</b>
<b>Samevatting</b> .....	<b>iii</b>
<b>Acknowledgements</b> .....	<b>iv</b>
<b>Contents</b> .....	<b>v</b>
<b>Chapter 1</b>	
<b>The phosphogypsum problem</b> .....	<b>1</b>
<b>1.1 Introduction</b> .....	<b>1</b>
<b>1.2 Production of phosphogypsum</b> .....	<b>2</b>
1.2.1 Phosphate ores and phosphate rock .....	2
1.2.2 Origin and properties of South African phosphate rock .....	3
1.2.3 Phosphoric acid production .....	3
<b>1.3 Disposal methods</b> .....	<b>5</b>
<b>1.4 Utilization of phosphogypsum</b> .....	<b>6</b>
1.4.1 Agricultural uses .....	6
1.4.2 Recovery of sulphur .....	7
1.4.3 Sulphuric acid process with simultaneous cement production ..	7
1.4.4 Building materials production .....	7
1.4.5 The use of phosphogypsum in Portland cement .....	8
<b>Chapter 2</b>	
<b>Hydration, setting and hardening of Portland cement</b> .....	<b>10</b>
<b>2.1 Introduction</b> .....	<b>10</b>
<b>2.2 Hydration of the individual phases in Portland cement</b> .....	<b>11</b>
2.2.1 Tricalcium silicate .....	11
2.2.2 Dicalcium silicate .....	11

2.2.3	Tricalcium aluminate .....	12
2.2.4	Calcium aluminoferrite .....	13
<b>2.3</b>	<b>Hydration of Portland cement .....</b>	<b>13</b>
<b>2.4</b>	<b>Setting of Portland cement .....</b>	<b>16</b>
<b>2.5</b>	<b>Strength development in Portland cement .....</b>	<b>17</b>
2.5.7	Optimum operating conditions .....	17
<b>2.6</b>	<b>X-ray Fluorescence analysis .....</b>	<b>18</b>
<b>Chapter 3</b>	<b>4.4.1 Introduction .....</b>	<b>19</b>
<b>Background on the aspects of treatment of phosphogypsum .....</b>		<b>19</b>
<b>3.1</b>	<b>Impurities in phosphogypsum .....</b>	<b>19</b>
<b>3.2</b>	<b>The influence of phosphogypsum impurities on the mechanical strength and hydration of Portland cement .....</b>	<b>19</b>
<b>3.3</b>	<b>Phases of the calcium sulphate/water system .....</b>	<b>22</b>
3.3.1	Description of the different phases .....	22
3.3.2	Dehydration, rehydration and crystal structure contributions ..	25
<b>3.4</b>	<b>Influence of the different phases of the calcium sulphate/water system on the properties of Portland cement .....</b>	<b>25</b>
<b>3.5</b>	<b>Existing treatment methods of phosphogypsum .....</b>	<b>27</b>
3.5.1	Thermal and washing treatments .....	27
3.5.2	Acid treatment .....	28
3.5.3	Treatment with ammonium hydroxide solutions .....	28
3.5.4	Wet sieving .....	29
<b>Chapter 4</b>		
<b>Experimental techniques applied in this study .....</b>		<b>30</b>
<b>4.1</b>	<b>Thermogravimetry (TG) .....</b>	<b>30</b>
<b>4.2</b>	<b>Differential Scanning Calorimetry (DSC) .....</b>	<b>30</b>
4.2.1	Heat-flux DSC .....	31
4.2.2	Calibration of the DSC apparatus .....	32
4.2.3	Applications of DSC .....	32
<b>4.3</b>	<b>Simultaneous TG-DSC .....</b>	<b>33</b>
4.3.1	The balance .....	33



4.3.2	Sample carrier system	33
4.3.3	The furnace	34
4.3.4	The Programmer	35
4.3.5	The data acquisition device (computer)	35
4.3.6	Sources of error during thermogravimetry	35
4.3.7	Optimum operating conditions	37
<b>4.4</b>	<b>X-ray Fluorescence analysis</b>	<b>38</b>
4.4.1	Introduction	38
4.4.2	Instrumentation	41
4.4.3	Qualitative analysis by XRF	44
4.4.4	Quantitative analysis by XRF	44
4.4.5	Sample preparation for XRF analysis	45
<b>4.5</b>	<b>Infrared spectroscopy</b>	<b>47</b>
4.5.1	Introduction	47
4.5.2	Instrumentation for Fourier-Transform Infrared spectroscopy	52
4.5.3	Sampling	55
4.5.4	Interpretation of an infrared spectrum	56
<b>4.6</b>	<b>BET surface area analysis</b>	<b>57</b>
<b>4.7</b>	<b>Cement tests</b>	<b>61</b>
4.7.1	Specific surface area and density	61
4.7.2	Setting times	63
4.7.3	Compressive strength	64

## Chapter 5

<b>Properties and characterization of South African phosphogypsum</b>		<b>66</b>
<b>5.1</b>	<b>Introduction</b>	<b>66</b>
<b>5.2</b>	<b>Experimental</b>	<b>66</b>
5.2.1	Samples	66
5.2.2	Thermal analysis	67
5.2.3	Infrared analysis	67
5.2.4	X-ray fluorescence analysis	67
7.3	Experimental	92

<b>5.3</b>	<b>Results and discussion</b> .....	<b>68</b>
5.3.1	X-ray fluorescence analysis .....	68
5.3.2	Infrared analysis .....	69
5.3.3	Thermal analysis .....	71
<b>5.4</b>	<b>Conclusion</b> .....	<b>76</b>
<b>Chapter 6</b>		
<b>Distribution of phosphorous impurities in particle size fractions of South African phosphogypsum</b> .....		
<b>6.1</b>	<b>Introduction</b> .....	<b>77</b>
<b>6.2</b>	<b>Experimental</b> .....	<b>78</b>
6.2.1	Samples .....	78
6.2.2	Instrumental analysis .....	78
6.2.3	Sieving .....	78
<b>6.3</b>	<b>Results and discussion</b> .....	<b>78</b>
6.3.1	Particle size distribution of the phosphogypsum samples .....	78
6.3.2	X-ray fluorescence analysis of the phosphogypsum particle size fractions .....	79
6.3.3	Thermal analysis of the phosphogypsum particle size fractions .....	80
6.3.4	Infrared spectroscopy analysis of the phosphogypsum particle size fractions .....	84
<b>6.4</b>	<b>Conclusion</b> .....	<b>87</b>
<b>Chapter 7</b>		
<b>Thermal and washing treatment of South African phosphogypsum</b> .....		
<b>7.1</b>	<b>Introduction</b> .....	<b>89</b>
<b>7.2</b>	<b>Description of the experimental conditions and results of the phosphogypsum purification process applied by Ölmez and Yilmaz</b> .....	<b>90</b>
<b>7.3</b>	<b>Experimental</b> .....	<b>92</b>

7.3.1	Samples .....	92
7.3.2	Instrumental analysis .....	92
7.3.3	Surface area determinations .....	92
7.3.4	Cement tests .....	92
7.3.5	Experimental procedures followed to optimise the thermal and washing treatments for South African phosphogypsum .....	93
<b>7.4</b>	<b>Results of the optimisation of the thermal and washing treatments for the South African phosphogypsum samples .....</b>	<b>94</b>
7.4.1	Washing of phosphogypsum with distilled water .....	94
7.4.2	Treatment of phosphogypsum with milk of lime .....	95
7.4.3	Thermal treatment of phosphogypsum .....	96
7.4.4	Treatment of the different phosphogypsum samples by combining the washing and thermal treatment methods .....	98
<b>7.5</b>	<b>Characterization of the untreated and treated phosphogypsum samples .....</b>	<b>98</b>
7.5.1	XRF analysis .....	98
7.5.2	Thermal analysis .....	100
7.5.3	Infrared analysis .....	104
7.5.4	Cement tests .....	107
<b>7.6</b>	<b>Conclusion .....</b>	<b>110</b>

## Chapter 8

<b>Sulphuric acid treatment of South African phosphogypsum .....</b>	<b>111</b>
<b>8.1 Introduction .....</b>	<b>111</b>
<b>8.2 Experimental .....</b>	<b>112</b>
8.2.1 Samples .....	112
8.2.2 Instrumental analysis .....	112
8.2.3 Jarosiński's method applied to South African phosphogypsum .....	112
8.2.4 Sulphuric acid treatment of phosphogypsum at a larger scale .....	113
8.2.5 Optimisation of the sulphuric acid method .....	113



8.2.6	The optimised sulphuric acid method on a large scale . . . . .	114
8.2.7	Sulphuric acid treatment combined with thermal treatment . .	114
8.2.8	Optimisation of the combined thermal and acid treating method . . . . .	115
8.2.9	The combined thermal and acid treatment of phosphogypsum at a larger scale . . . . .	115
8.2.10	Cement tests . . . . .	115
<b>8.3</b>	<b>Results and discussion of the sulphuric acid treatment of South African phosphogypsum . . . . .</b>	<b>116</b>
8.3.1	Application of Jarosiński's method to South African phosphogypsum . . . . .	116
8.3.2	Sulphuric acid treatment of phosphogypsum on a large scale . . . . .	120
8.3.3	Performance of cement tests on the untreated and sulphuric acid treated phosphogypsum samples . . . . .	129
8.3.4	Optimisation of the sulphuric acid treatment method . . . . .	131
8.3.5	The optimum sulphuric acid treatment of phosphogypsum on a large scale for performance of cement tests . . . . .	136
8.3.6	Performance of cement tests on the optimum sulphuric acid treated phosphogypsum samples . . . . .	142
<b>8.4</b>	<b>Results and discussion of the combined thermal and sulphuric acid treatment method, applied to the South African phosphogypsum samples . . . . .</b>	<b>145</b>
8.4.1	The combined thermal and sulphuric acid treatment method . . . . .	145
8.4.2	Optimisation of the combined thermal and sulphuric acid treatment method . . . . .	151
8.4.3	The combined thermal and sulphuric acid treatment on a large scale for the performance of cement tests . . . . .	153
8.4.4	Performance of cement tests on the combined thermal and sulphuric acid treated phosphogypsum samples . . . . .	158
<b>8.5</b>	<b>Conclusion . . . . .</b>	<b>160</b>

Chapter 9

Conclusion ..... 163

Appendix A

References ..... 176

.....

.....

.....



# Chapter 1 The phosphogypsum problem

## 1.1 Introduction

Natural gypsum is mainly used in the production of plasterboard and as an additive in Portland cement production. It is found and mined on all the continents, and can easily be processed with technologies that require very low capital investment (Coburn *et al.*, 1989). The usefulness of gypsum as an industrial product is due to its ability to release its water of crystallization when heated. This then produces partially or totally dehydrated gypsum. On addition of water, the dehydrated product can be rehydrated to the original material, that is, set and hardened gypsum.

Although there are generally generous supplies of natural gypsum available, increasing quantities of by-product gypsum are produced by the chemical industry. Residual phosphogypsum from phosphoric acid plants has been a worldwide problem concerning the environment, disposal and handling. Its utilization raises public interest, and may provide economic benefits by leading to the conservation of mineral resources. Social benefits include the making available of land and reduction in the risks of pollution of the environment.

Phosphogypsum is the largest single chemical by-product in the world in terms of annual turnover (Mehta and Brady, 1977). It is often offered for sale at extremely favourable prices, but contains impurities which need decontamination and neutralization. This gypsum is at a disadvantage in comparison with natural gypsum, because of higher investment and production costs. Its use will only be economical if it is close to a consumer region, when natural gypsum is not available, or when natural gypsum has more expensive transport costs.

# Chapter 1 The phosphogypsum problem

## 1.1 Introduction

Natural gypsum is mainly used in the production of plasterboard and as an additive in Portland cement production. It is found and mined on all the continents, and can easily be processed with technologies that require very low capital investment (Coburn *et al.*, 1989). The usefulness of gypsum as an industrial product is due to its ability to release its water of crystallization when heated. This then produces partially or totally dehydrated gypsum. On addition of water, the dehydrated product can be rehydrated to the original material, that is, set and hardened gypsum.

Although there are generally generous supplies of natural gypsum available, increasing quantities of by-product gypsum are produced by the chemical industry. Residual phosphogypsum from phosphoric acid plants has been a worldwide problem concerning the environment, disposal and handling. Its utilization raises public interest, and may provide economic benefits by leading to the conservation of mineral resources. Social benefits include the making available of land and reduction in the risks of pollution of the environment.

Phosphogypsum is the largest single chemical by-product in the world in terms of annual turnover (Mehta and Brady, 1977). It is often offered for sale at extremely favourable prices, but contains impurities which need decontamination and neutralization. This gypsum is at a disadvantage in comparison with natural gypsum, because of higher investment and production costs. Its use will only be economical if it is close to a consumer region, when natural gypsum is not available, or when natural gypsum has more expensive transport costs.

# Chapter 1 The phosphogypsum problem

## 1.1 Introduction

Natural gypsum is mainly used in the production of plasterboard and as an additive in Portland cement production. It is found and mined on all the continents, and can easily be processed with technologies that require very low capital investment (Coburn *et al.*, 1989). The usefulness of gypsum as an industrial product is due to its ability to release its water of crystallization when heated. This then produces partially or totally dehydrated gypsum. On addition of water, the dehydrated product can be rehydrated to the original material, that is, set and hardened gypsum.

Although there are generally generous supplies of natural gypsum available, increasing quantities of by-product gypsum are produced by the chemical industry. Residual phosphogypsum from phosphoric acid plants has been a worldwide problem concerning the environment, disposal and handling. Its utilization raises public interest, and may provide economic benefits by leading to the conservation of mineral resources. Social benefits include the making available of land and reduction in the risks of pollution of the environment.

Phosphogypsum is the largest single chemical by-product in the world in terms of annual turnover (Mehta and Brady, 1977). It is often offered for sale at extremely favourable prices, but contains impurities which need decontamination and neutralization. This gypsum is at a disadvantage in comparison with natural gypsum, because of higher investment and production costs. Its use will only be economical if it is close to a consumer region, when natural gypsum is not available, or when natural gypsum has more expensive transport costs.



# Chapter 1 The phosphogypsum problem

## 1.1 Introduction

Natural gypsum is mainly used in the production of plasterboard and as an additive in Portland cement production. It is found and mined on all the continents, and can easily be processed with technologies that require very low capital investment (Coburn *et al.*, 1989). The usefulness of gypsum as an industrial product is due to its ability to release its water of crystallization when heated. This then produces partially or totally dehydrated gypsum. On addition of water, the dehydrated product can be rehydrated to the original material, that is, set and hardened gypsum.

Although there are generally generous supplies of natural gypsum available, increasing quantities of by-product gypsum are produced by the chemical industry. Residual phosphogypsum from phosphoric acid plants has been a worldwide problem concerning the environment, disposal and handling. Its utilization raises public interest, and may provide economic benefits by leading to the conservation of mineral resources. Social benefits include the making available of land and reduction in the risks of pollution of the environment.

Phosphogypsum is the largest single chemical by-product in the world in terms of annual turnover (Mehta and Brady, 1977). It is often offered for sale at extremely favourable prices, but contains impurities which need decontamination and neutralization. This gypsum is at a disadvantage in comparison with natural gypsum, because of higher investment and production costs. Its use will only be economical if it is close to a consumer region, when natural gypsum is not available, or when natural gypsum has more expensive transport costs.

# Chapter 1 The phosphogypsum problem

## 1.1 Introduction

Natural gypsum is mainly used in the production of plasterboard and as an additive in Portland cement production. It is found and mined on all the continents, and can easily be processed with technologies that require very low capital investment (Coburn *et al.*, 1989). The usefulness of gypsum as an industrial product is due to its ability to release its water of crystallization when heated. This then produces partially or totally dehydrated gypsum. On addition of water, the dehydrated product can be rehydrated to the original material, that is, set and hardened gypsum.

Although there are generally generous supplies of natural gypsum available, increasing quantities of by-product gypsum are produced by the chemical industry. Residual phosphogypsum from phosphoric acid plants has been a worldwide problem concerning the environment, disposal and handling. Its utilization raises public interest, and may provide economic benefits by leading to the conservation of mineral resources. Social benefits include the making available of land and reduction in the risks of pollution of the environment.

Phosphogypsum is the largest single chemical by-product in the world in terms of annual turnover (Mehta and Brady, 1977). It is often offered for sale at extremely favourable prices, but contains impurities which need decontamination and neutralization. This gypsum is at a disadvantage in comparison with natural gypsum, because of higher investment and production costs. Its use will only be economical if it is close to a consumer region, when natural gypsum is not available, or when natural gypsum has more expensive transport costs.



# Chapter 1 The phosphogypsum problem

## 1.1 Introduction

Natural gypsum is mainly used in the production of plasterboard and as an additive in Portland cement production. It is found and mined on all the continents, and can easily be processed with technologies that require very low capital investment (Coburn *et al.*, 1989). The usefulness of gypsum as an industrial product is due to its ability to release its water of crystallization when heated. This then produces partially or totally dehydrated gypsum. On addition of water, the dehydrated product can be rehydrated to the original material, that is, set and hardened gypsum.

Although there are generally generous supplies of natural gypsum available, increasing quantities of by-product gypsum are produced by the chemical industry. Residual phosphogypsum from phosphoric acid plants has been a worldwide problem concerning the environment, disposal and handling. Its utilization raises public interest, and may provide economic benefits by leading to the conservation of mineral resources. Social benefits include the making available of land and reduction in the risks of pollution of the environment.

Phosphogypsum is the largest single chemical by-product in the world in terms of annual turnover (Mehta and Brady, 1977). It is often offered for sale at extremely favourable prices, but contains impurities which need decontamination and neutralization. This gypsum is at a disadvantage in comparison with natural gypsum, because of higher investment and production costs. Its use will only be economical if it is close to a consumer region, when natural gypsum is not available, or when natural gypsum has more expensive transport costs.

# Chapter 1      The phosphogypsum problem

## 1.1 Introduction

Natural gypsum is mainly used in the production of plasterboard and as an additive in Portland cement production. It is found and mined on all the continents, and can easily be processed with technologies that require very low capital investment (Coburn *et al.*, 1989). The usefulness of gypsum as an industrial product is due to its ability to release its water of crystallization when heated. This then produces partially or totally dehydrated gypsum. On addition of water, the dehydrated product can be rehydrated to the original material, that is, set and hardened gypsum.

Although there are generally generous supplies of natural gypsum available, increasing quantities of by-product gypsum are produced by the chemical industry. Residual phosphogypsum from phosphoric acid plants has been a worldwide problem concerning the environment, disposal and handling. Its utilization raises public interest, and may provide economic benefits by leading to the conservation of mineral resources. Social benefits include the making available of land and reduction in the risks of pollution of the environment.

Phosphogypsum is the largest single chemical by-product in the world in terms of annual turnover (Mehta and Brady, 1977). It is often offered for sale at extremely favourable prices, but contains impurities which need decontamination and neutralization. This gypsum is at a disadvantage in comparison with natural gypsum, because of higher investment and production costs. Its use will only be economical if it is close to a consumer region, when natural gypsum is not available, or when natural gypsum has more expensive transport costs.

# Chapter 1 The phosphogypsum problem

## 1.1 Introduction

Natural gypsum is mainly used in the production of plasterboard and as an additive in Portland cement production. It is found and mined on all the continents, and can easily be processed with technologies that require very low capital investment (Coburn *et al.*, 1989). The usefulness of gypsum as an industrial product is due to its ability to release its water of crystallization when heated. This then produces partially or totally dehydrated gypsum. On addition of water, the dehydrated product can be rehydrated to the original material, that is, set and hardened gypsum.

Although there are generally generous supplies of natural gypsum available, increasing quantities of by-product gypsum are produced by the chemical industry. Residual phosphogypsum from phosphoric acid plants has been a worldwide problem concerning the environment, disposal and handling. Its utilization raises public interest, and may provide economic benefits by leading to the conservation of mineral resources. Social benefits include the making available of land and reduction in the risks of pollution of the environment.

Phosphogypsum is the largest single chemical by-product in the world in terms of annual turnover (Mehta and Brady, 1977). It is often offered for sale at extremely favourable prices, but contains impurities which need decontamination and neutralization. This gypsum is at a disadvantage in comparison with natural gypsum, because of higher investment and production costs. Its use will only be economical if it is close to a consumer region, when natural gypsum is not available, or when natural gypsum has more expensive transport costs.



# Chapter 1      The phosphogypsum problem

## 1.1 Introduction

Natural gypsum is mainly used in the production of plasterboard and as an additive in Portland cement production. It is found and mined on all the continents, and can easily be processed with technologies that require very low capital investment (Coburn *et al.*, 1989). The usefulness of gypsum as an industrial product is due to its ability to release its water of crystallization when heated. This then produces partially or totally dehydrated gypsum. On addition of water, the dehydrated product can be rehydrated to the original material, that is, set and hardened gypsum.

Although there are generally generous supplies of natural gypsum available, increasing quantities of by-product gypsum are produced by the chemical industry. Residual phosphogypsum from phosphoric acid plants has been a worldwide problem concerning the environment, disposal and handling. Its utilization raises public interest, and may provide economic benefits by leading to the conservation of mineral resources. Social benefits include the making available of land and reduction in the risks of pollution of the environment.

Phosphogypsum is the largest single chemical by-product in the world in terms of annual turnover (Mehta and Brady, 1977). It is often offered for sale at extremely favourable prices, but contains impurities which need decontamination and neutralization. This gypsum is at a disadvantage in comparison with natural gypsum, because of higher investment and production costs. Its use will only be economical if it is close to a consumer region, when natural gypsum is not available, or when natural gypsum has more expensive transport costs.

## Chapter 2 Hydration, setting and hardening of Portland cement

### 2.1 Introduction

In chemical terms, hydration is a reaction of an anhydrous compound with water, yielding a new compound named a hydrate. In cement chemistry, hydration is understood to be the reaction of a non-hydrated cement or one of its components with water, associated with both chemical and physico-mechanical changes of the system, particularly with regard to setting and hardening. The chemical reactions taking place during hydration are generally more complex than simple conversion of anhydrous compounds into the corresponding hydrates (Hewlett, 1998a; Taylor, 1997).

A mixture of cement and water in such proportions that setting and hardening occur is called a paste. The mutual ratio of water and cement in the mix (the water/cement (w/c) ratio) refers to proportions by mass, which for a paste is typically 0.3-0.6. This ratio affects the rheology of the produced suspension, the progress of hydration and the properties of the hydrated material. Setting of cement is stiffening without a significant development of compressive strength, and typically occurs within a few hours. Hardening follows the setting of the cement paste, and means the development of compressive strength, which is normally a slower process. Curing means storage under conditions such that hydration occurs, which in laboratory studies include storage in moist air initially and then in water after the first 24 hours, or storage in air of 100% humidity and, less favourable, storage in a sealed container (Hewlett, 1998a; Taylor, 1997).

Because Portland cement is a multi-component system, its hydration is a complex process consisting of a series of individual chemical reactions that take place both simultaneously and successively. The process is initiated spontaneously upon contact of the binder with water, and is associated with liberation of heat.

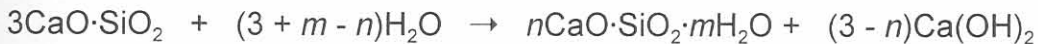


The progress of hydration and its kinetics are influenced by a number of factors, of which some are the phase composition of the cement and presence of foreign ions within the crystal lattices of the individual clinker phases, the fineness of the cement, the water-cement ratio, the curing temperature, and the presence of chemical admixtures and additives (Hewlett, 1998a).

## 2.2 Hydration of the individual phases in Portland cement

### 2.2.1 Tricalcium silicate

Tricalcium silicate,  $3\text{CaO}\cdot\text{SiO}_2$  (abbreviated as  $\text{C}_3\text{S}$ ), is the main component of Portland cement, and is the phase that primarily controls the early setting and hardening. The products of hydration of this phase at ambient temperatures are an ill-defined amorphous calcium silicate hydrate phase called the C-S-H phase and crystalline calcium hydroxide, also referred to as portlandite,  $\text{Ca}(\text{OH})_2$  (abbreviated as CH). The hydration reaction may be shown as



or abbreviated as



where  $m$  and  $n$  are not necessarily integers (Bye, 1999; Hewlett, 1998a).

### 2.2.2 Dicalcium silicate

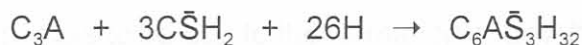
The  $\beta$ -modification of dicalcium silicate,  $2\text{CaO}\cdot\text{SiO}_2$  (abbreviation  $\text{C}_2\text{S}$ ) is the most regular constituent of  $\text{C}_2\text{S}$  in Portland cement. Similarly to  $\text{C}_3\text{S}$ , its hydration products are also C-S-H and calcium hydroxide. The amount of calcium hydroxide being produced during the hydration of  $\beta\text{-C}_2\text{S}$  is about a fifth of that produced in the hydration of  $\text{C}_3\text{S}$ , and the rate of hydration of  $\beta\text{-C}_2\text{S}$  is much slower than that of  $\text{C}_3\text{S}$  (Bye, 1999).

### 2.2.3 Tricalcium aluminate

The reaction of tricalcium aluminate,  $3\text{CaO}\cdot\text{Al}_2\text{O}_3$  (abbreviation  $\text{C}_3\text{A}$ ), with water in suspensions at ordinary temperatures gives  $\text{C}_2\text{AH}_8$  and  $\text{C}_4\text{AH}_{19}$ , which are subsequently converted into  $\text{C}_3\text{AH}_6$  (Taylor, 1997). The conversion to  $\text{C}_3\text{AH}_6$  is accelerated with increasing temperature and also depends on the water/solid ratio, the grain size of  $\text{C}_3\text{A}$  and the presence or absence of  $\text{CO}_2$ .

In the presence of calcium hydroxide, the rate of reaction slows down and only  $\text{C}_4\text{AH}_{19}$  is formed as primary product (Hewlett, 1998a). It again converts to  $\text{C}_3\text{AH}_6$  as the hydration progresses.

In the presence of calcium sulphate the amount of  $\text{C}_3\text{A}$  in the initial stage of hydration is noticeably reduced when compared to that consumed in the absence of  $\text{CaSO}_4$ . Ettringite (trisulphate),  $\text{C}_6\text{A}\bar{\text{S}}_3\text{H}_{32}$  is formed as the main product of hydration (Hewlett, 1998a, Taylor, 1997):



Ettringite belongs to the broad group of Aft phases with the general formula  $[\text{Ca}_3(\text{Al}, \text{Fe})(\text{OH})_6]\text{X}_3\cdot x\text{H}_2\text{O}$ , where X represents a formula unit of a doubly charged anion.

After a rapid initial reaction, the hydration rate is slowed down, and the length of this dormant period may vary with the amount of calcium sulphate present in the original paste. A faster hydration is initiated after all of the available gypsum has been consumed. Under these conditions, the ettringite formed initially reacts with additional amounts of  $\text{C}_3\text{A}$ , yielding calcium aluminate monosulphate hydrate (monosulphate),  $\text{C}_4\text{A}\bar{\text{S}}\text{H}_{12}$  (Taylor, 1997):



As ettringite is gradually consumed, calcium aluminate hydrate,  $\text{C}_4\text{AH}_{19}$ , also starts to form. In a paste hydration at ambient temperature, a nearly complete hydration of  $\text{C}_3\text{A}$  is attained within several months. The origin of the dormant period, which is characterised by a discretely reduced reaction rate, is not obvious and many theories exist to explain it.

The most widely accepted theory assumes the build-up of a layer of ettringite at the surface of  $C_3A$  which acts as a barrier responsible for the slowing down of the reaction. Ettringite is formed in a through solution reaction and precipitates at the surface of  $C_3A$  due to the limited solubility of  $C_3A$  in the presence of sulphates.

The termination of the dormant period appears to be due to a breakdown of the protective layer, as the added gypsum becomes consumed and ettringite is converted to monosulphate. During this solution reaction both  $C_3A$  and ettringite dissolve and monosulphate is precipitated from the liquid phase (Hewlett, 1998a).

#### 2.2.4 Calcium aluminoferrite

The composition of calcium aluminoferrite may vary between approximately  $C_2(A_{0.7}, F_{0.3})$  and  $C_2(A_{0.3}, F_{0.7})$  (Hewlett, 1998a). As with  $C_3A$ , the progress of hydration is slowed in the presence of calcium hydroxide and gypsum. The retardation in the presence of gypsum and calcium hydroxide appears to be due to the formation of an Aft layer at the  $C_2(A, F)$  surface.

### 2.3 Hydration of Portland cement

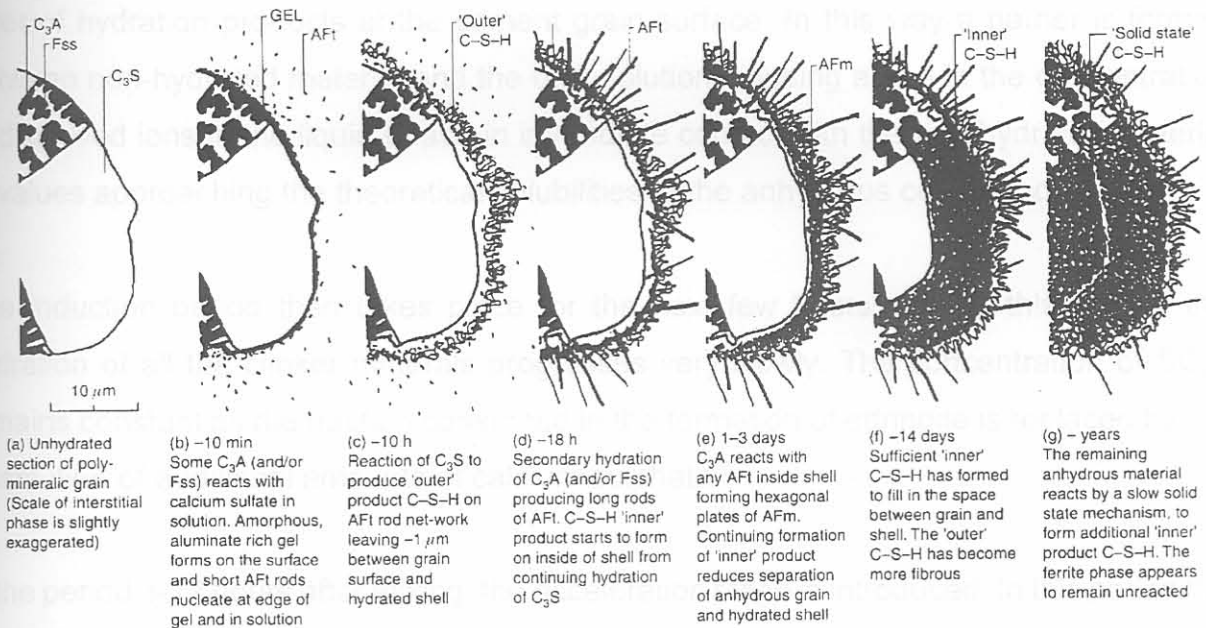
Chemically, the hydration of Portland cement consists of a series of reactions between the individual clinker minerals, calcium sulphate and water, which proceed both simultaneously and successively at different rates and influence each other (Hewlett, 1998a). The participants of the process are alite (tricalcium silicate doped with foreign ions), belite (dicalcium silicate doped by foreign ions), tricalcium aluminate, calcium aluminate ferrite, free calcium oxide, alkali sulphates, calcium sulphate in the form of dihydrate, hemihydrate or anhydrite interground with clinker, and mixing water.

The progress of the process depends on the rate of dissolution of the involved phases, the rate of nucleation and crystal growth of the hydrates to be formed, and the rate of diffusion of water and dissolved ions through the hydrated material already formed. At the beginning of hydration, the process tends to be controlled mainly by the rate of dissolution of the



clinker phases and calcium sulphate. The quantity and form of calcium sulphate plays an important role in the kinetics of the hydration process. A schematic presentation of the hydration of a polymineralic grain of Portland cement is given in Figure 2.1.

**Figure 2.1 Hydration of a grain of Portland cement (Bye, 1999; Taylor, 1997)**



The hydration of Portland cement is characterised by several stages (Hewlett, 1998a). During the pre-induction period, which takes place in the first minutes upon contact of cement with water, a rapid dissolution of ionic species into the liquid phase and the formation of hydrate phases is initiated. Alkali sulphates present in the cement dissolve completely within seconds, contributing  $K^+$ ,  $Na^+$  and  $SO_4^{2-}$  ions. Calcium sulphate dissolves until saturation, thus contributing  $Ca^{2+}$  and additional  $SO_4^{2-}$  ions.

Tricalcium silicate ( $C_3A$ ) dissolves similarly and a layer of the C-S-H phase precipitates at the cement particle surface. As the  $CaO/SiO_2$  ratio of the produced hydrate is lower than that of tricalcium silicate, the hydration of this phase is associated with an increase of the  $Ca^{2+}$  and  $OH^-$  concentration in the liquid phase. At the same time, silicate ions also enter



the liquid phase, although their concentration remains very low. Consequently, the ettringite that has been formed during the early stages of hydration. Tricalcium aluminate ( $C_3A$ ) dissolves and reacts with  $Ca^{2+}$  and  $SO_4^{2-}$  ions (from gypsum) present in the liquid phase, yielding ettringite that also precipitates at the cement particle surface. The ferrite phase reacts in a very similar way as  $C_3A$ , and also yields ettringite.

The early fast hydration reaction appears to be slowed down due to the deposition of the layer of hydration products at the cement grain surface. In this way a barrier is formed between non-hydrated material and the bulk solution, causing a rise in the concentration of dissolved ions in the liquid phase in immediate contact with the non-hydrated material to values approaching the theoretical solubilities of the anhydrous compound.

The induction period then takes place for the next few hours. During this period, the hydration of all the clinker minerals progresses very slowly. The concentration of  $SO_4^{2-}$  remains constant as the fraction consumed in the formation of ettringite is replaced by the dissolution of additional amounts of calcium sulphate.

In the period 3-12 hours after mixing, the acceleration stage is introduced. In this period the progress of hydration is accelerated again and is controlled by the nucleation and growth of the hydration products. The rate of  $C_3S$  hydration accelerates and the second-stage C-S-H starts to be formed. A noticeable hydration of dicalcium silicate also takes place. Crystalline calcium hydroxide precipitates from the liquid phase and together with it the concentration of  $Ca^{2+}$  in the liquid phase gradually declines. The calcium sulphate, interground with the cement becomes completely dissolved and the concentration of  $SO_4^{2-}$  in the liquid phase starts to decline due to the formation of ettringite, as well as the adsorption of  $SO_4^{2-}$  on the surface of the formed C-S-H phase.

During the post-acceleration period, the hydration rate slows down gradually, as the amount of still non-reacted material declines as the rate of the hydration process becomes diffusion controlled. The C-S-H phase continues to be formed due to the continuing hydration of both  $C_3S$  and  $\beta$ - $C_2S$ . The contribution of  $\beta$ - $C_2S$  to this process increases with time with a subsequent decline in the rate at which additional calcium hydroxide is formed. After the

supply of calcium sulphate has been depleted, the concentration of  $\text{SO}_4^{2-}$  in the liquid phase declines. Consequently, the ettringite that has been formed during the early stages of hydration starts to react in a through-solution reaction with additional  $\text{C}_3\text{A}$  to yield monosulphate. After the hydration process has been completed, ageing of the hydrated material takes place (Hewlett, 1998a; Taylor, 1997).

## 2.4 Setting of Portland cement

Setting is a process in which a 'fresh' cement paste of freely flowing or plastic consistency is converted into a set material which has lost its unlimited deformability and crumbles under the effect of a sufficiently great external force (Hewlett, 1998a).

After mixing a Portland cement with an adequate amount of water, the cement grains are initially evenly distributed in the liquid phase. Within minutes from mixing, flocculation of the cement particles takes place, which is associated with an increase in the viscosity of the paste. Individual aggregates of cement particles are formed which entrap a fraction of the mixing water, thus making it unable to participate in the flow of the paste. This initial flocculation of cement particles is caused by opposite zeta potentials and by weak van der Waals forces.

## 2.5 Strength development in Portland cement

In addition to flocculation, the viscosity of the paste also increases due to a progressive hydration of the cement that results in an increase of the solid/liquid ratio. During the acceleratory stage of hydration, the amount of hydrated material increases rapidly and the volume of the liquid phase declines. Chemical bonds develop at the points of contact between the individual cement particles, which are covered with the hydrated material. As the amount of hydrated material increases, the number of contacts between particles also increases and eventually a continuous three-dimensional network of solids develops within the paste, resulting in the set of the paste. The normal setting of Portland cement appears to be the consequence of both  $\text{C}_3\text{S}$  and  $\text{C}_3\text{A}$  hydration and the formation of the C-S-H and Aft phases (Hewlett, 1998a).



To produce a cement with acceptable setting characteristics, calcium sulphate has to be added or interground with the clinker to act as a set retarder. In the presence of sufficient amounts of  $\text{Ca}^{2+}$  and  $\text{SO}_4^{2-}$  in the liquid phase, the amount of  $\text{C}_3\text{A}$  and  $\text{C}_4\text{AF}$  hydrated in the initial pre-induction period is reduced, and ettringite (AFt) is formed during the hydration.

Flash set (also referred to as quick set) occurs when the amount of gypsum added is not sufficient. This is a rapid set, with much evolution of heat. Plasticity is not regained on continued mixing and the strength development of the paste is poor. It is associated with increased early reaction of the aluminate and ferrite phases with a subsequent formation of plates of the Afm ( $\text{Al}_2\text{O}_3\text{-Fe}_2\text{O}_3\text{-mono}$ ) phase throughout the paste, which accounts for the rapid stiffening (Taylor, 1997).

Another undesirable condition is called false set. It is also a rapid set, but there is no unusual high evolution of heat, and plasticity is regained on further mixing. The strength development is not affected noticeably. The most usual cause of false set is the presence of too much calcium sulphate in the form of hemihydrate, which is rehydrated to yield gypsum. The setting is attributable to the interlocking of gypsum crystals.

## 2.5 Strength development in Portland cement

The strength of cement is defined as the strength of mortar test specimens prepared, cured and tested according to a national or international testing standard, to eliminate the effect of factors other than cement quality on the obtained value.

The strength of a hardened cement paste is due to the presence of a continuous three-dimensional network of hydrate phases which can resist external stresses without being broken down. Of the three components of the hardened paste, i.e. hydrated material, non-hydrated residual cement and pores, the hydrated material is the constituent which is mainly responsible for the obtained strength. The non-hydrated material present acts as a filler and also exhibits the capacity to resist external stresses.





## Chapter 3      Background on the aspects of treatment of phosphogypsum

### 3.1 Impurities in phosphogypsum

The amounts of impurities in phosphogypsum depend upon the purity of the raw materials used, the operating conditions of the phosphoric acid process, and the age of the stockpile (Salyak, 1988). Classification of phosphogypsums from plant to plant is difficult due to variation in raw material, the fluctuation in the climatic conditions under which they are stored, and the operating conditions of the process ( $\text{H}_2\text{SO}_4$  concentration, acidulation temperature, oxidation conditions, amount of  $\text{H}_2\text{SO}_4$ ) (Gadalla *et al*, 1987).

To be able to use phosphogypsum for the control of cement hydration, it must first be purified of harmful impurities. These impurities can be classified into two groups, which are (1) free phosphoric acid, phosphates, sodium hexafluorosilicate, sodium sulphate, fluorosilicic acid and organic compounds that adhere to the surface of the gypsum crystals, and (2) dicalcium phosphate, monosodium phosphate and fluorophosphates that substitute in the crystal lattice of gypsum (Ölmez and Erdem, 1989; Wirsching, 1982). Unless neutralized, the impurities contained in phosphogypsum exist in acidic form (Mehta and Brady, 1977).

### 3.2 The influence of phosphogypsum impurities on the mechanical strength and hydration of Portland cement

Tabikh and Miller (1971) stated that the chemical process employed in the production of phosphogypsum yields a product of widely varying impurity concentrations. Presence of large amounts of impurities interfere in an unpredictable way with the hydration of Portland cement.

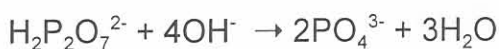


Saltgitter Industriebau GmbH (1979) reported that the soluble impurities contained in phosphogypsum react with the free CaO in the cement, and form an insoluble precipitate which settles on the cement particles. This coating process then restricts the hydration of the cement, with a resulting delay of the setting time.

Murakami (1968) found that the impurities in phosphogypsum increased the setting time of Portland cement, but not the mechanical strength at any stage. Singh *et al.* (1993) have shown that the mechanical strength of cement is considerably reduced at all ages on using unprocessed phosphogypsum in place of natural gypsum. They both argued that the impurities in phosphogypsum delayed the hydration of tricalcium silicate, which is the main compound in Portland cement. Water-soluble impurities of phosphogypsum gradually enter the aqueous phase of the cement paste, and deposition of a protective coating occurs on the surface of the cement particle. This deposition leads to subsequent suppression of cement hydration. When processed phosphogypsum was used, the compressive strength was improved as a result of the removal of impurities.

Murakami (1968), Singh (1987), as well as Tabikh and Miller (1971) proposed the following mechanisms for the action of some impurities in the hydrating phase:

1. The region of the paste in the immediate vicinity of hydrating particles is very alkaline. Neutralization of phosphatic and fluoride species results in the deposition of basic insoluble tricalcium phosphate and calcium fluoride on the surface of cement grains which provides a protective layer against the attack of water. The formation of this protective layer ( $\text{Ca}_3(\text{PO}_4)_2$  and  $\text{CaF}_2$ ) can be shown by the following reaction equations:



and



2. The action of species such as  $\text{Na}_2\text{SiF}_6$  or  $\text{CaH}_2\text{P}_2\text{O}_7$  takes place through two different retarding mechanisms, namely
  - (a) simple depositional covering of the hydrating cement particles, or
  - (b) the ability of these species to serve as “bridges” or “cross-linking agents” between hydrating cement grains, involving chemical bonding through *Si-O-Si* or *Si-O-P-O-Si* linkages. These structures form more rigid and ordered protective coatings than a simple deposition.
  
3. The action of lattice-substituted impurities is believed to be due to the slow release of these impurities during dissolution of gypsum, resulting in a more efficient dispersion of the protective material throughout the system.

Bensted (1995) found that when natural gypsum is replaced with by-product gypsums in Portland cement, the amount of ettringite that forms at the beginning of hydration is increased. The alite ( $\text{C}_3\text{S}$ ) hydration is retarded at first, giving less C-S-H development initially, allowing extra space for the aluminate ( $\text{C}_3\text{A}$ ) and ferrite ( $\text{C}_4\text{AF}$ ) to hydrate in and hence apparently to accelerate the initial formation of ettringite. Water-soluble phosphate and fluoride play a significant role in retarding the onset of setting.

A possible solution was offered by Mehta and Brady (1977), who reported that when phosphogypsum was added to the cement plant raw mix in the range of 2%  $\text{SO}_3$ , the clinkering temperature was reduced, the retarding effect was reduced and there was an increase in the early strengths. When added in this way, the phosphogypsum acted as both a mineralizer for clinker and a set retarder for cement made from this clinker.

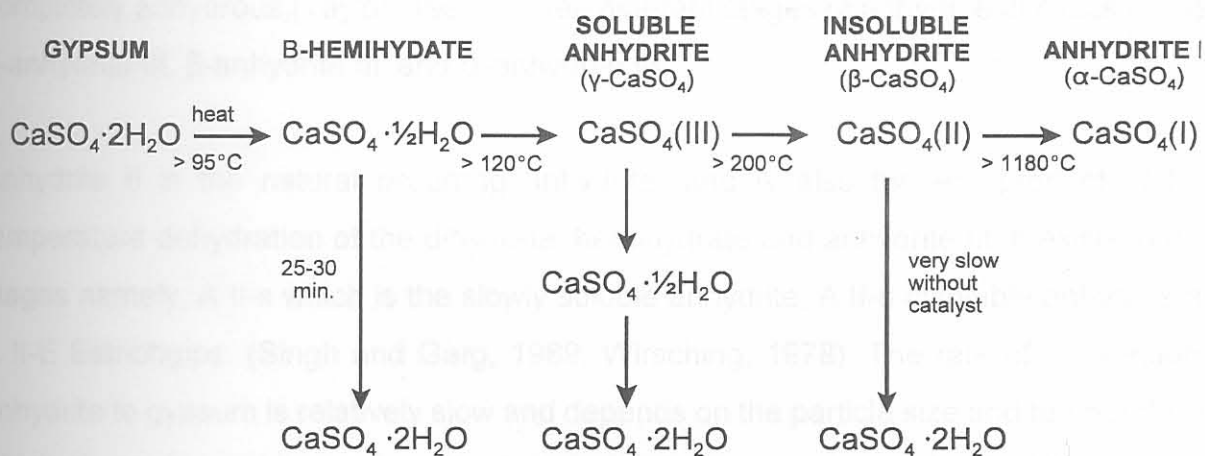


### 3.3 Phases of the calcium sulphate/water system

#### 3.3.1 Description of the different phases

The  $\text{CaSO}_4/\text{H}_2\text{O}$  system consists of five phases, of which four can exist under normal conditions. These phases are calcium sulphate dihydrate ( $\text{CaSO}_4 \cdot 2\text{H}_2\text{O}$ ), calcium sulphate hemihydrate ( $\text{CaSO}_4 \cdot \frac{1}{2}\text{H}_2\text{O}$ ), anhydrite III ( $\gamma\text{-CaSO}_4$ ), anhydrite II ( $\beta\text{-CaSO}_4$ ) and anhydrite I ( $\alpha\text{-CaSO}_4$ ). Anhydrite I only exists at temperatures above 1180 °C. An overview of these phases is presented in Figure 3.1.

**Figure 3.1** The different phases of the calcium sulphate/water system (Bensted, 1995; Luckevich, 2000)



Calcium sulphate dihydrate is both the starting material for dehydration and the end product of rehydration. It occurs naturally as the mineral gypsum, and is the most common sulphate mineral (Hand, 1997).

Calcium sulphate hemihydrate exists in two forms, termed  $\alpha$  and  $\beta$ . These two forms of hemihydrate are the two limiting states of this phase, and are distinguished from each other by their properties, energy relationships and methods of preparation. The  $\alpha$ -hemihydrate is produced under pressure in a humid atmosphere and consists of compact, well-formed,

mostly transparent, large primary particles (Wirsching, 1978). When the hemihydrate is produced at atmospheric pressure, the water of crystallization is driven off as steam, which causes a disruption in the crystal structure to form the fragmentary crystals of  $\beta$ -hemihydrate (Coburn *et al.*, 1989).  $\beta$ -Hemihydrate forms flaky, irregular secondary particles which consist of extremely small individual crystals.

The  $\alpha$ -hemihydrate has a lower water demand on hydration, and this then leads to a stronger hydrated product than the  $\beta$ -hemihydrate. The only reliable method for determining which of these hemihydrates are present is by differential scanning calorimetry, as the two hemihydrates produce qualitatively different traces on heating (Hand, 1997).

The anhydrite III form is also called soluble anhydrite (Wirsching, 1978). Soluble anhydrite has essentially the same crystal structure as hemi-hydrate and readily absorbs water to rehydrate to the hemihydrate form. This form of calcium sulphate is probably never completely anhydrous (Taylor, 1997). Three different stages of anhydrite III exists namely,  $\beta$ -anhydrite III,  $\beta$ -anhydrite III' and  $\alpha$ -anhydrite III.

Anhydrite II is the natural occurring anhydrite, and is also the end-product of high-temperature dehydration of the dihydrate, hemihydrate and anhydrite III. It exists in three stages namely, A II-s which is the slowly soluble anhydrite, A II-u insoluble anhydrite and A II-E Estrichgips. (Singh and Garg, 1989; Wirsching, 1978). The rate of conversion of anhydrite to gypsum is relatively slow and depends on the particle size and temperature at which it was formed as well as the temperature, composition and pH of the hydration solution. Table 3.1 describes some of the physical properties of the phases of the  $\text{CaSO}_4/\text{H}_2\text{O}$  system.

Phase	1. Features	2. Water of crystallization (% weight)	3. Density (g/cm <sup>3</sup> )	4. Lattice structure	5. Solubility in water at 20 °C (g/100 g solution)	6. Thermodynamic stability (°C)	7. Production temperature in laboratory (°C)	8. Production temperature in industry (°C)
		~11.2	~1.76	Monoclinic	~0.2	<40	~120	~140

Table 3.1 Physical properties of the phases of the  $\text{CaSO}_4/\text{H}_2\text{O}$  system (Wirsching, 1978)

Phase	$\text{CaSO}_4 \cdot 2\text{H}_2\text{O}$	$\text{CaSO}_4 \cdot \frac{1}{2}\text{H}_2\text{O}$		$\text{CaSO}_4$ III	$\text{CaSO}_4$ II	$\text{CaSO}_4$ I
1. Features		2 Forms:  $\alpha$ -Form $\beta$ -Form		3 stages: $\beta$ -Anhydrite III $\beta$ -Anhydrite III' $\alpha$ -Anhydrite III	3 stages of reaction of calcined anhydrite II: A II-s :slowly soluble A II-u :insoluble A II-E :Estrichgips	
2. Water of crystallization (% weight)	20.92	6.21	6.21	0.00	0.00	0.00
3. Density ( $\text{g}/\text{cm}^3$ )	2.31	2.619 - 2.637	2.757	2.580	2.93 - 2.97	
4. Lattice structure	Monoclinic	rhombohedral		hexagonal	rhombic	cubic
5. Solubility in water at 20°C (g/100 g solution)	0.21	0.88	0.67	0.67-0.88	0.27	insoluble
6. Thermodynamic stability (°C)	<40	metastable		metastable	40 - 1180	>1180
7. Production temperature in laboratory (°C)	<40	45 - 200 in dry air	>45 aqueous medium	50 Vacuum: $\alpha$ - and $\beta$ -A III 100 Air: $\alpha$ - and $\beta$ -A III 100 dry: $\beta$ -A III'	200 - 1180	>1180 not stable below
8. Production temperature in industry (°C)	<40	120 - 180 (dry)	80 - 180 (wet)	290 (dry) $\beta$ -A III 290 (dry) $\beta$ -A III' 110 (wet) $\alpha$ -A III	between 300 - 900: <500:       A II-s 500 - 700:  A II-u >700:       A II-E	-



### 3.3.2 Dehydration, rehydration and crystal structure contributions

Calcium sulphate dihydrate forms a layered lattice, with the water of crystallization arranged between the layers. It may therefore be split easily along the water layers. During its conversion to the hemihydrate, the lattice volume shrinks, and broad channels parallel to the  $\text{CaSO}_4$  chains are formed in which the water of crystallization of the hemihydrate is loosely bound at definite points. The water can enter and leave relatively easily, which is demonstrated by the ready conversion into anhydrite III in which these channels are free of water. Anhydrite II exhibits a more dense packing of ions and only reacts slowly with water, which explains why it has the highest solubility of the calcium sulphates (Wirsching, 1978).

### 3.4 Influence of the different phases of the calcium sulphate/water system on the properties of Portland cement

During the early and middle periods of reaction in a cement paste, calcium sulphate dissolves and reacts at the surfaces of the cement grains. The factor most directly influencing the course of these reactions is not so much the amount of calcium sulphate available, but the rates at which the relevant ionic species are made available at the surface of the cement grains. The rates at which  $\text{Ca}^{2+}$  and  $\text{SO}_4^{2-}$  ions are supplied by the calcium sulphate thus depend on both the amount of calcium sulphate and on its physical and chemical nature. Hemihydrate supplies ions more quickly than gypsum, which in turn supplies them more quickly than insoluble anhydrite (Taylor, 1997). Therefore, the calcium sulphate phases present in the Portland cement mixture will affect the setting time of the cement considerably due to its difference in solubility.

The heat produced on grinding can cause partial conversion of the gypsum into hemihydrate ( $\text{CaSO}_4 \cdot \frac{1}{2}\text{H}_2\text{O}$ ) or  $\gamma\text{-CaSO}_4$ . The extent to which calcium sulphate dihydrate is dehydrated in a cement mill depends on the temperature and relative humidity existing in it. The conversions affect the rate at which the calcium sulphate dissolves on hydration. Partial conversion to hemihydrate may be desirable, as the water present in gypsum can

cause the particles of cement to adhere during storage, with subsequent formation of lumps (Bye, 1999; Taylor, 1997).

The calcium sulphate hemihydrate formed does not have the precise composition implied by its name because compositions covering the range  $\text{CaSO}_4 \cdot 0.01 - 0.63\text{H}_2\text{O}$  are obtained. The name soluble anhydrite is sometimes used for the lower end of the range. These compositions can be interconverted simply by a change in relative humidity or temperature since water molecules can enter or leave the porous structure. In contrast, conversion to calcium sulphate dihydrate involves its dissolution in water from which the dihydrate crystallises as the stable phase at temperatures below approximately  $43^\circ\text{C}$  (Bye, 1999).

Hewlett (1998b) reported that at grinding temperatures between  $115^\circ\text{C}$  and  $130^\circ\text{C}$ , the dihydrate form can dehydrate to the hemihydrate form and to a lesser extent to calcium sulphate anhydrite. These calcium sulphate forms produce a supersaturated solution with regard to the dihydrate form upon mixing with water. This leads to gypsum precipitation and stiffening of the cement or mortar, making it necessary to add more water for workability, which results in a lowering of strength properties. This process is referred to as "False set". The ratios between the different calcium sulphate forms are thus crucial for the cement industry.

The percentages of the dihydrate, hemihydrate and anhydrite forms of calcium sulphate in the gypsum samples can vary significantly among different gypsum types, especially for phosphogypsum originating from different process routes, plants and operating conditions. These percentages can influence the dehydration behaviour of the gypsums. It is necessary to study the dehydration behaviour of each material used in industry separately to obtain an indication of the dihydrate composition of a gypsum in a milled cement sample, as it would have a major effect on the setting behaviour of cement (Strydom and Potgieter, 1999).



### 3.5 Existing treatment methods of phosphogypsum

Several methods have been proposed or adopted for minimizing the effects of impurities in phosphogypsum. Many of these methods have in common a step of rendering soluble, acidic materials insoluble and alkaline.

Suitable and technically applied methods of processing phosphogypsum had been developed in Japan in 1940 and in Germany in 1960. All other processes designed for the use of phosphogypsum failed technically and resulted in their plants having to close down after a short operation period (Wirsching, 1982).

The wet purification units for by-product gypsum consist mostly of slurry containers, flotation machines, hydrocyclones, and filter or centrifuge installations. Investment and expenditure on purification can vary according to the resulting utilisation of the product (Wirsching, 1978).

#### 3.5.1 Thermal and washing treatments

Treatment of phosphogypsum with lime water or aqueous cement extracts, converts phosphates into  $\text{Ca}_3(\text{PO}_4)_2$  and complex fluoranions into  $\text{CaF}_2$  and insoluble silicates and aluminates. These insoluble impurities have smaller effects on the setting behaviour of cement. Another method, which also involves reduction of acidity, involves heating of the unprocessed phosphogypsum with limestone, lime, or cement at 700 - 800°C. The gypsum is then converted to anhydrite, and the impurities are simultaneously converted to insoluble compounds. Simple washing with water can be effective in dissolving surface absorbed water-soluble impurities, but still leaves the lattice-substituted impurities behind (Tabikh and Miller, 1971).

Ölmez and Erdem (1989) as well as Erdogan *et al.* (1994) investigated the effect of washing of phosphogypsum with water and milk of lime, with and without preceding thermal treatment. They both reported that the untreated phosphogypsum retarded the setting times of Portland cement and also reduced strength, but can be used to control the hydration of Portland cement if washed with milk of lime.



Smadi *et al.* (1999) obtained a better quality of phosphogypsum by calcining washed and unwashed phosphogypsum at temperatures between 170 and 950°C. The treated phosphogypsum samples were used in replacing cement in mortar mixes, and have shown an improvement in mechanical properties compared to the mortars containing untreated phosphogypsum.

### 3.5.2 Acid treatment

Impurities incorporated isomorphically into the gypsum crystal lattice, mainly phosphates, cause lime sensitivity in calcined cement products, with a considerable effect on the setting time. They are not removed by flotation and washing but can be precipitated and rendered harmless by dehydration and recrystallization. They may go into solution during hydrothermal recrystallization if their affinity for the hemihydrate is less than for the dihydrate (Wirsching, 1978).

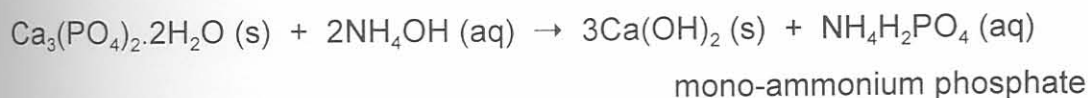
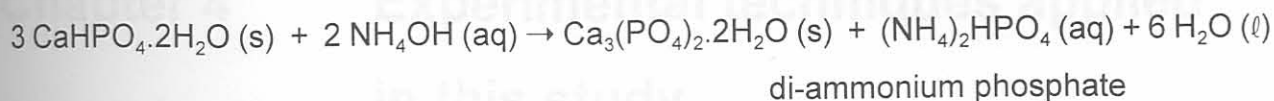
Jarosiński (1994) treated phosphogypsum in sulphuric acid solutions to purify and convert it into anhydrite II. By applying this method, they could reduce the impurities in phosphogypsum to the level below the requirements for use in anhydrite cement.

### 3.5.3 Treatment with ammonium hydroxide solutions

When phosphatic and fluoride compounds are dissolved in an ammonium hydroxide solution, the solubilities of these compounds increase with an increase in the ammonium hydroxide concentration (Singh *et al.*, 1993). This led to the conclusion that the phosphorous impurities present in phosphogypsum, will combine with the ammonium hydroxide to form water-soluble mono-ammonium phosphate and di-ammonium phosphatic compounds:



mono-ammonium phosphate



Similarly, fluorides present in phosphogypsum will form water-soluble ammoniated compounds .

This method was found to be successful in reducing the impurities contained in Indian phosphogypsum, by treating the phosphogypsum with 10-20% aqueous ammonium hydroxide and subsequent washing of water. This purified gypsum was suitable for use in cement manufacture, and the cement produced had properties similar to cement containing natural gypsum.

#### 3.5.4 Wet sieving

Singh *et al.* (1996) adopted a method which consists of wet sieving the sample through a 300  $\mu\text{m}$  sieve. The results have shown that the amount impurities were significantly reduced in the finer fraction that passed through the sieve, as against to the coarser fraction (10-15% of the sample) that retained over the sieve. The amount of phosphorous impurities contained in the phosphogypsum sample was reduced from 1.28% before sieving, to 0.41% in the finer fraction after sieving.

Al-Jabbari *et al.* (1988) washed the phosphogypsum with water using a 100  $\mu\text{m}$  sieve. They then burned the phosphogypsum and added accelerators (for example calcium hydroxide) to the calcined phosphogypsum in order to improve the setting time and compressive strength of the produced material. The purified phosphogypsum was chemically analysed, and the results indicated that the best and cheapest method of purification was through washing with water using a 100  $\mu\text{m}$  sieve followed by neutralization with calcium hydroxide.

## Chapter 4 Experimental techniques applied in this study

### 4.1 Thermogravimetry (TG)

Thermogravimetry is a group of techniques in which the mass of a sample is measured as a function of temperature or time, while subjected to a controlled heating programme in a specified atmosphere. The technique has a wide range of applications, of which some important ones are (Dodd *et al*, 1987; Haines, 1995):

- investigation of phase changes e.g. a liquid changes to a gas
- characterisation of materials
- to evaluate the thermal stability of materials
- to investigate thermal decomposition
- qualitative analysis
- quantitative analysis
- used in quality control to do purity assessment
- to investigate the chemical reactivity, e.g. the influence of addition of a catalyst
- kinetic studies

The sources of error during thermogravimetry and optimum operating conditions of the technique will be discussed in Chapter 4.3.6 and 4.3.7.

### 4.2 Differential Scanning Calorimetry (DSC)

DSC is a technique in which the difference in heat flow to a sample and to a reference is monitored against temperature or time while the temperature of the sample, in a specified atmosphere, is programmed (Haines, 1995).

Thermal events in the sample appear as deviations from the DSC baseline curve, in either endothermic or exothermic direction. Because of the absorption of more power by a sample,



endothermic responses are usually represented as positive (above the baseline). The melting of well-known material, such as indium, is used to calibrate the instruments.

Two types of DSC are recognised, namely power-compensated DSC and heat-flux DSC. In the first type, the sample and reference are heated by separate, individual heaters, and the temperature difference is kept close to zero while the difference in electrical power needed to maintain equal temperatures are measured (Haines, 1995). Heat-flux DSC was used during this study. The sample and reference are heated from the same source and the temperature difference between them is measured. This signal is then converted to a power difference.

#### 4.2.1 Heat-flux DSC

In heat-flux DSC the thermocouples are positioned beneath the sample and reference pans. A shift in the baseline is not influenced by any property of the sample, but by a change in the specific heat capacity of the sample. It is also dependent on the characteristics of the sample holders. Therefore, the apparatus has to be calibrated by using known standard materials.

The area under the DSC peak is directly proportional to the heat of the reaction by the following equation (Haines, 1995):

$$\Delta H = K \int \Delta T dt = K \cdot (\text{peak area}) \quad (4.1)$$

where  $\Delta H$  = heat of the reaction  
 $\Delta T$  = temperature difference between the sample and the reference  
 $t$  = time  
 $K$  = the calibration constant that converts peak area into joules, and is a thermal factor that may vary with temperature

#### 4.2.2 Calibration of the DSC apparatus

The DSC apparatus must be calibrated for calorimetric sensitivity. Usually the melting points of pure metals are used, and because the value of the calibration constant ( $K$ ) is markedly dependent upon temperature, calibrations have to be carried out over the full operating range of the instrument. ICTAC (International Confederation for Thermal Analysis and Calorimetry) has approved a set of standard substances that can be used for the calibration (Haines, 1995). The calibration factor is specific to a particular instrument under one set of operating conditions, since the geometry and thermal conductivity of the sample and reference system contribute to the value of the calibration factor.

The integrated peak area of a pure substance may be used to calculate the calorimetric sensitivity constant:

$$K_T = \Delta H_s \cdot \frac{m_s}{A_s} \quad (4.2)$$

where

$\Delta H_s$	=	enthalpy of fusion of the calibration substance
$m_s$	=	sample mass of the calibration substance
$A_s$	=	peak area
$K_T$	=	calorimetric sensitivity constant at temperature T

#### 4.2.3 Applications of DSC

The DSC curve can be used to estimate the purity of samples. Melting endotherms are very sharp if the substance is pure, but are broader for impure substances. Physical changes and measurements can be investigated, such as melting, phase changes, enthalpies of vaporization and of sublimation, heat capacity, glass transitions and thermal conductivity. The path of chemical reactions such as dehydration, decompositions, polymer curing, glass formation and oxidative attack can also be followed (Brown, 1988; Charsley and Warrington, 1992; Dodd *et al*, 1987; Haines, 1995).

### 4.3 Simultaneous TG-DSC

Thermal methods sometimes require complementary techniques for a more comprehensive understanding of the process occurring. In simultaneous TG-DSC systems, the designs are based on a thermobalance which is modified to weigh both the sample and the reference and to measure the temperature of each. The sample and reference are contained in crucibles, which are located on a heat-flux DSC plate. Therefore, both techniques are sensed simultaneously. This technique saves time and also gives the results for two or more techniques under precisely the same experimental conditions. A shortcoming of this technique is that the sensitivity of both techniques is reduced on combination, because of compromises in instrumental design (Charsley and Warrington, 1992).

The instrument used during this study was the NETZSCH-STA 409 EP, which enables the simultaneous execution of Thermogravimetry (TG) and Heat-flux-Differential Scanning Calorimetry (DSC). The instrument can measure in a temperature range of 20°C up to 1400°C. Both measuring techniques are applied simultaneously and on the same sample. By using the software, developed by NETZSCH-Gerätebau GmbH, characteristic temperatures, enthalpy values, and mass changes were obtained. A simplified diagram of the NETZSCH-STA 409 EP is given in Figure 4.1.

#### 4.3.1 The balance

The STA 409 contains a highly sensitive analytical balance that works according to the principle of the substitution beam balance. The change in mass occurring during a reaction, causes deviation of the weighing beam, which is registered as a change in voltage. The presence of oxidising or corrosive gases near the balance mechanism is undesirable. Therefore, the balance enclosure is often purged with an inert gas.

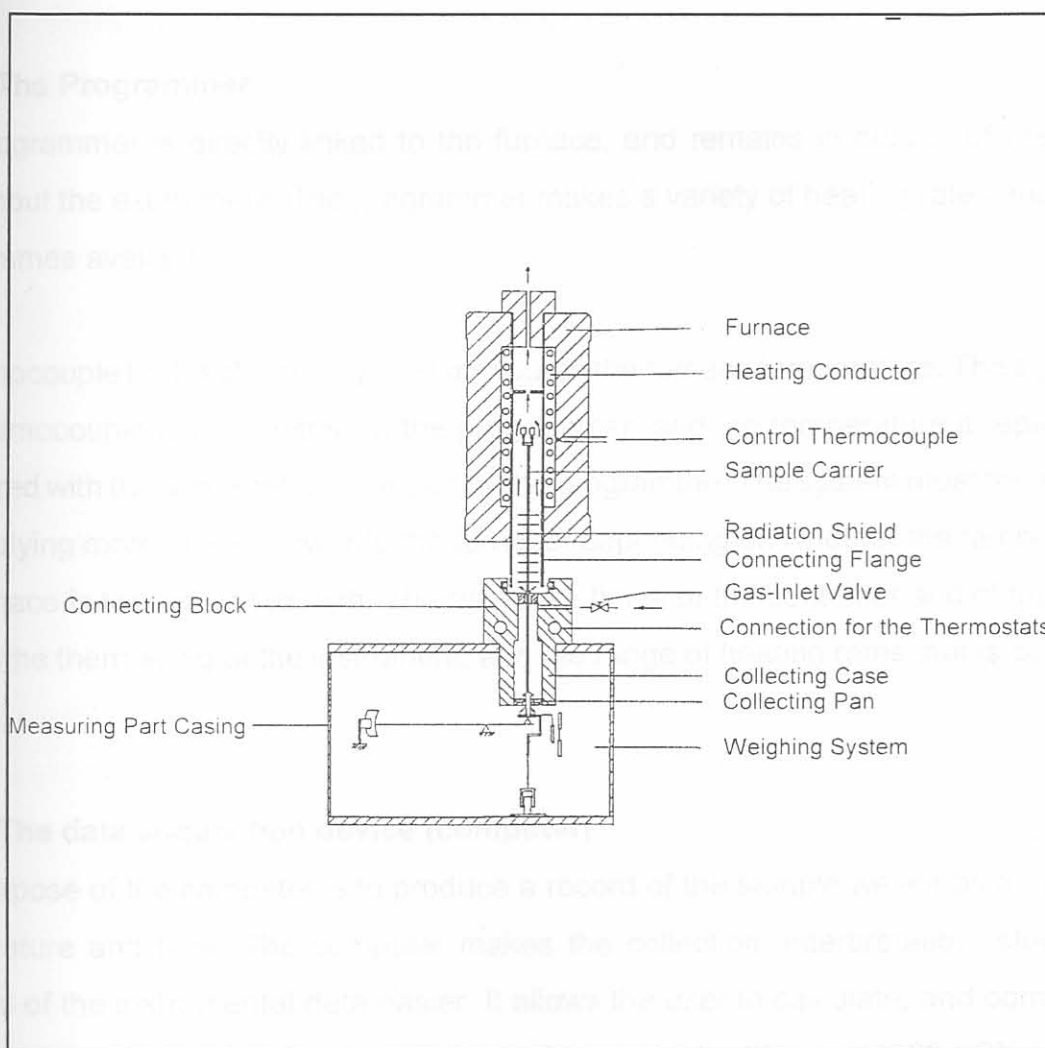
#### 4.3.2 Sample carrier system

The sample carrier system is connected to the balance. It contains the thermocouples (Pt10%Rh-Pt) to measure the temperature and the temperature difference between the sample and reference sides. The sample and reference materials are contained in



crucibles, located on and supported by a heat-flux DSC plate. Below the crucibles, the thermocouple wires of the temperature sensors go through the alumina support rod to the balance and detector systems.

**Figure 4.1 The structure of the measuring part of the Netzsch-STA 409 EP (Netzsch-Gerätebau)**



### 4.3.3 The furnace

Maximum temperatures of approximately 1400°C are produced by the tube furnace of the STA 409 EP, which is heated with a resistance coil. The furnace should be capable of reaching temperatures 100 to 200°C above the maximum desired working temperature. If operated in the presence of a corrosive atmosphere the linings of the furnace must consist

of a material that can resist chemical attack.

The uniform heating zone must be of reasonable length to provide a uniform sample temperature, and the furnace should not affect the balance mechanism through radiation or convection. Inclusion of radiation shields and convection baffles reduces transfer of heat to the balance mechanism.

#### 4.3.4 The Programmer

The programmer is directly linked to the furnace, and remains in control of the furnace throughout the experiment. The programmer makes a variety of heating rates and thermal programmes available.

A thermocouple that is chemically inert measures the furnace temperature. The signal from the thermocouple is transmitted to the programmer, and the temperature it represents is compared with the temperature required by the programme. The system must then respond by supplying more or less power to the furnace, depending on whether the temperature of the furnace is too low or too high. The response times of the controller and of the furnace govern the thermal lag of the instrument, and the range of heating rates that is achievable.

#### 4.3.5 The data acquisition device (computer)

The purpose of the computer is to produce a record of the sample weight as a function of temperature and time. The computer makes the collection, interpretation, storage and retrieval of the instrumental data easier. It allows the user to calculate, and compare, the results of an experiment more easily and accurately (Brown, 1988; Charsley and Warrington, 1992; Dodd *et al*, 1987; Haines, 1995; Wunderlich, 1990).

#### 4.3.6 Sources of error during thermogravimetry

Errors in thermogravimetric measurements can lead to inaccuracies in the recorded temperature and mass data. Some sources of error are discussed below (Dodd *et al*, 1987).

The buoyancy effect of the sample container refers to the apparent mass gain that can occur when an empty, and thermally inert crucible is heated. This effect is due to thermomolecular flow that can occur when the balance is operating at low pressure. As the sample is heated, the density of the atmosphere around the sample decreases, and the upthrust, caused by the gas, will decrease. The crucible will therefore show an apparent gain in measured mass.

Running a "blank" buoyancy curve with an empty crucible can compensate for this effect over the significant temperature range. This curve is then subtracted from the experimental curve for a specific sample. The use of very small samples and crucibles will also reduce this effect.

Gas flowing over and around the sample container may cause turbulence and the heat from the oven can cause convection effects. This can also be reduced by smaller sample masses.

The actual temperature of the sample will usually lag behind the temperature recorded by the thermocouple. This thermal lag is related to several factors that include the time in which a weight change is recorded, the heating rate, the gas flow, the geometry of the sample container, and the thermal conductivity of the sample. The heat of the reaction will also affect the sample temperature. An endothermic reaction at a specific temperature will cause a larger thermal lag, while an exothermic reaction will have the opposite effect. However, these effects are of very small magnitude.

Other factors that must be considered to cause errors in thermogravimetry are:

- condensation on the balance suspension
- reaction between the sample and crucible
- random fluctuations of the balance system
- electrostatic effects on the balance mechanism
- induction effects from the furnace
- the environment of the thermobalance

Well-designed thermobalances usually exclude most of these factors causing errors.



### 4.3.7 Optimum operating conditions

Many factors affect the nature, accuracy, and precision of experimental results. Comparison of samples can only be made when their curves are run under the same conditions, or when differences are clearly stated.

Large sample masses cause poor resolution in thermogravimetric curves. This is due to the significant temperature gradient within a large sample and the greater difficulty of volatile products to escape from a large sample. These factors can lead to irreproducibility, and therefore the sample mass should be kept as small as possible, especially for kinetic studies. Sample masses of less than 50 mg are normally used.

The sample must preferably be in powdered form, and should be spread uniformly in the sample container. The particle size must also be considered, because the thermal properties of powders differ from those of the bulk material (Brown, 1988; Dodd *et al*, 1987; Haines, 1995).

Thermogravimetric measurements can be done in a static or dynamic atmosphere. The transfer of heat and chemistry of the sample will depend upon the surrounding atmosphere. Even if there is no reaction between the sample and the atmosphere, the heat transfer by the gas may affect the results. Changing the surrounding atmosphere can alter the course of a chemical reaction completely. Usually an inert gas is used, which quickly removes the gaseous products from the sample, but the gas may also be used as a reactant in the reaction.

A flowing gas atmosphere will also reduce condensation of reaction products on the cooler parts of the weighing mechanism. It will flush out corrosive products, reduce secondary reactions, and act as a coolant for the balance system. The flow rate of the gas must also be considered. A very low gas flow will not sweep away reaction products, or act as a heat transfer agent. A very high gas flow can interfere with the balance mechanism or cause turbulence effects (Haines, 1995).

The sample holder should not react chemically with the sample during the experiment. Changing from an aluminium crucible to silica, alumina or platinum may change the heat transfer, because of the different thermal conductivity of these materials. It can also influence the chemistry of a process, for example, if a reaction occurs that can be catalysed by platinum.

The shape of the crucible is important, since a shallow container will allow a more significant exchange of gas between the sample and its gaseous surroundings. A narrow, deep crucible may restrict heat flow (Brown, 1988; Dodd *et al*, 1987; Haines, 1995; Wunderlich, 1990).

Increasing heating rates result in an inhomogeneous temperature distribution in the sample. The thermal lag between the actual temperature of the sample and the recorded temperature will increase with increasing heating rate, and the resolution of the thermogravimetric curve will decrease. Working with the lowest heating rate that is possible for the specific circumstances is best (Brown, 1988; Charsley and Warrington, 1992; Dodd *et al*, 1987; Haines, 1995; Wunderlich, 1990).

## 4.4 X-ray Fluorescence analysis

### 4.4.1 Introduction

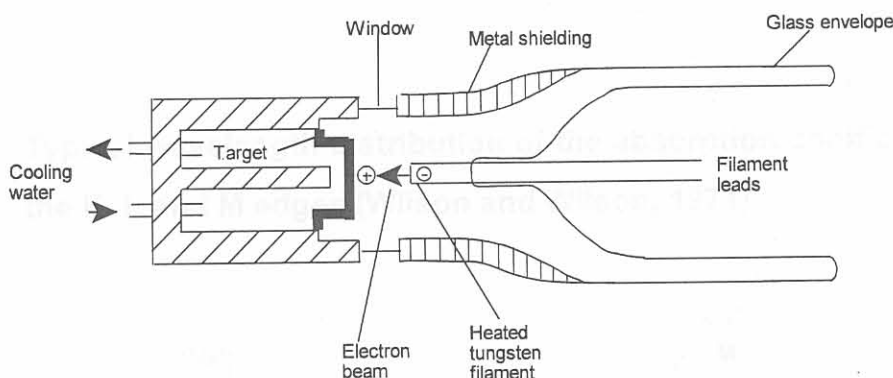
Since the discovery of X-rays in 1895, a variety of X-ray techniques have been developed. These include radiography, X-ray fluorescence analysis, X-ray crystallography, and radiotherapy.

In the devices used to apply these techniques, X-rays are being produced in X-ray tubes. Electrons are produced by an electrically heated tungsten filament, and are then accelerated towards the target by applying a large potential difference. The high speed electrons are stopped by the atoms of the target, resulting in X-rays being produced in all

directions from the surface of the target. Since X-rays are harmful, the tube is partly covered with a heavy absorbing metal such as lead. The X-rays then leave the tube through a window, consisting of a light metal such as aluminium or beryllium.

Only a fraction of the energy supplied to the tube is converted to X-rays, most is converted into heat. To prevent the target from melting, it is cooled by running water. The target material must be made of a high melting material which has good thermal conductivity and for the production of high-intensity X-rays, the target element should have a high atomic number. Pure transition metals such as molybdenum, wolfram, copper and chromium are typical target materials. Figure 4.2 shows a schematic diagram of an X-ray tube.

**Figure 4.2 Schematic diagram of an X-ray tube (Whiston, 1987)**



Characteristic X-rays are produced when high speed electrons remove inner K, L or M electrons from target atoms, and outer electrons fill the vacancies. The continuous spectrum arises from the conversion of the electron's kinetic energy to radiant energy on impact.

All matter absorbs X-ray to a certain extent. An X-ray beam of original intensity  $I_0$  becomes reduced to intensity  $I$  on passing through a distance  $\chi$  of absorbing medium of density  $\rho$ .



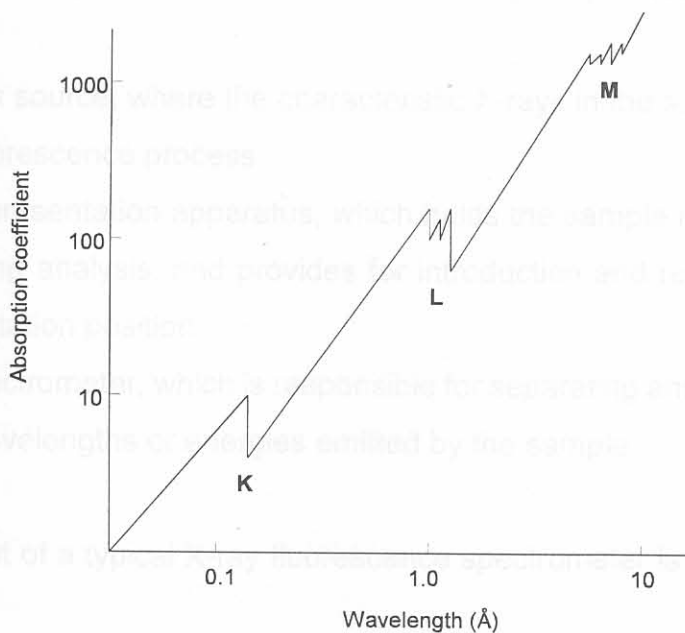
The intensities are related by the equation (Whiston, 1987):

$$I = I_0 e^{-\mu_m \rho x} \quad (4.3)$$

where  $\mu_m$  is the mass absorption coefficient, which is characteristic of a particular medium.

The typical distribution of the mass absorption coefficient against wavelength is shown in Figure 4.3. Mass absorption generally increases with increasing wavelength, but in the graph of  $\mu_m$  versus  $\lambda$ , a number of vertical discontinuities, called absorption edges, is observed. These correspond to the ionisation energies of the K, L and M electrons of the absorbing medium. The X-rays having wavelengths less than these absorption edges have sufficient energy to displace inner electrons resulting in the emission of characteristic radiation called X-ray fluorescence.

**Figure 4.3 Typical wavelength distribution of the absorption coefficient, showing the K, L and M edges (Wilson and Wilson, 1971)**



The planes of atoms in a crystal will only reflect an X-ray beam when the Bragg equation is fulfilled (Whiston, 1987, Wilson and Wilson, 1971):

$$2d \sin \theta = n\lambda \quad (4.4)$$

- where
- d = the interplanar spacing
  - $\theta$  = the angle between the planes and the X-ray beam (Bragg angle)
  - $\lambda$  = the X-ray wavelength
  - n = the order of reflection

#### 4.4.2 Instrumentation

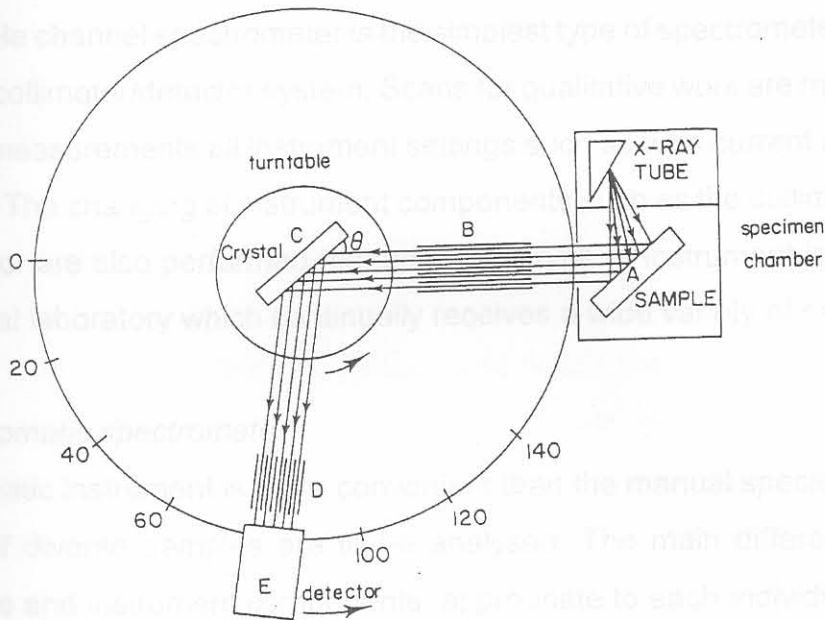
X-ray fluorescence is a rapid, non-destructive, qualitative and quantitative method of determining elements in solids and liquids. In principle, the technique is based on the measurement of wavelengths and intensities of X-rays emitted by a sample, when excited by the rays from a primary X-ray tube. Since the beam doesn't penetrate very far into the specimen, it is essentially a surface technique (Whiston, 1987).

An X-ray fluorescence spectrometer consists of three principal sections (Jenkins *et al*, 1981):

- the excitation source, where the characteristic X-rays in the sample are excited via the X-ray fluorescence process
- the sample presentation apparatus, which holds the sample in a precisely defined position during analysis, and provides for introduction and removal of the sample from the excitation position
- the X-ray spectrometer, which is responsible for separating and counting the X-rays of various wavelengths or energies emitted by the sample

The simplified layout of a typical X-ray fluorescence spectrometer is shown in Figure 4.4.

**Figure 4.4 Simplified layout of a typical wavelength dispersive spectrometer (Whiston, 1987)**



A primary X-ray beam irradiates the sample (A) causing it to fluoresce. Each element will emit its own characteristic X-radiation. Part of the radiation is collimated by a system of slits (B) onto an analysing crystal (C). Since a number of different crystals are necessary to cover the full wavelength range of the spectrometer, a multi-position crystal changer is usually incorporated. This usually consists of a turntable arrangement holding up to six crystals. The particular crystal in use is mounted on a turntable which can be rotated by a motor.

As the crystal rotates, so the angle ( $\theta$ ) presented to the fluorescent rays changes. Whenever the Bragg equation is fulfilled for a particular X-ray wavelength, this part of the beam is reflected by the crystal. The reflected beam passes through a set of collimating slits (D) and enters the detector (E). The detector and crystal table are connected in such a way that they always rotate together. Furthermore, they are geared so that when the crystal rotates through an angle  $\theta$ , the detector rotates through  $2\theta$ . This results in the detector always being in the correct position to receive any rays reflected by the crystal.



There are four basic types of XRF instruments. These will be discussed shortly below.

(a) *Manual spectrometer*

The manual single channel spectrometer is the simplest type of spectrometer, and consists of a one crystal/collimator/detector system. Scans for qualitative work are motor driven, but for quantitative measurements all instrument settings such as tube current and voltage are made manually. The changing of instrument components such as the collimator, analysing crystal or detector are also performed manually. This type of instrument is sufficient for a general analytical laboratory which continually receives a wide variety of samples.

(b) *Semi-automatic spectrometer*

The semi-automatic instrument is more convenient than the manual spectrometer when a large number of diverse samples are to be analysed. The main difference is that the machine settings and instrument components, appropriate to each individual sample, are selected by a simple operation.

(c) *Automatic sequential spectrometer*

This instrument is adequate for routine analysis of large numbers of similar samples. The spectrometer is usually interfaced with a computer which has been programmed to control the entire sequence of the analysis. This involves control of samples, changing of settings and of instrument components applicable to each element of interest in each sample, moving the spectrometer from one  $2\theta$  setting to another, collection of intensity data, and calculation of element concentration.

(d) *Simultaneous automatic spectrometer*

This type of spectrometer is also suitable for the routine analysis of a large number of samples. The instrument consists of up to 26 single channel instruments situated around the X-ray tube and samples. Each channel is fixed at the  $2\theta$  angle of a specific element, and each channel is fitted with instrument components most suited for that element. The intensities are collected from each channel and fed to a computer for calculation of element concentration.

This type of instrument has several advantages when compared to the automatic sequential spectrometer. It has no moving parts and much time is saved by measuring the intensities simultaneously rather than sequentially. This makes the simultaneous spectrometer ideal for on-line analysis for production control. Another advantage lies in trace analysis, where intensities are likely to be very weak. Higher sensitivity can be obtained by having two or more output channels set on the same element line and combining their outputs.

The simultaneous spectrometer also has disadvantages when compared to a sequential spectrometer. The automatic spectrometer is more compact than the simultaneous instrument, and has fewer instrument components which means that it should be less expensive. The sequential spectrometer is more flexible in its use, since it can be programmed to detect any element, while simultaneous spectrometers are constructed to detect specific elements. Sequential instruments can be programmed to use machine parameters which are optimised for each element, with simultaneous instruments certain machine parameters are fixed and may not be optimum for all the elements being analysed.

#### **4.4.3 Qualitative analysis by XRF**

For qualitative analysis, the crystal is rotated so that all angles between about  $15^\circ$  and  $145^\circ$  are presented to the X-ray beam. Detected X-rays are amplified and recorded as a series of peaks. A scale of  $2\theta$  is automatically recorded, and elements are identified from their  $2\theta$  values in conjunction with an appropriate set of tables.

For a particular analysing crystal, the line-to- $2\theta$  tables list the wavelength and  $2\theta$  values of the characteristic elements that can be dispersed by the crystal. The data are listed in order of increasing atom number.  $2\theta$ -to-line tables list similar data, but in increasing magnitude of  $2\theta$ . The interpretation of an XRF trace involves the reading off the  $2\theta$  values of the peaks and then consulting  $2\theta$ -to-line tables, applicable to the analysing crystal used.



#### 4.4.4 Quantitative analysis by XRF

For quantitative analysis, the crystal remains stationary, set at the appropriate angle to reflect a particular element's radiation. The recorded intensity is related to the element's concentration in the sample.

There is usually not a linear relationship between analyte line intensity and concentration, because of matrix effects, which can arise from absorption and enhancement. Spectral interference can arise from overlap of analyte line with either a matrix line or an X-ray tube line. This may be overcome by using a different analyte line, by using a crystal with a higher dispersion, by using filters, or by reducing the voltage or current of the X-ray tube.

The three most common ways of overcoming matrix effects include the use of calibration curves, making standard additions, and correcting mathematically. Calibration curves are suitable to do routine analyses of samples where standards are readily available. Standard additions are applicable to infrequent analyses where standards are not available, while mathematical corrections are ideal for the routine analysis of large numbers of samples.

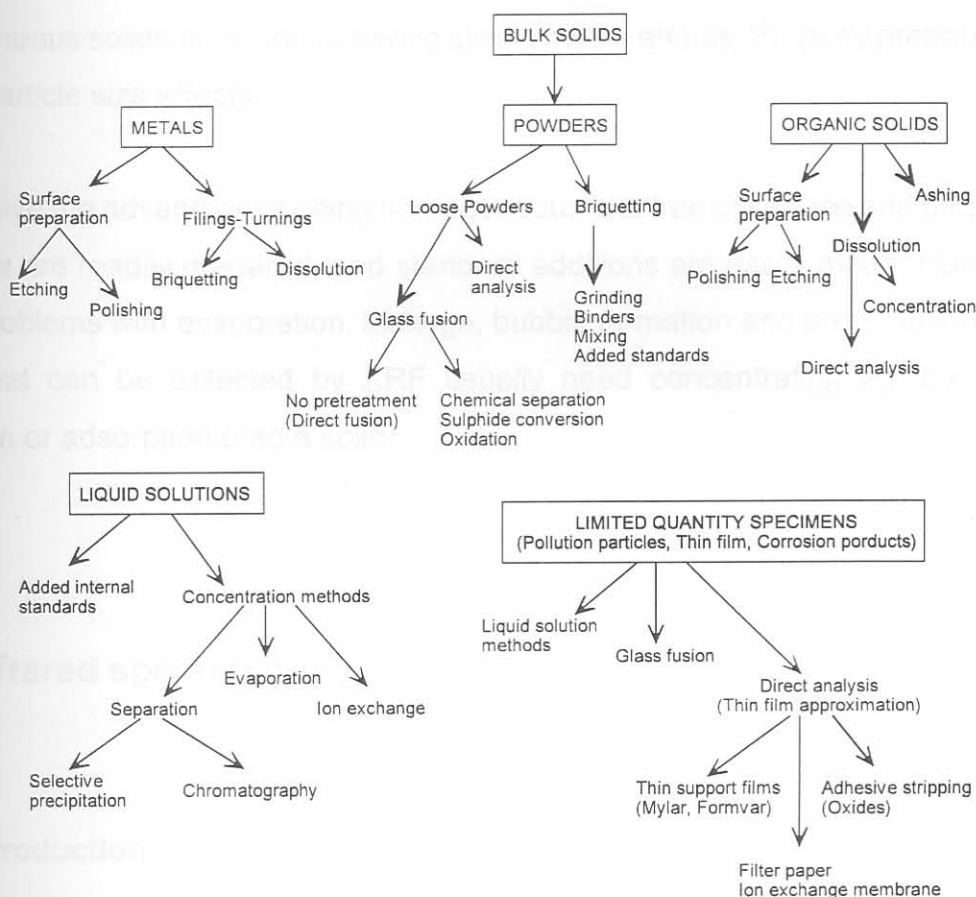
#### 4.4.5 Sample preparation for XRF analysis

For qualitative analysis, the only prerequisite is usually that the sample fits into the sample holder. However, for quantitative work sample preparation may be necessary, particularly for solids where the analyte line intensity can be dependent on surface roughness, particle shape, particle size, size distribution and packing density (Jenkins, 1981 *et al*; Whiston, 1987).

The guiding principles for sample preparation techniques are reproducibility, accuracy, simplicity, low cost, and rapidity of preparation. A broad outline of different sample preparation procedures is shown in Figure 4.5. The details of some of these techniques are discussed below.



**Figure 4.5 A summary of sample preparation procedures for XRF analysis (Jenkins *et al*, 1981)**



Bulk solids such as metals and ceramics should preferably be in the form of a small cylinder about 5 cm in diameter. To eliminate the surface texture effects, one surface should be smoothed to a finish of about 50  $\mu\text{m}$ . This can be achieved by making use of graded papers, machining, electropolishing and spark planing. The standards and unknown samples should have an identical surface finish. If standards are not available, the solid may be transformed into a powder or to a solution, to facilitate standard additions (Whiston, 1987).

To ensure homogeneity and to eliminate particle size effects, powdered samples are usually milled to a fineness of about 300 mesh. They may then be loosely packed into a cell, compacted into a pellet (with or without binder), or supported on a substrate such as filter paper, Scotch tape or Mylar film. Standards and unknowns should be prepared under

identical conditions.

Fusion with borax or with lithium tetraborate to produce a “glass” disc may be useful for heterogeneous solids or for solids having strong matrix effects. Properly prepared discs will give no particle size effects.

Liquids have the advantage of being homogeneous and free of surface and particle effects. Standards are readily prepared, and standard additions are easily made. However, there can be problems with evaporation, leakage, bubble formation and precipitation of analyte. Gases that can be detected by XRF usually need concentrating eg. by dissolution, absorption or adsorption onto a solid.

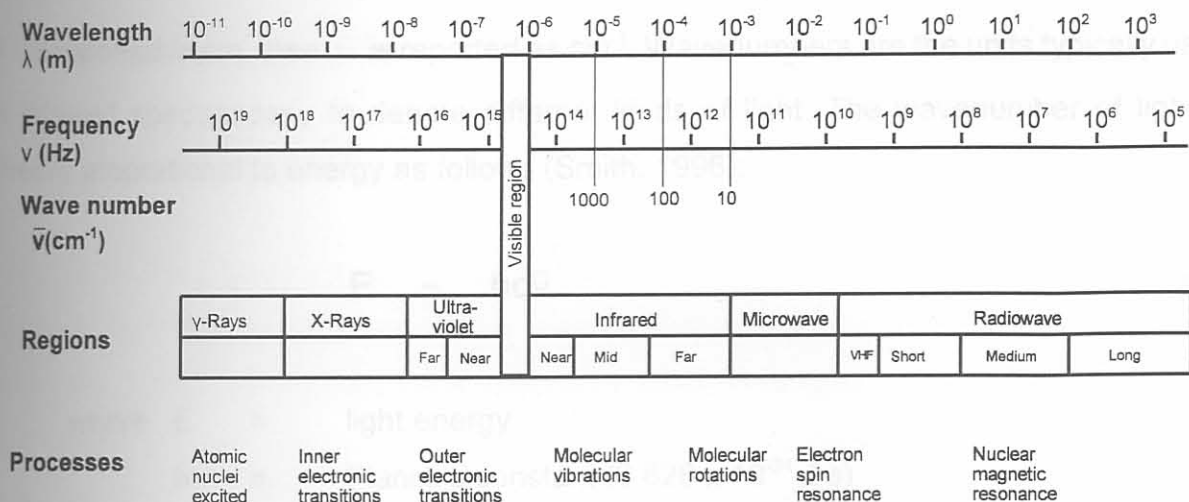
## 4.5 Infrared spectroscopy

### 4.5.1 Introduction

Infrared spectroscopy is the investigation of the interaction between infrared radiation and matter. When a substance is exposed to infrared radiation, the amount of radiation absorbed is different for components of the radiation having different wavenumbers, which means that the absorption is selective. The IR spectrum is obtained by recording passing radiation through a sample and determining what fraction of the incident radiation is absorbed at a particular energy. The energy at which any peak in an absorption spectrum appears, corresponds to the frequency of a vibration of a part of a sample molecule (Stuart, 1996; Svehla, 1976).

When light constituted of components of various wavelengths is resolved according to wavelength with a monochromator, a spectrum of electromagnetic radiation is obtained. The division of the electromagnetic spectrum into its various regions is shown in Figure 4.6.

Figure 4.6 The electromagnetic spectrum



The electromagnetic spectrum and the varied interactions between these radiations and many forms of matter can either be considered in terms of classical or quantum theories. The nature of the various radiations shown in Figure 4.6 have been interpreted by Maxwell's classical theory of electro- and magnetodynamics, consequently the term of electromagnetic radiation.

According to this theory, light is composed of electric and magnetic waves. These two waves are in planes perpendicular to each other, and the light wave moves through space in a plane perpendicular to the planes containing the electric and magnetic waves. It is the electric part of light, called the electric vector, that interacts with molecules. The amplitude of the electric vector changes with time, and it has the form of a sine wave. The wavelength ( $\lambda$ ) of the light wave is the distance between adjacent crests or troughs in the sine wave. The wavenumber ( $\bar{\nu}$ ) of a light wave is the number of waves in a length of one centimetre, and is given by the following relationship (Smith, 1996; Stuart, 1996)

$$\bar{\nu} = \frac{1}{\lambda} = \frac{\nu}{c} \quad (4.5)$$



where  $c$  = the speed of light ( $2.997925 \times 10^8 \text{ m s}^{-1}$ )  
 $\nu$  = the frequency (number of cycles per second)

If  $\lambda$  is reported in cm, then  $\bar{\nu}$  is reported as  $\text{cm}^{-1}$ . Wavenumbers are the units typically used in infrared spectroscopy to denote different kinds of light. The wavenumber of light is directly proportional to energy as follows (Smith, 1996):

$$E = hc\bar{\nu} \quad (4.6)$$

where  $E$  = light energy  
 $h$  = Planck's constant ( $6.626 \times 10^{-34} \text{ J s}$ )  
 $\bar{\nu}$  = wavenumber

This indicates that high wavenumber light has more energy than low wavenumber light. Most FT-IR instruments operate in the wavenumber range between  $4000$  and  $400 \text{ cm}^{-1}$ , which is defined as mid-infrared radiation.

According to the quantum theory, processes of electronic change (including vibration and rotation) can be represented in terms of quantised discrete energy levels  $E_0, E_1, E_2$  etc. Each atom or molecule in a system must exist in one or other of these levels. In a large group of molecules there will be a distribution of all atoms among these various energy levels. These energy levels are a function of the quantum number and a parameter associated with the particular atomic or molecular process associated with that state. Whenever a molecule interacts with radiation, a quantum of energy (or a photon) is either emitted or absorbed. In each case the energy of the quantum of radiation must exactly fit the energy gap  $E_1 - E_0, E_2 - E_1$ , etc. The energy of the quantum is related to the frequency by the following (Stuart, 1996):

$$\Delta E = h\nu \quad (4.7)$$

Therefore, the frequency of emission or absorption of radiation for a transition between the energy states  $E_0$  and  $E_1$  is given by the following relationship:

$$\nu = \frac{E_1 - E_0}{h} \quad (4.8)$$

When infrared radiation interacts with matter, it can be absorbed, causing the chemical bonds in the material to vibrate. The presence of chemical bonds in a material is a necessary condition for infrared absorbance to occur. Functional groups within molecules tend to absorb infrared radiation in the same wavenumber range, regardless of the structure of the rest of the molecule that the functional group is in. This means there is a correlation between the wavenumbers at which a molecule absorbs infrared radiation and its structure. This correlation allows the structure of unknown molecules to be identified from the molecule's infrared spectrum (Smith, 1996).

Molecules are considered as rigid ball-like atoms, connected by bonds with spring-like characteristics. The absorption of infrared radiation sets the molecule into vibrational or rotational motion, or a combination of the two. Similarly, emission of infrared radiation is accompanied by a decrease of the vibration or rotation. In order for the infrared radiation to be absorbed, the vibration frequency of the molecule must be identical to the frequency of radiation.

A molecule having  $N$  atoms can undergo  $3N - 6$  fundamental modes of vibration, or  $3N - 5$  if it is a linear molecule. Each of these fundamental modes has associated with it a ground-state energy:

$$E = \frac{1}{2} h\nu \quad (4.9)$$

This means that the absorption of energy is quantised. In addition, higher frequencies can be excited with energy

$$E = (n + \frac{1}{2})h\nu \quad n = 1, 2, 3, \dots \quad (4.10)$$

The spectroscopist observes the frequencies of absorbed radiation and assigns the corresponding molecular vibrational frequencies to particular modes of oscillation. He can then use the known geometry and atomic masses with the observed vibrational frequencies to calculate the force constant ( $k$ ), or stiffness, of the interatomic bonds. The reduced mass ( $\mu$ ) is defined as

$$\mu = \frac{m_1 m_2}{m_1 + m_2} \quad (4.11)$$

where  $m_1$  and  $m_2$  are the masses of the atoms at the end of the bond. The equation relating the force constant to the reduced mass and wavenumber values for bond vibrational frequencies is as follows (Stuart, 1996):

$$\bar{\nu} = \frac{1}{2\pi c} \sqrt{\frac{k}{\mu}} \quad (4.12)$$

where  $c$  is the speed of light.

The rotational energy levels of a molecule are also restricted to certain discrete values,

$$E = BJ(J + 1) \quad J = 0, 1, 2, \dots \quad (4.13)$$

where  $B$  is a constant determined by the moment of inertia of the molecule about one of its axis, and  $J$  is the rotational quantum number. The spacing of these energy levels increases with increasing values of  $J$ . Each vibrational state of a gaseous molecule is accompanied by a set of rotational levels, which means that each vibrational band is a complex band containing many possible rotational transitions. The selection rules for rotational transitions depend on the geometry of the molecule and the particular mode in question (Stewart, 1970).



The infrared spectra of polyatomic molecules are quite complex, but the spectrum of a particular chemical bond is a unique characteristic of that compound. It reflects the geometry, bond strength, and atomic masses of the substance. This makes infrared spectroscopy important in the identification of unknown compounds.

#### 4.5.2 Instrumentation for Fourier-Transform Infrared (FT-IR) spectroscopy

Fourier-transform infrared spectroscopy is based on the interference of radiation between two beams to yield an interferogram, which is a signal produced as a function of the change of pathlength between the two beams. The distance and frequency are interchangeable by the mathematical method of Fourier transformation.

The basic components of an FT-IR spectrometer are shown schematically in Figure 4.7. The radiation emerging from the source is passed to the sample through an interferometer, before reaching a detector. After high-frequency contributions have been eliminated by a filter, the signal is amplified and the data is converted to a digital form by an analog-to-digital converter. It is then transferred to the computer, for Fourier transformation to be carried out.

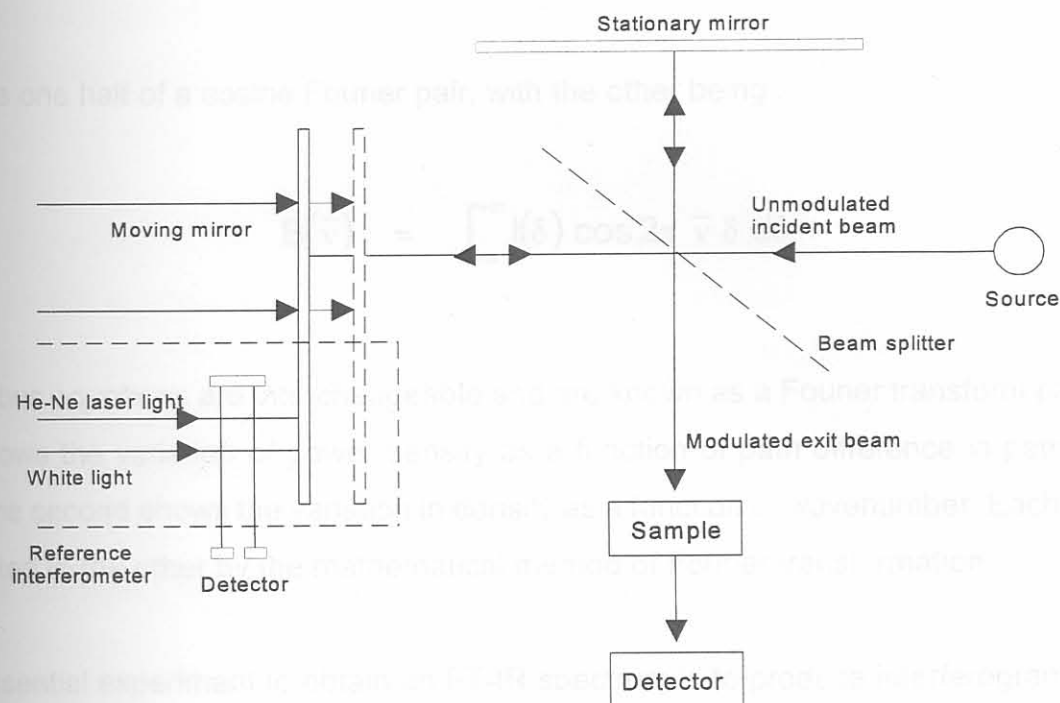
Figure 4.7 The basic components of a FT-IR spectrometer (Stuart, 1996)



The most conventional interferometer used is a Michelson interferometer. A simplified schematic layout is shown in Figure 4.8. It consists of two perpendicular plane mirrors, one of which travel in a direction perpendicular to the plane. A semi-reflecting film, the beamsplitter, crosses the planes of these two mirrors. The beamsplitter material has to be chosen according to the region to be examined. Materials such as germanium or iron oxide are coated on to an infrared-transparent substrate such as potassium bromide or caesium

iodide to produce beamsplitters for the mid- or near-infrared regions. Thin organic films, such as poly(ethylene terephthalate), are used in the far-infrared region.

Figure 4.8 A Michelson interferometer (Stuart, 1996)



If a collimated beam of monochromatic radiation of wavelength  $\lambda$  is passed into a perfect beam splitter, 50% of the incident radiation will be passed to the stationary mirror and 50% will be transmitted to the movable mirror, which can move along the axis shown in Figure 4.8. After each beam has been reflected back to the beamsplitter, they are again partially reflected and partially transmitted. Thus, 50% of the beam reflected from the stationary mirror is transmitted through the beamsplitter to sample and then to the detector, while the other 50% is reflected back in the direction of the source. The beam which emerges from the interferometer at  $90^\circ$  to the input beam is called the transmitted beam, and is the beam which is detected in FT-IR spectroscopy (Griffiths, 1975).

For more sensitive work, a mercury cadmium telluride (MCT) detector can be used, which requires that the detector has to be cooled by liquid nitrogen.

The intensity falling on the detector,  $I(\delta)$ , can be related to the spectral power density, given as  $B(\bar{\nu})$ , at a particular wavenumber ( $\bar{\nu}$ ), as follows (Stuart, 1996):

$$I(\delta) = \int_0^{+\infty} B(\bar{\nu}) \cos 2\pi \bar{\nu} \delta \, d\bar{\nu} \quad (4.14)$$

which is one half of a cosine Fourier pair, with the other being:

$$B(\bar{\nu}) = \int_{-\infty}^{+\infty} I(\delta) \cos 2\pi \bar{\nu} \delta \, d\delta \quad (4.15)$$

These two equations are interchangeable and are known as a Fourier transform pair. The first shows the variation of power density as a function of path difference in pathlength, while the second shows the variation in density as a function of wavenumber. Each can be converted to the other by the mathematical method of Fourier transformation.

The essential experiment to obtain an FT-IR spectrum is to produce interferograms, both with and without a sample in the beam, and then transform these interferograms into spectra of the source with and without sample absorptions.

FT-IR spectrometers use a Nernst or Globar source for infrared emission in the mid-infrared region. The Globar source is constructed of silicon carbide, while the Nernst filament is a mixture of the oxides of zirconium, yttrium and erbium.

A detector must have adequate sensitivity to the radiation arriving from the sample over the whole spectral region required. There are two types of detectors which are generally used. The normal detector for routine use is a pyroelectric device, which incorporates deuterium tryglycine sulphate (DTGS) in a temperature-resistant alkali halide window. For more sensitive work, a mercury cadmium telluride (MCT) detector can be used, which requires that the detector has to be cooled by liquid nitrogen.



The moving mirror is the most crucial component of the interferometer, and produces an optical path difference between the two arms of the interferometer. It is either moved at a constant velocity, or is held at equidistant points for fixed short periods and is rapidly stepping between these points. It has to be accurately aligned and must be capable of scanning two distances so that the path difference corresponds to a known value. A number of factors associated with the moving mirror needs to be considered when calculating an infrared spectrum (Stuart, 1996).

### 4.5.3 Sampling

It is possible to analyse samples in liquid, solid or gaseous form by FT-IR. Gaseous samples are examined by using gas cells. Liquid samples can be analysed in fixed-pathlength sealed cells, which are particularly useful for volatile liquids. These cells cannot be taken apart for cleaning. Semi-permanent cells can also be used, and are demountable so that the windows can be cleaned. An important consideration in the choice of infrared cells is the type of window material. The material must be transparent to the incident infrared radiation, and therefore alkali halides are normally used (Stewart, 1970; Stuart, 1996).

Liquid films also provide a quick method for examining liquid samples. A drop of liquid is placed between two infrared plates, which are then mounted in a cell holder. However, a common problem encountered in obtaining good quality spectra from liquid films is sample volatility. The recorded spectrum progressively becomes weaker due to evaporation which takes place during the recording period.

There are three methods of examining solid samples in infrared spectroscopy, which are alkali halide discs, mulls and films. The use of alkali halide discs involves the mixing of a few milligrams of solid sample with 100 - 200 mg of a dry alkali halide powder (normally KBr). The mixture is then ground with a mortar and pestle and subjected to a pressure of approximately  $1.58 \times 10^5 \text{ kg cm}^{-2}$ , in an evacuated die. This sinters the mixture and produces a clear transparent disc, which is used in the spectrometer (Stewart, 1970).

When using a mull for determining an infrared spectrum, about 50 mg of the solid sample is ground and then suspended in 1 - 2 drops of a mulling agent. This is followed by further grinding until a smooth paste is obtained. The most common mulling agent is Nujol (liquid paraffin).

Films can be produced by either solvent casting or by melt casting. In solvent casting the solid sample is dissolved in an appropriate solvent, at a concentration which depends on the required film thickness. The solution is then poured on to a levelled glass plate and spread to a uniform thickness. The solvent is evaporated in an oven, and once dry, the film can be stripped from the plate. Alternatively, it is possible to cast a film straight on to the infrared window to be used. Solid samples which melt at relatively low temperatures without decomposition can be prepared by melt casting. A film is prepared by hot-pressing the sample in a hydraulic press between heated metal plates (Stuart, 1996).

#### **4.5.4 Interpretation of an infrared spectrum**

In an infrared spectrum, two different types of absorption bands are present. The first type of band is attributable to distinct parts of a molecule, also called group frequencies. The group frequencies are localised at certain regions in the infrared spectrum, and are very useful for the identification of the functional groups of a molecule. The other type of bands are caused by vibrations of the molecule as a whole, and is referred to as skeletal modes. The skeletal frequencies are characteristic for a particular molecule, are not localised, and normally occur below  $1500\text{ cm}^{-1}$  (the region which is also referred to as the fingerprint region) (van der Maas, 1969).

The interpretation of a spectrum will have to start with the identification of the localised group frequencies. A functional group can give rise to none, one, or more absorption bands, depending on the nature of the group. Group regions can overlap for different functional groups. Previously obtained data, which indicates the regions where a certain functional group will absorb radiation, are tabulated in tables and correlation charts. This information is used to interpret an obtained infrared spectrum. The intensities and shape of the bands can also provide additional information (George and McIntyre, 1987).



## 4.6 BET surface area analysis

Any solid can take up relatively large volumes of condensable gas, and this volume of gas taken up differs from solid to solid. Two important factors that play a role in the volume of gas adsorbed by a solid are the surface area and porosity (or pore volume) of the solid. This means that measurements of adsorption of gases or vapours can be made to obtain information regarding the surface area and pore structure of a solid.

The term adsorption implies the condensation of gases on free surfaces, in contradiction to gaseous absorption where the molecules of gas penetrate into the mass of the absorbing solid. Adsorption is internationally defined as the enrichment (i.e. positive adsorption or simply adsorption) or depletion (i.e. negative adsorption) of one or more components in an interfacial layer (Gregg and Sing, 1982).

The instrument used for the determination of surface area during this study was the Micromeritics FlowSorb 2300. This instrument is designed to rapidly measure the surface area on the molecular level of stable, granulated, and powdered materials. Surface area measurements can be accomplished either by a simplified, single point procedure or by the more conventional multipoint BET technique. The BET equation, that describes the adsorption of a gas upon a solid surface, is given below (Micromeritics Instruction manual, 1985):

$$\frac{\left(\frac{P}{P_0}\right)}{V \left[1 - \left(\frac{P}{P_0}\right)\right]} = \frac{1}{V_m C} + \left(\frac{C-1}{V_m}\right) \left(\frac{P}{P_0}\right) \quad (4.16)$$

- where V = the volume (at standard temperature and pressure, STP) of gas adsorbed at pressure P
- $P_0$  = the saturation pressure which is the vapour pressure of gas at the adsorbing temperature
- $V_m$  = the volume of gas (at STP) required to form an adsorbed monomolecular layer
- C = a constant related to the energy of adsorption



The FlowSorb 2300 measures the surface area of a solid sample, by determining the quantity of a gas that adsorbs on a single layer of molecules on a sample. The surface area of the sample is calculated from this monolayer adsorbed gas volume by using the following equation:

$$S = \frac{V_m AN}{M} \quad (4.17)$$

- where S = the surface area of the sample  
 $V_m$  = the monolayer adsorbed gas volume at STP  
 A = Avogadro's number, which expresses the number of gas molecules in a mole of gas at STP  
 M = the molar volume of the gas  
 N = the area of each adsorbed gas molecule

This adsorption is done at or near the boiling point of the adsorbate gas. Under specific conditions, the area covered by each gas molecule is known within relatively narrow limits. This means that the area of the sample is directly calculated from the number of adsorbed molecules, which is derived from the gas quantity at the prescribed conditions, and the area occupied by each.

The FlowSorb2300 instrument permits the measurement of surface areas by the single point or multipoint procedures. Measurements for this study were performed using the single point determination method. In single point surface area determinations, the constant C of equation 4.16 is typically a relatively large number, i.e.  $C \gg 1$ . This reduces equation 4.16 to

$$V \left[ \frac{\left(\frac{P}{P_0}\right)}{1 - \left(\frac{P}{P_0}\right)} \right] = \frac{1}{V_m} \left[ \left(\frac{1}{C}\right) + \left(\frac{P}{P_0}\right) \right] \quad (4.18)$$

If  $P/P_0 \gg 1/C$ , then equation 4.18 can be represented by

$$\frac{\left(\frac{P}{P_0}\right)}{V\left[1-\left(\frac{P}{P_0}\right)\right]} = \frac{1}{V_m}\left(\frac{P}{P_0}\right) \quad (4.19)$$

which rearranges to

$$V_m = V\left[1-\frac{P}{P_0}\right] \quad (4.20)$$

Substituting equation 4.20 into equation 4.17 yields

$$S = \frac{VAN\left[1-\frac{P}{P_0}\right]}{M} \quad (4.21)$$

The surface area of the sample is then determined from equation 4.21, once the volume of gas adsorbed ( $V$ ) is measured and appropriate values for the other terms are incorporated. For nitrogen gas adsorbed from a mixture of 30 %  $N_2$  (mole percentage) and 70 % He using a liquid nitrogen bath, the respective values are obtained as set out below (Micromeritics Instruction manual, 1985):

- The volume ( $V$ ) of gas with which the FlowSorb 2300 is calibrated is injected at room temperature and the current atmospheric pressure. This volume must be multiplied by the following ratio to convert it to standard conditions:

$$\frac{273.2 \text{ K}}{\text{Room temperature (K)}} \times \frac{\text{Atmospheric pressure (mmHg)}}{760 \text{ mmHg}} \quad (4.22)$$

- Avogadro's number (A) is  $6.023 \times 10^{23}$  molecules  $\text{mol}^{-1}$
- The molar volume (M) of a gas at standard conditions is  $22414 \text{ cm}^3 \text{ mol}^{-1}$
- The accepted value for the area (N) of a solid surface occupied by an adsorbed nitrogen molecule is  $16.2 \times 10^{-20} \text{ m}^2$ .
- Since the adsorption takes place at atmospheric pressure, the pressure (P) is obtained as

$$P = \frac{\%N_2}{100\%} \times \text{atmospheric pressure} \quad (4.23)$$

- The saturation pressure of liquid nitrogen ( $P_0$ ) is typically a small amount greater than atmospheric pressure, due to thermally induced circulation, dissolved oxygen, and other factors. With fresh, relatively pure liquid nitrogen, the saturation pressure is typically about 15 mmHg greater than atmospheric pressure.

When these values, for a 30%  $N_2$  / 70% He mixture, adsorbed at liquid nitrogen temperature, when room temperature is  $22^\circ\text{C}$  and atmospheric pressure is 760 mmHg, are substituted into equation 4.21 a surface area of  $2.84 \times V$  is obtained. For calibration purposes, this means that a syringe injection of  $V = 1.00 \text{ cm}^3$  of nitrogen at  $22^\circ\text{C}$  and 760 mmHg, should produce an indicated surface area of  $2.84 \text{ m}^2$ .

When the surface areas of hydrated cements are determined by the BET technique, different surface area values are obtained for different adsorbates used (Micromeritics Instruction manual, 1985). According to Brunauer, the co-developer of the BET-equation, the surface area measured by  $N_2$ -adsorption is inaccurate and suggests the use of  $H_2O$ -adsorption for hydrated cement samples. Only gypsum and phosphogypsum samples were characterised during this study, and measurements were compared relative to each other. Subsequently, nitrogen gas was chosen as adsorbent.



## 4.7 Cement tests

### 4.7.1 Specific surface area and density

The fineness of cement is an important factor influencing the rate of hydration, since the hydration reactions occur at the interface of the cement particle with water. Ordinary Portland cement is usually ground to a surface area in the range 3000 - 3500 cm<sup>2</sup> g<sup>-1</sup>, but it should be kept in mind that the value obtained in the determination of surface area depends on the method used to measure it (Bye, 1983).

The weight specific surface area of cement ( $S_w$ ) is usually determined by an air permeability method, on what is called a Lea and Nurse constant flow apparatus. The correlation between the specific area and the measured resistance to flow of a powder bed, for a specific surface in the range in which laminar flow occurs (250 - 500 m<sup>2</sup> kg<sup>-1</sup>), is given by the Carman-Kozeny equation (Bye, 1983):

$$S_w = \frac{N}{\rho(1-\epsilon)} \frac{\epsilon^3 A \Delta p}{\eta QL} \quad (4.24)$$

where $S_w$	=	weight specific surface area
$A$	=	bed cross-sectional area
$L$	=	thickness of the bed
$\epsilon$	=	porosity of the bed
$\eta$	=	the Stokes viscosity of air
$Q$	=	rate of air flow
$\rho$	=	density of the powder
$\Delta p$	=	the drop in pressure across the bed
$N$	=	a dimensionless constant depending on the chosen units

In the Lea and Nurse apparatus dry air is passed continuously at a constant pressure, first through a compacted cylindrical bed of cement (25 mm diameter, 10 mm deep) and then through a length of capillary tubing. A manometer is used to measure the drop in pressure

across the bed of cement ( $h_1$ ). A second manometer measures the drop in pressure across the capillary, which acts as a flowmeter. For this apparatus, equation 4.24 becomes:

$$S_w = \frac{k}{\rho} \sqrt{\frac{h_1}{h_2}} \quad (4.25)$$

where  $\frac{h_1}{h_2}$  = the average of the ratios of the two manometer readings at two air flow rates

$k$  = a constant dependent on the dimensions of the apparatus

The density of Portland cement usually lies in the range of 3050 - 3250 kg m<sup>-3</sup>, and is determined by the displacement of kerosine. A vacuum pump is used to ensure complete displacement of air. The mass of cement used in the apparatus is adjusted to produce a bed with a porosity of 0.475.

The specific surface area of cement can also be determined by a constant volume method developed in 1943 by Rigden and Blaine (Bye, 1983). This method is based on the fact that the time required to pass a fixed volume of air through a bed of cement with standard porosity, is related to the specific surface area of the cement by the following relationship:

$$S_w = K\sqrt{t} \quad (4.26)$$

where  $t$  is the time, and  $K$  is a constant for an apparatus determined by means of a cement with a known specific surface area.

The simplicity of constant-volume permeameters makes them suitable for use in the cement industry. They are normally permitted as complying to the standard, if calibrated against a Lea and Nurse apparatus.

One version of the constant-volume permeameter incorporates the use of an U-tube. Kerosine in one limb of the U-tube is raised to produce a head of about 100 mm. This is then allowed to fall, forcing air through the cement, which is compacted in a cell attached to the second limb. The time it takes for the meniscus to fall between two marks on the U-tube, which define the fixed volume, is noted and used to calculate the specific surface area.

#### 4.7.2 Setting times

An essential property of cement is that it should exhibit setting when mixed with a limited quantity of water. Two setting times are described in all Standard procedures, namely an initial and a final set. There is no well-defined physical meaning of these terms, but the setting time of cement is usually described as the time at which a neat cement paste presents chosen resistance to the penetration of a needle (Bye, 1983; Hewlett, 1998c).

The main variables influencing penetration are the water content of the paste, the temperature, the load on the needle, the dimension of the needle, and the reactivity of the cement. The apparatus for the determination of setting times is shown in Figure 4.9. The needle, which has a diameter of 1.13 mm and a total load of 300 g, is named after Vicat (1828). It is released at the surface of the hydrating paste, at intervals, until it penetrates only to a point  $5 \pm 1$  mm from the bottom of the standard mould. When the paste has attained this degree of stiffness it has reached initial set.

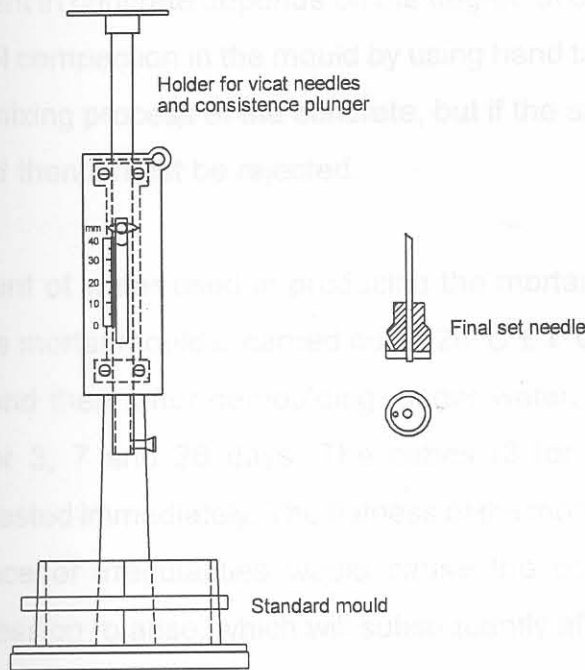
The needle is then replaced by cylindrical knife edge attachment for the final setting time determination. Final set is reached when the knife edge makes only a shallow impression on the surface of the paste but does not penetrate the 0.5 mm necessary to mark the surface.

The amount of water used in making the standard cement paste is determined by the standard consistence of the paste. This is achieved when a 10 mm diameter plunger, which is held in the apparatus used for the Vicat needle, can be forced under its own weight to penetrate to  $5 \pm 1$  mm from the bottom of the mould. Trial and error methods determine the



correct amount of water to form this paste consistence.

Figure 4.9 Apparatus for the determination of setting times and standard consistence (Bye, 1983).



### 4.7.3 Compressive strength

Compressive strength is the most important material parameter used to characterize cement quality. Usually the term implies the crushing strength of concrete or mortar cubes cast in steel moulds, either 100 or 150 mm in length. The compressive strengths developed in these cubes, depend on the material used, the mix proportions, the efficiency with which the mix is compacted into the mould, and the temperature, humidity and time of curing. Materials and procedures are therefore described in detail in national standards, which enables inter-laboratory co-operative testing.

Concrete strength is related to the volumes of cement (C), water (W) and air (A) it contains by Feret's empirical law (Bye, 1983):

$$S = k \left( \frac{C}{C + W + A} \right)^2 \quad (4.27)$$

where  $k$  is a constant for the aggregates, cement and curing employed.

The volume of air present in concrete depends on the degree of compaction achieved, and the aim is to achieve full compaction in the mould by using hand tamping. Some air may be introduced during the mixing process of the concrete, but if the amount is abnormal with a particular batch of sand then it must be rejected.

The effect of the amount of water used in producing the mortar is significant, but easily controlled. Curing of the mortar mould is carried out at  $20^{\circ}\text{C} \pm 1^{\circ}\text{C}$ , in a high humidity room for the first 24 hours and then, after demoulding, under water. Compressive strength is usually measured after 3, 7 and 28 days. The cubes (3 for each curing period) are superficially dried and tested immediately. The flatness of the mortar cube face is important, because the occurrence of irregularities would cause the concentration of abnormal stresses during compression to arise, which will subsequently affect the results.

The procedures as set out in SABS EN 196-1:1996 (Determination of strength) and SABS EN 196-3:1996 (Determination of setting time and soundness) were followed as standard methods of cement testing during this study.

# Chapter 5 Properties and characterization of South African phosphogypsum

## 5.1 Introduction

South African phosphogypsum will have to be purified, particularly with respect to phosphorous and fluorine impurities, before it can be used in the building and construction industry. Before this phosphogypsum can be purified, it is important to characterize the impure samples so that the composition of the starting material is known. In this study, the influence of only phosphorous impurities and the hydrated form of calcium sulphate, contained in the South African phosphogypsum samples, on the properties of Portland cement was investigated.

This chapter reports on the results of characterization of different batches of phosphogypsum, obtained from two South African phosphoric acid producers. Two batches of phosphogypsum were obtained from each phosphoric acid producer, in order to study the homogeneity (or inhomogeneity) of samples prepared at different time periods by the same phosphoric acid production method.

## 5.2 Experimental

### 5.2.1 Samples

Phosphogypsum samples were obtained from two South-African phosphoric acid producers, Omnia and Kynoch. Two different batches were obtained from each producer. Both batches of Kynoch phosphogypsum were taken from a ten-year-old disposal site at Modderfontein, Johannesburg. The first batch of the Omnia phosphogypsum was taken from an old dumping site at Rustenburg, while the second batch was obtained in the form of a wet filter



cake, taken directly from the phosphoric acid plant. All samples were oven-dried overnight at 45 °C.

### 5.2.2 Thermal analysis

Simultaneous TG and DSC analyses were performed on a NETZSCH STA 409 simultaneous TG/DSC instrument. Open platinum pans as well as crimped hermetic aluminium pans were used. For all analyses a heating rate of 5 °C/min were used in a static air atmosphere, with sample masses between 10 and 15 mg. Temperature and enthalpy calibrations were achieved using the ICTAC recommended DTA standards.

### 5.2.3 Infrared analysis

A Bruker IFS113v FTIR-spectrometer was used for Infrared spectroscopy analysis. KBr pellets were prepared by mixing 4 mg of sample with 100 mg of dry KBr.

### 5.2.4 X-ray fluorescence analysis

The X-ray fluorescence analyses were performed on an ARL8429 XRF spectrometer. To determine the loss on ignition, all samples were roasted for 8 hours at 950 °C. Then 1.000 g of the sample was mixed with 6.000 g of  $\text{Li}_2\text{B}_4\text{O}_7$  flux, and melted at 1050 °C in a platinum crucible. The samples were cast in a platinum casting, and analyses of the main elements were performed on a pre-calibrated main element program. Three certified standards were analysed with all samples.

	0.18	0.03	0	0
$\text{TiO}_2$	0	0	0	0
$\text{V}_2\text{O}_5$	0	0	0	0
$\text{ZrO}_2$	0	0	0	0
Sr	0.23	0.27	0.32	0.13
$\text{SO}_3$	44.06	45.76	61.24	47.66
Loss on ignition	22.21	21.29	10.06	20.90
Total	100.73	101.47	101.93	102.64

\*0 means that the compound was present in a quantity below the detection limit

## 5.3 Results and discussion

### 5.3.1 X-ray fluorescence analysis

The XRF analyses of both batches of the respective phosphogypsum samples are given in Table 5.1.

**Table 5.1** The XRF results of the different batches of the Omnia and Kynoch phosphogypsum samples

Compounds (%)	Kynoch phosphogypsum		Omnia phosphogypsum	
	Batch 1	Batch 2	Batch 1	Batch 2
Al <sub>2</sub> O <sub>3</sub>	0.11	0.08	0.04	0
CaO	33.04	33.16	38.38	33.94
Cr <sub>2</sub> O <sub>3</sub>	0*	0	0	0
Fe <sub>2</sub> O <sub>3</sub>	0.09	0.04	0.05	0.09
K <sub>2</sub> O	0	0	0	0.01
MgO	0.13	0.07	0.16	0.10
MnO	0	0	0	0
Na <sub>2</sub> O	0	0	0	0
<b>P<sub>2</sub>O<sub>5</sub></b>	<b>0.71</b>	<b>0.77</b>	<b>1.68</b>	<b>1.34</b>
SiO <sub>2</sub>	0.16	0.03	0	0
TiO <sub>2</sub>	0	0	0	0
V <sub>2</sub> O <sub>5</sub>	0	0	0	0
ZrO <sub>2</sub>	0	0	0	0
Sr	0.28	0.27	0.32	0.18
SO <sub>3</sub>	44.06	45.76	51.24	47.85
Loss on ignition	22.21	21.29	10.06	20.90
<b>Total</b>	<b>100.79</b>	<b>101.47</b>	<b>101.93</b>	<b>102.64</b>

\*0 means that the compound was present in a quantity below the detection limit

For phosphogypsum to be used as a set retarder in cement, the total percentage of  $P_2O_5$  must be lower than 0.5% (PPC report 13/88, Gypsum retarder specifications). From the results in the table, it can be observed that none of the obtained South African phosphogypsum samples satisfied this guideline. The amount of phosphorous impurities in both batches of the Omnia phosphogypsum was significantly higher than for the Kynoch phosphogypsum.

### 5.3.2 Infrared analysis

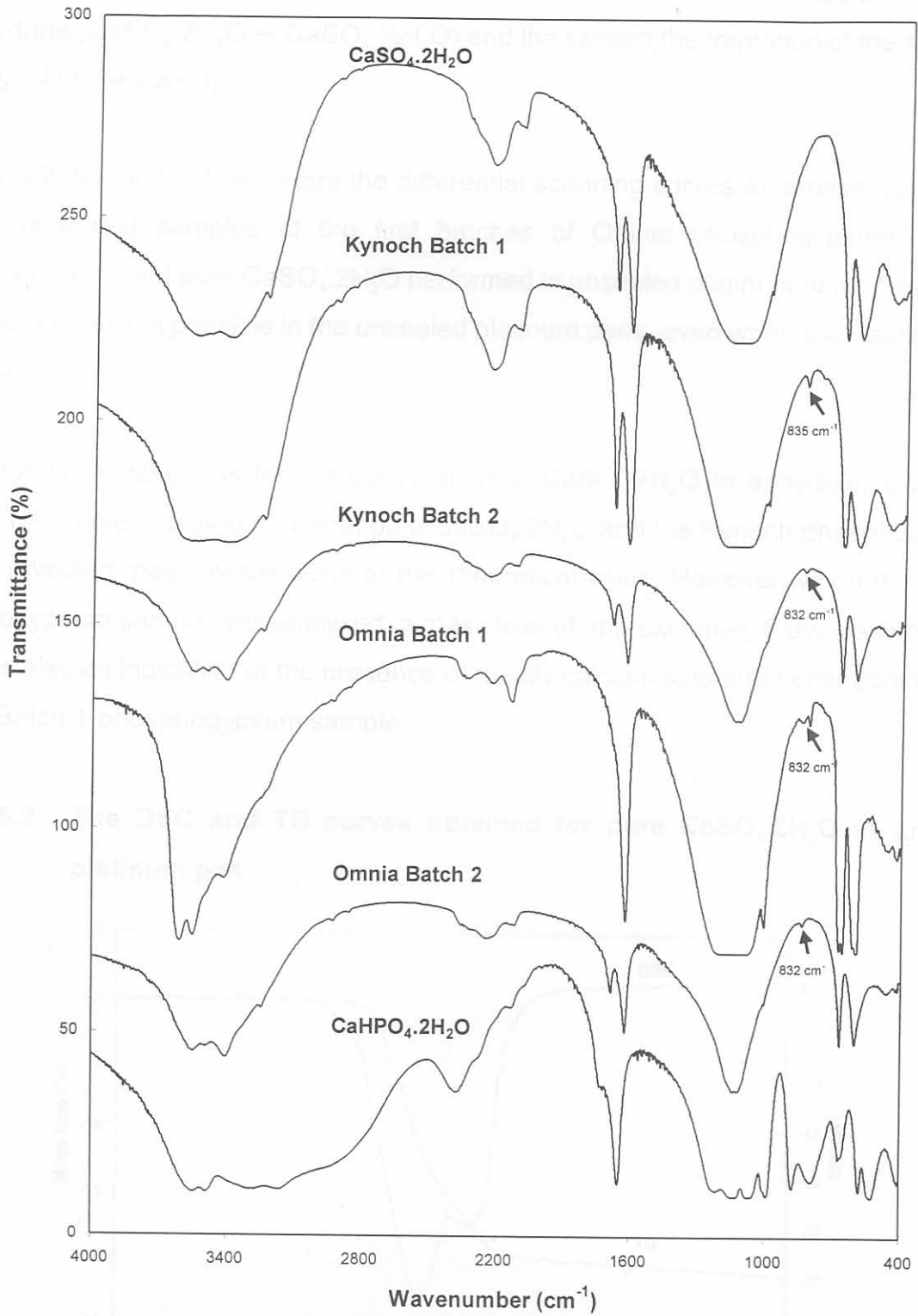
Murakami (1968) showed that phosphogypsum produces weak absorptions at about  $1015\text{ cm}^{-1}$  and  $837\text{ cm}^{-1}$  in the related characteristic absorption bands of  $HPO_4^{2-}$ . These displacements can be ascribed to the formation of the solid solution of gypsum with dicalcium phosphate equivalent to the amount of phosphorous impurities in the crystal lattice of phosphogypsum. Ölmez and Yilmaz (1988) have also successfully identified the phosphorous impurities contained in phosphogypsum by using infrared analysis.

If the FT-IR spectra of pure  $CaSO_4 \cdot 2H_2O$ , pure  $CaHPO_4 \cdot 2H_2O$ , and the different batches of Kynoch and Omnia phosphogypsum samples in Figure 5.1 are compared, the small band characteristics (indicated in the figure) at  $837\text{ cm}^{-1}$  and  $1015\text{ cm}^{-1}$  can be attributed to the water-insoluble phosphorous impurities in phosphogypsum.

According to Todorovsky *et al* (1997), the presence of  $CaSO_4 \cdot \frac{1}{2}H_2O$  can be confirmed in an IR spectrum when a split in each of the peaks at  $600\text{ cm}^{-1}$  and  $667\text{ cm}^{-1}$  is observed. Only the Omnia Batch 1 phosphogypsum sample has shown this characteristic, and was also the only sample that produced a single peak in the region between  $1600\text{--}1700\text{ cm}^{-1}$ . The peaks between  $3400\text{--}4000\text{ cm}^{-1}$  were narrower than those of the other gypsum samples. This serves as a further indication of the presence of mainly calcium sulphate hemihydrate.



Figure 5.1 The FT-IR spectra of pure  $\text{CaSO}_4 \cdot 2\text{H}_2\text{O}$ , pure  $\text{CaHPO}_4 \cdot 2\text{H}_2\text{O}$  and the different batches of the Kynoch and Omnia phosphogypsum samples



### 5.3.3 Thermal analysis

The DSC curve obtained for pure calcium sulphate dihydrate gives a two-step dehydration process. The first endothermic peak represents the formation of calcium sulphate hemihydrate ( $\text{CaSO}_4 \cdot 2\text{H}_2\text{O} \rightarrow \text{CaSO}_4 \cdot \frac{1}{2}\text{H}_2\text{O}$ ) and the second the formation of the anhydrite ( $\text{CaSO}_4 \cdot \frac{1}{2}\text{H}_2\text{O} \rightarrow \text{CaSO}_4$ ).

Figures 5.2, 5.3 and 5.4 represent the differential scanning curves and mass loss curves for the untreated samples of the first batches of Omnia phosphogypsum, Kynoch phosphogypsum and pure  $\text{CaSO}_4 \cdot 2\text{H}_2\text{O}$  performed in unsealed platinum pans. Separation of the peaks was not possible in the unsealed platinum pans, even when low heating rates were used.

The theoretical mass loss for the dehydration of  $\text{CaSO}_4 \cdot 2\text{H}_2\text{O}$  to anhydrite,  $\text{CaSO}_4$ , is 20.9%. The curves obtained for both pure  $\text{CaSO}_4 \cdot 2\text{H}_2\text{O}$  and the Kynoch phosphogypsum sample revealed mass losses close to this theoretical value. However, when the Omnia phosphogypsum sample was analysed, a mass loss of approximately 8.0% was obtained. This was also an indication of the presence of mainly calcium sulphate hemihydrate in the Omnia Batch 1 phosphogypsum sample.

**Figure 5.2** The DSC and TG curves obtained for pure  $\text{CaSO}_4 \cdot 2\text{H}_2\text{O}$  in an open platinum pan

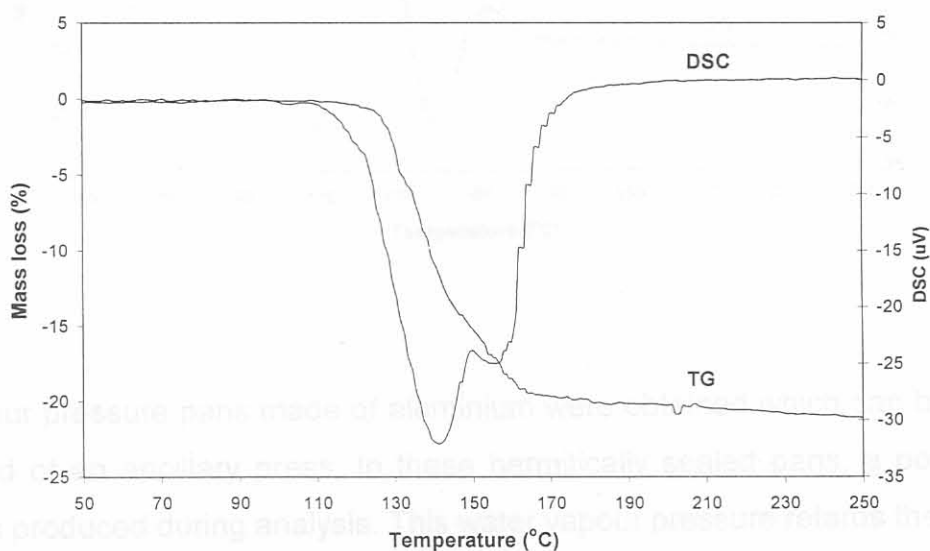


**Figure 5.3** The DSC and TG curves obtained for Omnia phosphogypsum (Batch 1) in an open platinum pan

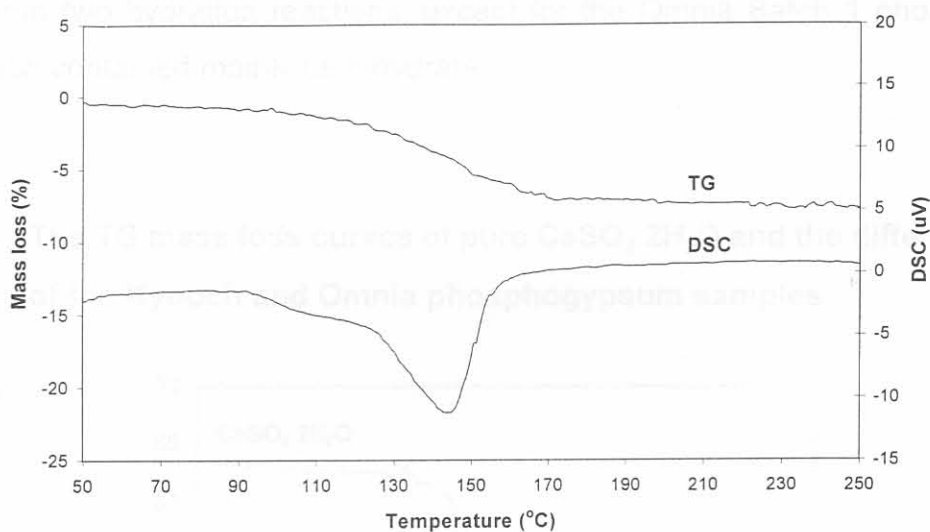
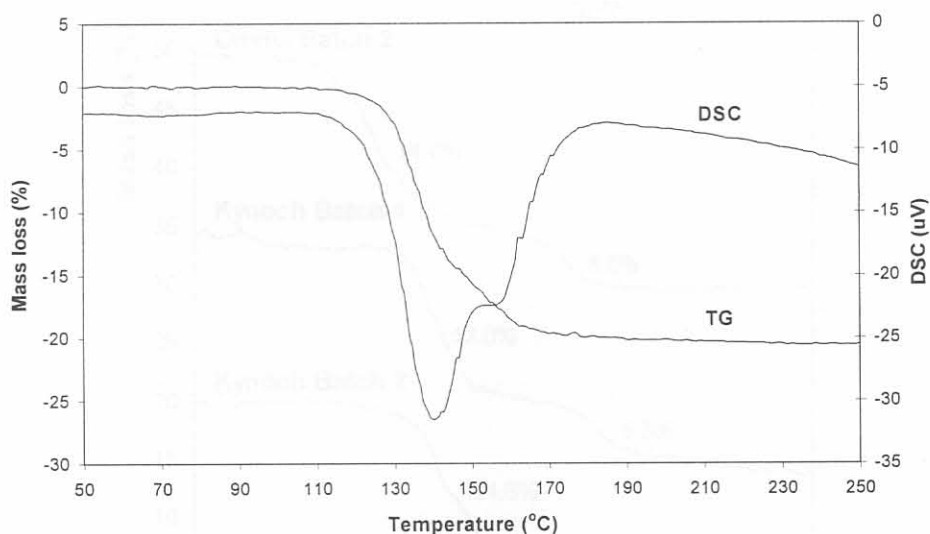


**Figure 5.4** The DSC and TG curves obtained for Kynoch phosphogypsum (Batch 1) in an open platinum pan



Small vapour pressure pans made of aluminium were obtained which can be tightly shut with the aid of an ancillary press. In these hermitically sealed pans, a positive vapour pressure is produced during analysis. This water vapour pressure retards the onset of the second dehydration reaction, resulting in better separation in the TG curve and DSC peaks.



The TG and DSC curves given in Figures 5.5 and 5.6 were obtained by encapsulating the samples in aluminium hermetic pans. This method proved to resolve the two peaks, thus separating the two hydration reactions, except for the Omnia Batch 1 phosphogypsum sample, which contained mainly hemihydrate.

**Figure 5.5** The TG mass loss curves of pure  $\text{CaSO}_4 \cdot 2\text{H}_2\text{O}$  and the different batches of the Kynoch and Omnia phosphogypsum samples

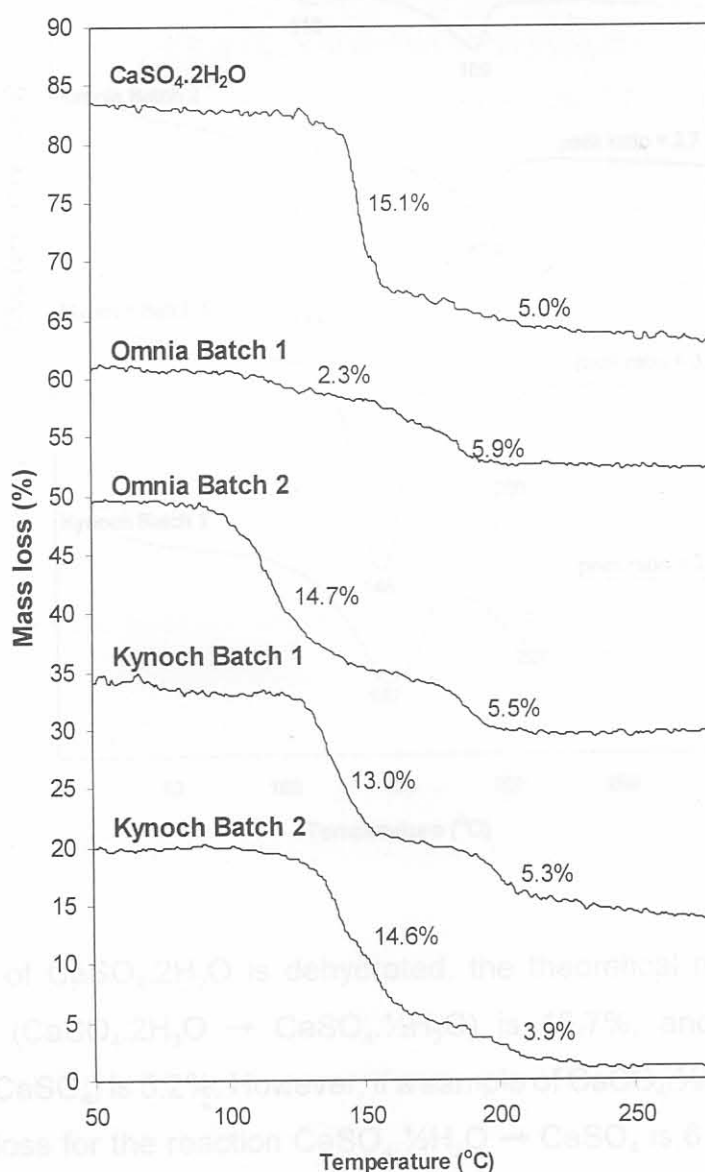
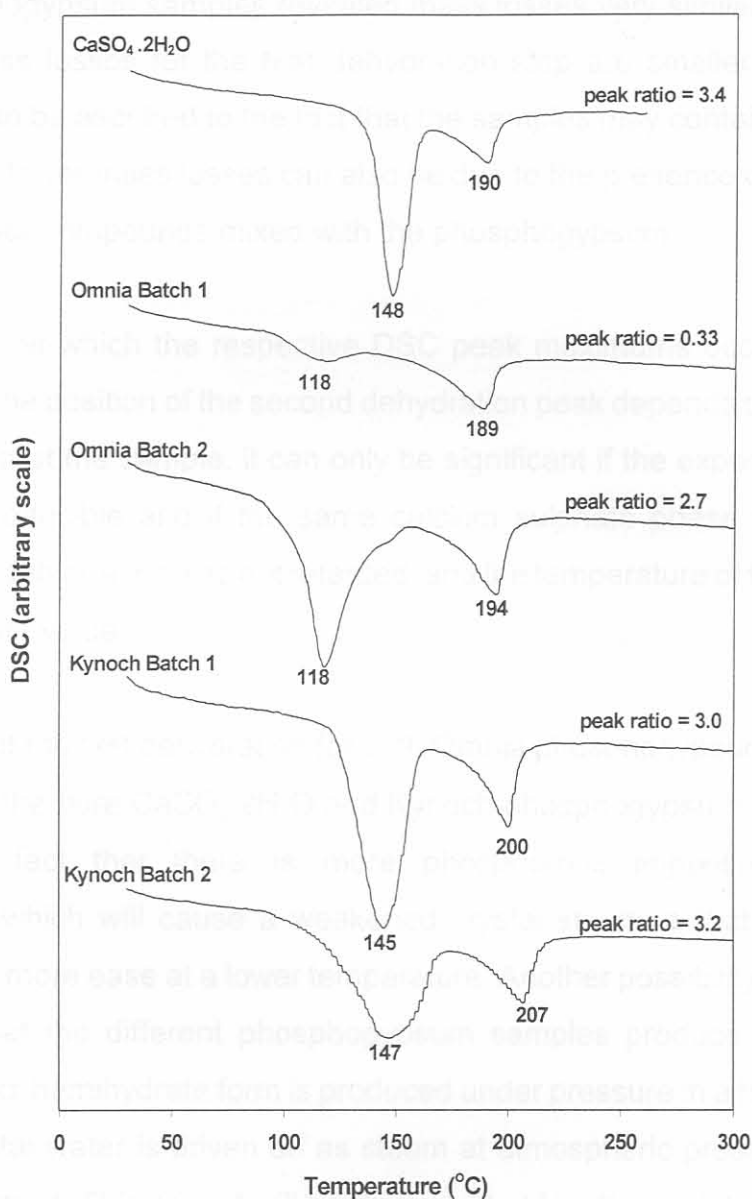


Figure 5.6 The DSC curves of pure  $\text{CaSO}_4 \cdot 2\text{H}_2\text{O}$  and the different batches of the Kynoch and Omnia phosphogypsum samples



If a pure sample of  $\text{CaSO}_4 \cdot 2\text{H}_2\text{O}$  is dehydrated, the theoretical mass loss for the first dehydration step ( $\text{CaSO}_4 \cdot 2\text{H}_2\text{O} \rightarrow \text{CaSO}_4 \cdot \frac{1}{2}\text{H}_2\text{O}$ ) is 15.7%, and that of the second ( $\text{CaSO}_4 \cdot \frac{1}{2}\text{H}_2\text{O} \rightarrow \text{CaSO}_4$ ) is 5.2%. However, if a sample of  $\text{CaSO}_4 \cdot \frac{1}{2}\text{H}_2\text{O}$  is dehydrated, the theoretical mass loss for the reaction  $\text{CaSO}_4 \cdot \frac{1}{2}\text{H}_2\text{O} \rightarrow \text{CaSO}_4$  is 6.2%. This explains the higher second mass loss of 5.9% for the Omnia Batch 1 phosphogypsum sample. As confirmed by the IR results, this sample contained more hemihydrate than dihydrate, resulting in a very low mass loss for the first dehydration step, followed by a higher mass

loss for the second step.

The other phosphogypsum samples revealed mass losses very similar to that of the pure gypsum. The mass losses for the first dehydration step are smaller than that for pure gypsum, which can be ascribed to the fact that the samples may contain small amounts of hemihydrate. The lower mass losses can also be due to the presence of small amounts of impurities and other compounds mixed with the phosphogypsum.

The temperatures at which the respective DSC peak maximums occur are indicated in Figure 5.6. Since the position of the second dehydration peak depends on the water vapour pressure produced at the sample, it can only be significant if the experimental conditions were exactly reproducible and if the same calcium sulphate phase was present in all samples. The first dehydration was not retarded, and the temperature of this peak maximum can be of significant value.

The temperature of the first dehydration for both Omnia phosphogypsum samples is much lower than that of the pure  $\text{CaSO}_4 \cdot 2\text{H}_2\text{O}$  and Kynoch phosphogypsum. This can partly be ascribed to the fact that there is more phosphorous impurities in the Omnia phosphogypsum, which will cause a weakened crystal structure that will lose water of crystallization with more ease at a lower temperature. Another possibility that needs further investigation is that the different phosphogypsum samples produce different forms of hemihydrate. The  $\alpha$ -hemihydrate form is produced under pressure in a humid atmosphere, but when the crystal water is driven off as steam at atmospheric pressure, crystals of  $\beta$ -hemihydrate is formed. This aspect will be discussed at length at a later stage.

The peak ratios of the DSC peaks of the different gypsum samples are also indicated in Figure 5.6. Dunn *et al* (1987) reported the DSC peak ratio for the two stage dehydration of pure gypsum as 3.3. This is in agreement with the DSC peak ratio of 3.4 obtained experimentally for pure  $\text{CaSO}_4 \cdot 2\text{H}_2\text{O}$ . The DSC curves also confirmed the presence of mainly hemihydrate for the Omnia Batch 1 phosphogypsum sample, which revealed a peak ratio of only 0.33. All other phosphogypsum samples produced DSC curves with peak ratios similar to that of pure  $\text{CaSO}_4 \cdot 2\text{H}_2\text{O}$ .



## Chapter 5 Distribution of phosphorous

### 5.4 Conclusion

FT-IR analysis can be used to identify the phosphorous impurities contained in phosphogypsum, and can also indicate the presence of calcium sulphate hemihydrate. TG and DSC analyses can serve as useful tools in determining more comprehensively which form of the calcium sulphate phases are present in the phosphogypsum samples.

By using the abovementioned techniques, most of the phosphogypsum samples have shown characteristics close to that of pure gypsum in terms of the calcium sulphate phase. Only the Omnia Batch 1 phosphogypsum sample contained mainly the hemihydrate form, while the other samples contained predominantly calcium sulphate dihydrate.

The different South African phosphogypsum samples were analysed and found to contain a significant amount of phosphorous impurities. In addition to this high phosphorous content, the presence of a relevant amount of hemihydrate underpins its unsuccessful utilization as a set retarder in cement. Therefore, the harmful phosphorous impurities contained in the phosphogypsum must be removed or neutralized, and the hemihydrate must be rehydrated to dihydrate. These two aspects will be dealt with in the following chapters.

statistical errors in their determinations

Krempl (1972) found that the impurities in phosphogypsum are concentrated in the fractions larger than 165 µm and smaller than 25 µm. By washing the fraction between 25 µm and 165 µm, the water-soluble phosphorous was removed completely.

The aim of this chapter is to establish the particle size distribution of dried South African phosphogypsum and to determine the amount of phosphorous impurities contained in each fraction.

## Chapter 6

# Distribution of phosphorous impurities in particle size fractions of South African phosphogypsum

### 6.1 Introduction

The particle size distribution of phosphogypsum has a major influence on its technological properties. The particle sizes of phosphogypsum depend on the type of phosphoric acid process applied, the application of crystal modifiers in the process, as well as on the degree of grinding of the raw phosphate rock used.

According to Eipeltauer *et al* (1981) the particle size distribution in a raw slurry determines whether it is necessary to apply further size reduction in order to meet the requirements for a specific purpose. In their investigation, particle size determinations were done on the wet phosphogypsum samples, obtained from the wet phosphoric acid process, after being washed with water. They found that the presence of organic substances resulted in large statistical errors in their determinations.

Krempff (1972) found that the impurities in phosphogypsum are concentrated in the fractions larger than 168  $\mu\text{m}$  and smaller than 25  $\mu\text{m}$ . By washing the fraction recovered between 25  $\mu\text{m}$  and 168  $\mu\text{m}$ , the water-soluble phosphorous was removed completely.

The aim of this chapter is to establish the particle size distribution of dried South African phosphogypsum and to determine the amount of phosphorous impurities contained in each fraction.

Approximately 85% of the Ornia phosphogypsum and 76% of the Kynoch phosphogypsum are found in fractions smaller than 150  $\mu\text{m}$ , which indicates that Ornia phosphogypsum is a finer waste product than Kynoch phosphogypsum.

## 6.2 Experimental

### 6.2.1 Samples

Phosphogypsum samples were obtained from two South-African phosphoric acid producers, Omnia and Kynoch. Batch 2 of both of the Kynoch and Omnia phosphogypsum was used in this study. The samples were dried overnight at 45°C.

### 6.2.2 Instrumental analysis

Thermal analysis, Infrared analysis and X-ray fluorescence analysis were done as described in Chapter 5.2.

### 6.2.3 Sieving

A Fritsch Analysette 3 vibratory sieve shaker was used to sieve the phosphogypsum samples. A set of sieves between 75 and 1700 IS  $\mu\text{m}$  were used and 10.0 g of the respective phosphogypsum samples were sieved for 10 minutes.

## 6.3 Results and discussion

### 6.3.1 Particle size distribution of the phosphogypsum samples

The particle size distribution of the phosphogypsum samples is presented in Table 6.1. Approximately 85% of the Omnia phosphogypsum and 76 % of the Kynoch phosphogypsum are found in fractions smaller than 150  $\mu\text{m}$ , which indicates that Omnia phosphogypsum is a finer waste product than Kynoch phosphogypsum.

Particle size ( $\mu\text{m}$ )	% P <sub>2</sub> O <sub>5</sub>	
	Omnia phosphogypsum	Kynoch phosphogypsum
Unsieved	1.50	1.00

Due to the small percentage sample obtained, XRF analysis, was not performed.



**Table 6.1 Particle size distribution of the phosphogypsum samples**

Particle size ( $\mu\text{m}$ )	Size distribution (mass %)	
	Omnia phosphogypsum	Kynoch phosphogypsum
> 1700	0	4.6
600 - 1700	0	5.4
300 - 600	0.1	3.6
150 - 300	14.1	11.1
75 - 150	48.7	27.7
< 75	37.1	47.5

### 6.3.2 X-ray fluorescence analysis of the phosphogypsum particle size fractions

Although there are many other impurities contained in the phosphogypsum samples, only phosphorous was studied during this investigation. The phosphorous content of each fraction, determined by XRF analysis, is listed in Table 6.2.

**Table 6.2 The total phosphorous content of the particle size fractions of the phosphogypsum samples, as determined by XRF analysis**

Particle size ( $\mu\text{m}$ )	% $\text{P}_2\text{O}_5$ (%)	
	Omnia phosphogypsum	Kynoch phosphogypsum
600 - 1700	-	1.09
300 - 600	*	1.08
150 - 300	1.55	1.04
75 - 150	1.29	0.98
< 75	1.29	0.97
Unsieved	1.50	1.00

\* Due to the small percentage sample obtained, XRF analysis, was not performed.

The 150 - 300  $\mu\text{m}$  and 300 - 600  $\mu\text{m}$  Omnia phosphogypsum fractions also contained dark particles that can be attributed to unreacted iron oxide and/or magnesium oxide present from the wet phosphoric acid process. The presence of iron oxide was confirmed by the XRF results. From the table, it can also be seen that the amount of phosphorous impurities contained in the Omnia phosphogypsum sample is reduced the finer fractions, when compared to the larger and untreated fractions. However, the amount of phosphorous impurities contained in the different particle size fractions of the Kynoch phosphogypsum did not differ significantly.

### 6.3.3 Thermal analysis of the phosphogypsum particle size fractions

The thermogravimetric mass losses obtained for each fraction of the sieves, are given in Table 6.3. The mass losses obtained for Kynoch phosphogypsum are all close to the theoretical mass loss of 20.9%. The mass losses obtained for the Omnia particle size fractions up to 300  $\mu\text{m}$  were also similar to that of the theoretical value. However, the fraction between 300 and 600  $\mu\text{m}$  revealed a mass loss of only 15.2%.

**Table 6.3** The mass losses obtained from the thermogravimetric analysis for the different particle size fractions of the phosphogypsum samples

Particle size ( $\mu\text{m}$ )	TG mass loss (%)	
	Omnia phosphogypsum	Kynoch phosphogypsum
600 - 1700	-	21.1
300 - 600	15.2	19.2
150 - 300	20.0	21.7
75 - 150	20.0	19.3
< 75	21.1	19.9
Unsieved	19.8	20.7

Omnia phosphogypsum contains a high percentage phosphorous, and it is possible that in the particle size fraction between 300 and 600  $\mu\text{m}$ , the phosphorous content is higher than in the other fractions. These impurities can cause a slight decrease in the mass loss of the sample, but not to the extent shown here. A more obvious explanation for the decrease in the mass loss percentage for this particle size fraction is that the hemihydrate form of calcium sulphate, which is also contained in the Omnia phosphogypsum sample, mainly accumulates in this fraction.

**Figure 6.1** The DSC curves of the particle size fractions and unsieved Omnia phosphogypsum

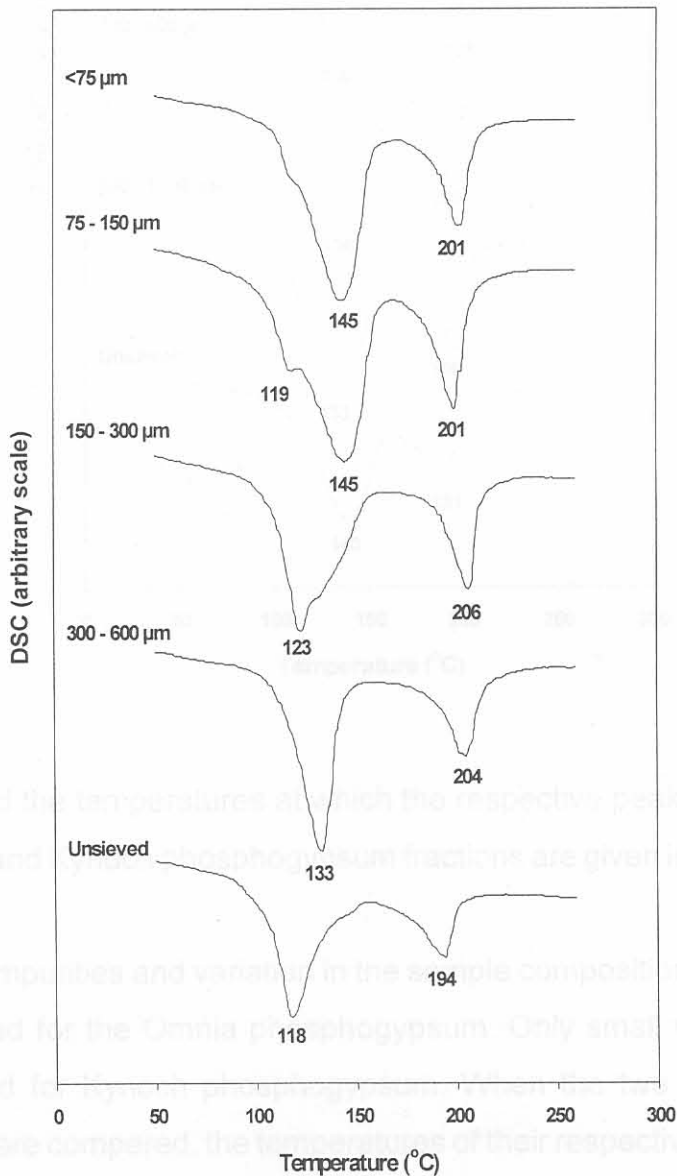
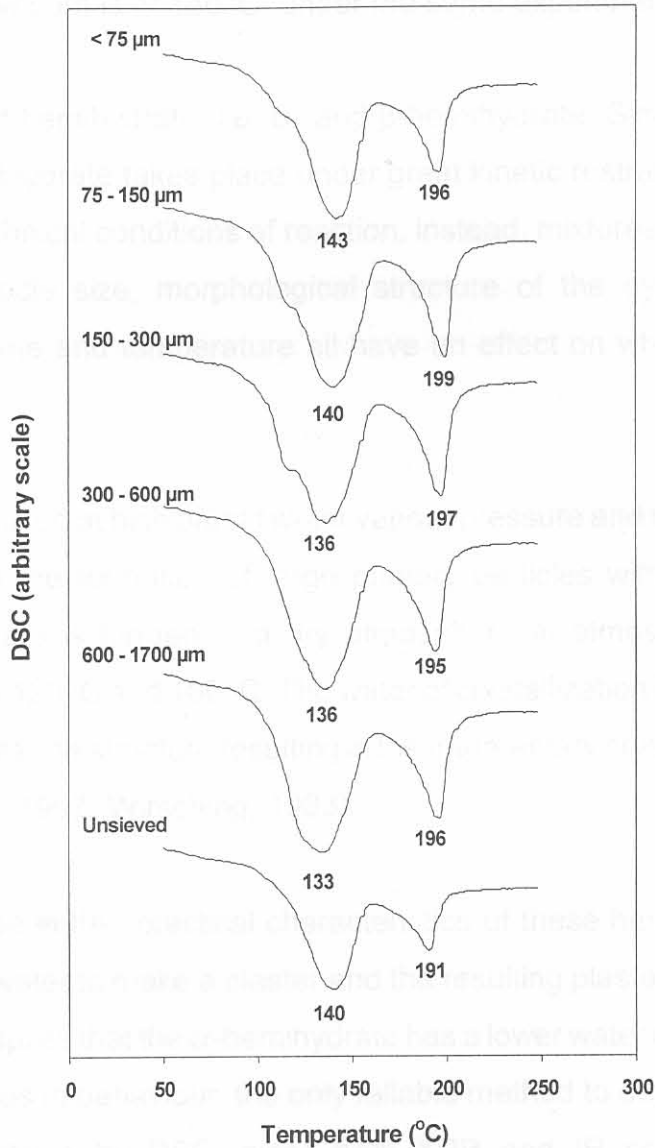




**Figure 6.2** The DSC curves of the particle size fractions and unsieved Kynoch phosphogypsum



The DSC curves and the temperatures at which the respective peak maximums occur for the different Omnia and Kynoch phosphogypsum fractions are given in Figures 6.1 and 6.2.

The contribution of impurities and variation in the sample composition are noticeable in the DSC curves obtained for the Omnia phosphogypsum. Only small variations in the DSC curves are observed for Kynoch phosphogypsum. When the two unsieved samples in Figures 6.1 and 6.2 are compared, the temperatures of their respective peak maximums for

the dehydration to the hemihydrate differed significantly. The peak temperature for the unsieved Omnia phosphogypsum is 118°C, while the corresponding peak temperature for the Kynoch phosphogypsum is at 140°C, under the same experimental conditions.

There are two types of hemihydrate, i.e.  $\alpha$ - and  $\beta$ -hemihydrate. Since the phase change from dihydrate to hemihydrate takes place under great kinetic restraints, pure phases are not obtained under technical conditions of reaction, instead, mixtures of phases are nearly always obtained. Particle size, morphological structure of the gypsum, water vapour pressure, residence time and temperature all have an effect on which calcium sulphate phase will form.

$\alpha$ -Hemihydrate is produced at high partial water vapour pressure and temperatures of 80°C to 180°C, resulting in the formation of large primary particles with an even crystalline structure.  $\beta$ -Hemihydrate is formed in a dry atmosphere at atmospheric pressure and temperatures between 120°C and 180°C. The water of crystallization is driven off as steam, which disrupts the crystalline structure resulting in the fragmentary crystals of  $\beta$ -hemihydrate (Coburn, 1989; Taylor, 1997; Wirsching, 1983).

The principle difference in the practical characteristics of these hemihydrates is that the  $\beta$ -form requires more water to make a plaster and the resulting plaster will set more quickly and be weaker. This implies that the  $\alpha$ -hemihydrate has a lower water demand on hydration. Despite their differences in behaviour, the only reliable method to determine the presence of  $\alpha$ - or  $\beta$ -hemihydrate is by DSC, since both XRD and IR spectroscopy of these hemihydrates result in traces in which peaks are in identical positions.

The hydration behaviour and subsequently the DSC traces of autoclaved  $\alpha$ - and calcined  $\beta$ -hemihydrates are different. However, there has been substantial disagreement about how these differences arise and whether or not any other subhydrate species exists. In particular, it has been suggested that there are whole series of subhydrates of the form  $\text{CaSO}_4 \cdot n\text{H}_2\text{O}$ , where  $n$  varies from 0 to 2/3 or even between 0 and 1. Alternatively, it has been suggested that there is only one other subhydrate apart from hemihydrate, but there

is disagreement over the amount of water in the structure as  $\text{CaSO}_4 \cdot 3/5\text{H}_2\text{O}$ ,  $\text{CaSO}_4 \cdot 2/3\text{H}_2\text{O}$ , or even  $\text{CaSO}_4 \cdot 4/5\text{H}_2\text{O}$  have all been suggested as the chemical formula of the additional subhydrate. Some authors have claimed that the higher subhydrate ( $\text{CaSO}_4 \cdot 2/3\text{H}_2\text{O}$ ) actually is the referred to hemihydrate. On the whole, it seems likely that at high water partial pressure another subhydrate exists (Hand, 1997).

It is therefore most probable that the Kynoch and Omnia phosphogypsum samples produced these different types of hemihydrates. The  $\alpha$ -hemihydrate is formed at a lower temperature, and it seemed to be the form that was produced from the dehydration of unsieved Omnia phosphogypsum. If this was the case, then  $\beta$ -hemihydrate was formed when the Kynoch phosphogypsum was dehydrated. In the DSC curves of the sieved phosphogypsum samples, the existence of a shoulder and occasionally a second peak was observed in the region of the first dehydration reaction. This suggested that these two types of hemihydrates were produced simultaneously.

For the Kynoch phosphogypsum, the  $\beta$ -hemihydrate was formed predominantly in all size fractions. From Figure 6.1 it can be seen that the temperature of the first dehydration peak is higher for the two smaller particle size fractions than for the particle size fractions larger than  $150\ \mu\text{m}$ . This indicates that the Omnia phosphogypsum formed mainly  $\beta$ -hemihydrate in the dehydration of the smaller particle size fractions and  $\alpha$ -hemihydrate for the larger fractions.

#### 6.3.4 Infrared spectroscopy analysis of the phosphogypsum particle size fractions

The results of the FT-IR analyses of the different size fractions are given in Figures 6.3 and 6.4. In all spectra, small bands at  $832\ \text{cm}^{-1}$  can be observed, indicating the presence of phosphorous impurities.

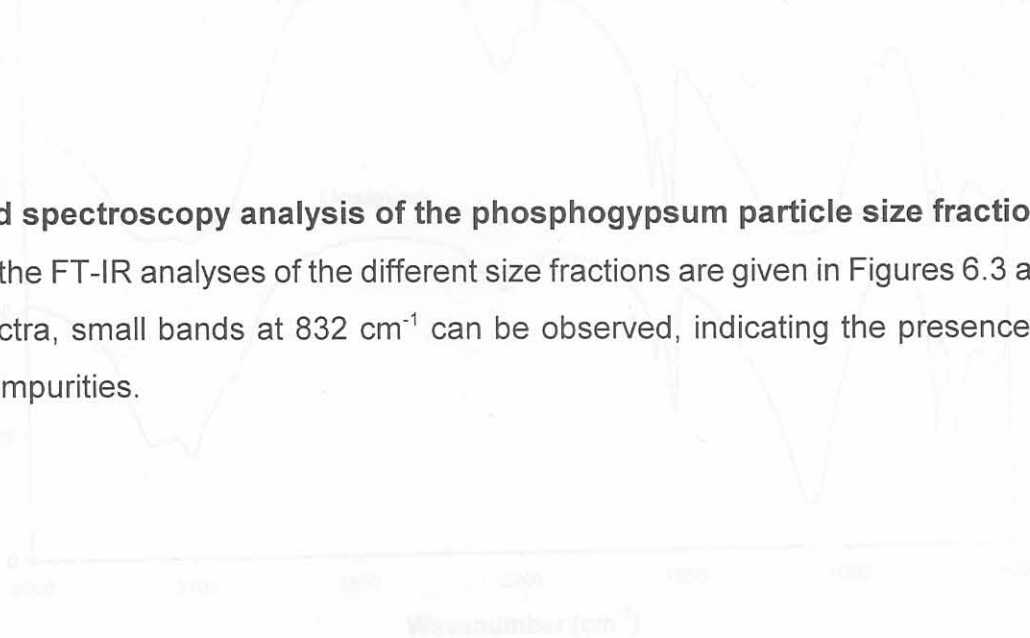




**Figure 6.3** The IR spectra of the particle size fractions and unsieved Kynoch phosphogypsum

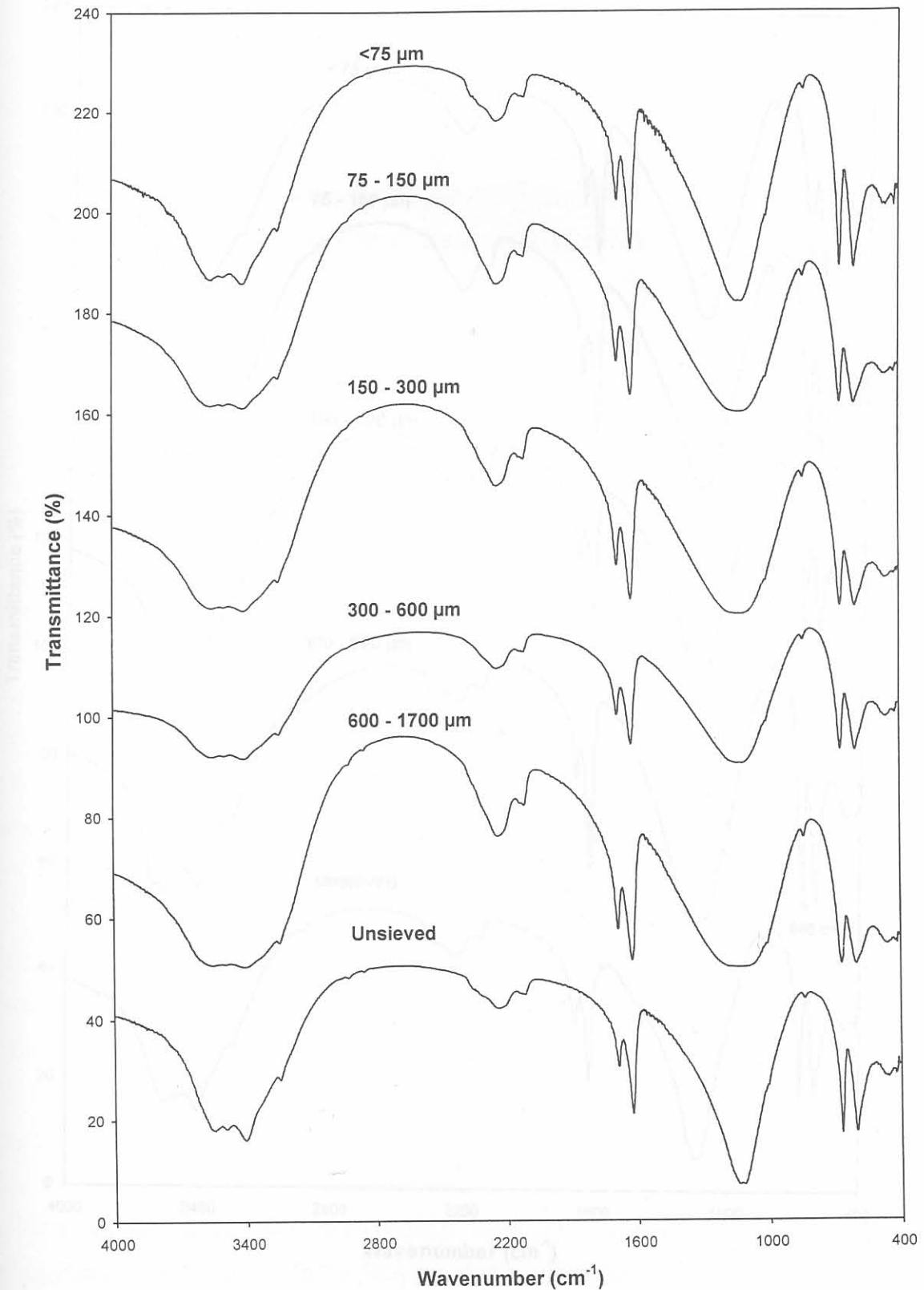
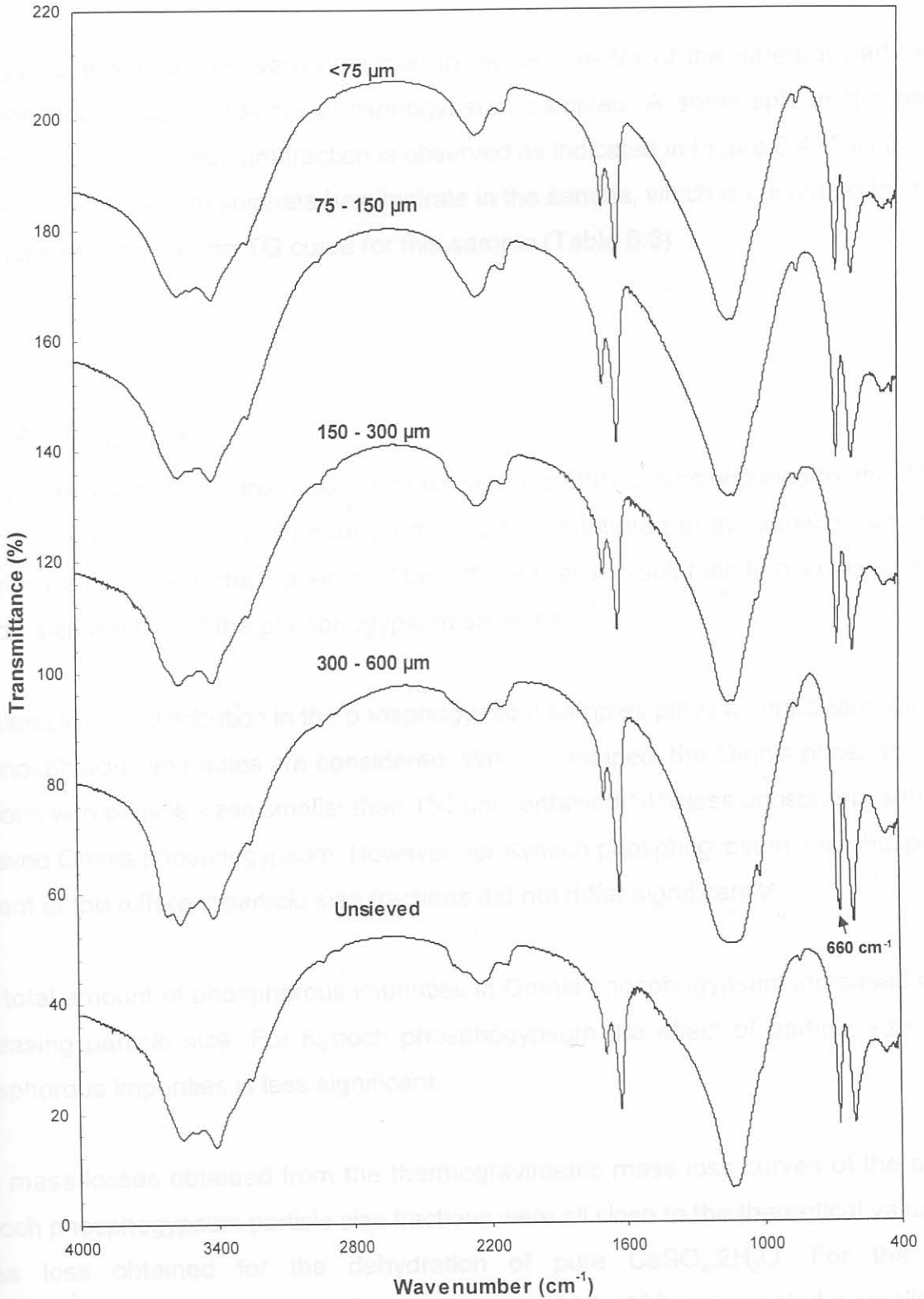


**Figure 6.4** The IR spectra of the particle size fractions and unsieved Omnia phosphogypsum



In the IR spectra obtained for the Kynoch phosphogypsum samples, the < 75 and 75 -150  $\mu\text{m}$  fractions, and also the sample of unsieved Kynoch phosphogypsum, contained higher amounts of dihydrate, resulting in a broadening of the 3000 - 4000  $\text{cm}^{-1}$  band.

No significant differences were observed in the IR spectra of the different particle size fractions and unsieved Omnia phosphogypsum samples. A small split in the peak at 660  $\text{cm}^{-1}$  for the 300 - 600  $\mu\text{m}$  fraction is observed as indicated in Figure 6.4. This indicates the presence of calcium sulphate hemihydrate in the sample, which is confirmed by the low mass loss obtained in the TG curve for this sample (Table 6.3).

## 6.4 Conclusion

The differences in the infrared spectra, mass loss and DSC curves obtained for the different particle size fractions of phosphogypsum, could be attributed to the variable amounts of impurities, as well as by the presence of the different calcium sulphate forms present in each particle size fraction of the phosphogypsum samples.

The particle size distribution in the phosphogypsum samples plays an important role when the phosphorous impurities are considered. When combined, the Omnia phosphogypsum fractions with particle sizes smaller than 150  $\mu\text{m}$  contained 14% less phosphorous than the unsieved Omnia phosphogypsum. However, for Kynoch phosphogypsum, the phosphorous content of the different particle size fractions did not differ significantly.

The total amount of phosphorous impurities in Omnia phosphogypsum increased with an increasing particle size. For Kynoch phosphogypsum the effect of particle size on the phosphorous impurities is less significant.

The mass losses obtained from the thermogravimetric mass loss curves of the different Kynoch phosphogypsum particle size fractions were all close to the theoretical value of the mass loss obtained for the dehydration of pure  $\text{CaSO}_4 \cdot 2\text{H}_2\text{O}$ . For the Omnia phosphogypsum, the particle size fraction between 300 - 600  $\mu\text{m}$  revealed a smaller mass



loss, which indicated the presence of calcium sulphate hemihydrate. All other Omnia particle size fractions contained mainly the dihydrate form of calcium sulphate. These results were confirmed by the FT-IR analyses of the respective particle size fractions for both Kynoch and Omnia phosphogypsum.

It seemed as if the Kynoch and Omnia phosphogypsum samples formed different types of calcium sulphate hemihydrate on dehydration. These results were obtained from the DSC curves of the respective phosphogypsum particle size fractions. Mainly the  $\alpha$ -Hemihydrate was obtained, as measured in a lower temperature from the dehydration of unsieved Omnia phosphogypsum; while the  $\beta$ -hemihydrate was primarily formed as observed in the higher dehydration temperatures for the unsieved Kynoch phosphogypsum. In the sieved particle size fractions of both Kynoch and Omnia phosphogypsum, both types of hemihydrates were produced.

The temperature at the peak maximum of the DSC curve serves as an indicative measure of the amount of impurities present in the fraction (Singh *et al*, 1996). There was no significant change in the amount of phosphorous impurities contained in the different particle size fractions of Kynoch phosphogypsum, and therefore the DSC peak maximums for the different particle size fractions could not be compared in this regard. The results obtained for Omnia phosphogypsum were difficult to analyse due to the unpredictable formation of the different hemihydrate species.

Naturally occurring gypsum and phosphogypsum contain various amounts of calcium sulphate dihydrate, calcium sulphate hemihydrate and anhydrous. The ratios in which these calcium sulphate forms occur can have a profound effect on the setting behaviour of cement, because their respective solubilities in water are significantly different from one another (Strydom and Potgieter, 1999). The dihydrate form is preferred in the cement industry.

# Chapter 7 Thermal and washing treatment of South African phosphogypsum

## 7.1 Introduction

The impurities that should be removed or neutralised, to be able to use phosphogypsum for the control of cement hydration, are mainly water-soluble phosphorous compounds, water-soluble fluoride, and phosphorous substituted in the gypsum crystal lattice. Only the effect of phosphorous impurities on the properties of Portland cement was investigated in this study.

Ölmez and Yilmaz (1998) successfully converted the phosphorous impurities in Turkish phosphogypsum into inactive, insoluble compounds by calcination of the sample and subsequent treatment with a milk of lime solution. Only water-soluble impurities can be removed by washing with water and milk of lime. Calcium hydrogen phosphate ( $\text{CaHPO}_4 \cdot 2\text{H}_2\text{O}$ ) substitutes in the gypsum crystal lattice to form a solid solution, because of its similar crystalline parameters when compared to  $\text{CaSO}_4 \cdot 2\text{H}_2\text{O}$ . The  $\text{HPO}_4^{2-}$  ions exist in exchanged state with  $\text{SO}_4^{2-}$  ions in these solid solutions. If the phosphogypsum is converted to the hemihydrate form, the  $\text{HPO}_4^{2-}$  ions can be removed by a calcination process, because of the subsequent change in crystal structure that occur (Ölmez and Erdem, 1989).

Naturally occurring gypsum and phosphogypsum contain various amounts of calcium sulphate dihydrate, calcium sulphate hemihydrate and anhydrite. The ratios in which these calcium sulphate forms occur can have a profound effect on the setting behaviour of cement, because their respective solubilities in water are significantly different from one another (Strydom and Potgieter, 1999). The dihydrate form is preferred in the cement industry.

The treatment of South African phosphogypsum samples by the method developed by Ölmez and Yilmaz (1988) will be investigated in this chapter. The aim of the study will be to reduce the amount of phosphorous impurities contained in South African phosphogypsum, and to ensure that the treated phosphogypsum occurs in the dihydrate form. The effect of the treated phosphogypsum as a set retarder in Portland cement will also be investigated.

## 7.2 Description of the experimental conditions and results of the phosphogypsum purification process applied by Ölmez and Yilmaz

In the process applied by Ölmez and Yilmaz (1988), the phosphogypsum sample was first oven-dried at 45°C. In order to investigate favourable conditions for the purification treatment, the sample was then treated with distilled water according to the procedure described in Table 7.1.

**Table 7.1 Experimental procedure followed by Ölmez and Yilmaz (1988) to remove the impurities in Turkish phosphogypsum**

	Solid mass (%)	Stirring time (min)	Temperature (°C)
<b>Step 1:</b> Optimisation of Solid ratio	12, 14, 18, 25	5	20
<b>Step 2:</b> Optimisation of Stirring time	14	1, 2, 3, 4, 5, 6, 9, 12, 15	20
<b>Step 3:</b> Optimisation of Temperature	14	5	20, 30, 40, 50, 60, 70



Two treatment methods for inactivating the impurities in phosphogypsum were used. The first method involved the neutralisation of the water-soluble impurities in the phosphogypsum with a 0.4% milk of lime solution. The untreated phosphogypsum sample was mixed with the milk of lime solution in a solid mass percentage of 14%, and was then stirred for 5 minutes at 20°C.

The other method claimed to remove the phosphorous substituted in the gypsum crystal lattice by means of thermal treatment. Untreated phosphogypsum was calcined at 130, 135, 140 and 150 °C for 5, 10, 15, 30 and 60 minutes respectively. The sample was then stirred in a 0.4% milk of lime solution for 5 minutes at 20°C.

The results obtained by Ölmez and Yilmaz (1998) are summarised in Table 7.2.

**Table 7.2 The percentages of phosphorous impurities in untreated and treated Turkish phosphogypsum samples, as reported by Ölmez and Yilmaz (1998)**

	Untreated	Washing with water	Washing with milk of lime	Calcination and washing with milk of lime	
				130 °C	150 °C
<b>Water-soluble</b>	0.25	0.07	Nil	Nil	Nil
<b>In crystal lattice</b>	0.51	0.51	0.51	0.20	Nil
<b>Water-insoluble</b>	0.26	0.26	0.51	0.82	1.02
<b>Total</b>	1.02	0.84	1.02	1.02	1.02

The results in the table indicated that all the water-soluble phosphorous impurities in phosphogypsum were converted into insoluble matter by washing it with milk of lime. There was no change in the amount of phosphorous impurities in the gypsum crystal lattice by washing the sample with milk of lime. By washing the sample with water, similar results were obtained. All the water-soluble and co-crystalline impurities were converted into insoluble compounds when the Turkish phosphogypsum samples were treated thermally followed by neutralisation with a milk of lime solution.

## 7.3 Experimental

### 7.3.1 Samples

Phosphogypsum was obtained from two South-African phosphoric acid producers, Omnia and Kynoch. Batch 1 of both of the Kynoch and Omnia phosphogypsum was used in this study. Samples were dried overnight at 45°C. Pure chemicals were obtained from Merck.

### 7.3.2 Instrumental analysis

Thermal analysis, Infrared analysis and X-ray fluorescence analysis were done as described in Chapter 5.2.

### 7.3.3 Surface area determinations

A Micromeritics Flowsorb II 2300 BET instrument was used to determine the surface areas of the gypsum samples. Nitrogen gas was adsorbed at low temperatures achieved by liquid nitrogen.

### 7.3.4 Cement tests

All cement control tests were performed according to standard methods described by the South African Bureau of Standards (SABS EN 196-1). The phosphogypsum samples as well as natural gypsum (used as reference) were interground with Hercules clinker. The SO<sub>3</sub> contents of the clinker and of each gypsum sample was first determined by a wet chemical analysis method, and each of the gypsum samples was then interground with the clinker to achieve a final SO<sub>3</sub> content of 2.3% in the cement. The sample was then milled to a fineness of approximately 3200 cm<sup>2</sup>/g Blaine surface area. The relative density, initial and final setting time and compressive strength of the cement after 2, 7 and 28 days were then determined.

The  $\text{SO}_3$  content of the gypsum samples was determined by a PPC internal standard test method, SR3 (1999): "Determination of gravimetric sulphate ( $\text{SO}_3$ )". In this method the sulphate ions are released by dissolving the gypsum in hydrochloric acid, and are then precipitated at the boiling point by a solution of barium chloride at a pH of 1.0-1.5. The  $\text{SO}_3$  content of the solution is then determined gravimetrically.

### 7.3.5 Experimental procedures followed to optimise the thermal and washing treatments for South African phosphogypsum

The method used by Ölmez and Yilmaz (1988) was applied to both the Omnia and Kynoch phosphogypsum. The purpose of the treatment was to investigate its effect on the total amount of phosphorous impurities contained in South African phosphogypsum, and to study the hydrated form of calcium sulphate obtained from the treatment. The process was adjusted for South African phosphogypsum, and entailed the optimisation of the following three individual steps:

1. The phosphogypsum sample was washed with distilled water to determine the optimum solid to liquid ratio, by means of surface area analysis, at constant temperature and pressure. Solid to liquid ratios used were 10, 12, 14, 16, and 18 mass percent solid.
2. By using the optimum solid to liquid ratio, obtained from the maximum surface area, in (1), the effect of different time periods was studied stirring the phosphogypsum sample in a 0.1% milk of lime solution. (A 0.1% milk of lime solution was used due to the low solubility of  $\text{Ca}(\text{OH})_2$ ). The stirring times applied were 1, 5, 10, 20 and 30 minutes.
3. The effect of thermal treatment on the phosphogypsum, for various time periods, was then studied. The temperatures used were 90, 100, 110, 120, 130 and 140°C, and samples were heated at these respective temperatures for 5, 10, 20, 30, 45, 60, 90 and 120 minutes.



Surface area measurements were used to determine the optimum treatment condition for each step. The change in surface area can be an indication of the reactivity of the compounds, as an increase in the surface area indicates an increase in the number of surface active points and nuclei, where the reaction starts (Bamford and Tipper, 1969).

#### 7.4.2 Treatment of phosphogypsum with milk of lime

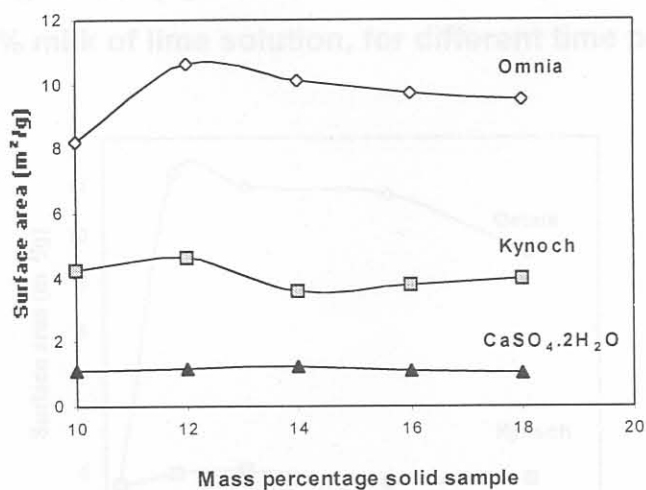
Figure 7.2 shows the results of the surface area measurements for the treatment of 12% (by mass) of solid with 0.1% milk of lime solution, for different time periods. Kynoch phosphogypsum and the Omnia phosphogypsum samples with a 0.1% milk of lime solution revealed a maximum surface area at 12 minutes.

### 7.4 Results of the optimisation of the thermal and washing treatments for the South African phosphogypsum samples

#### 7.4.1 Washing of phosphogypsum with distilled water

The results obtained from the surface area analyses for the washing of Kynoch phosphogypsum, Omnia phosphogypsum and  $\text{CaSO}_4 \cdot 2\text{H}_2\text{O}$  with distilled water in different mass percentages, are given in Figure 7.1.

Figure 7.1 Washing of the Omnia phosphogypsum, Kynoch phosphogypsum and pure  $\text{CaSO}_4 \cdot 2\text{H}_2\text{O}$  with distilled water in different mass percentages



Pure  $\text{CaSO}_4 \cdot 2\text{H}_2\text{O}$  was included as a reference. The Omnia phosphogypsum revealed a higher surface area, compared to the Kynoch phosphogypsum and  $\text{CaSO}_4 \cdot 2\text{H}_2\text{O}$ . Both Kynoch and Omnia phosphogypsum revealed a maximum value for the surface area, and

thus reactivity, when the sample was stirred in distilled water at a solid mass percentage of 12%.

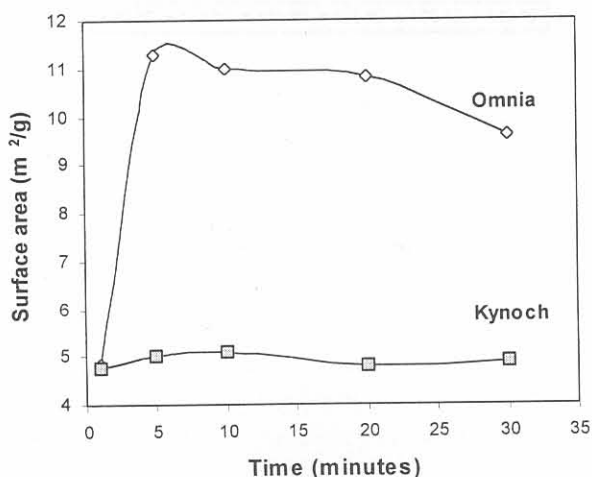
#### 7.4.2 Treatment of phosphogypsum with milk of lime

Figure 7.2 represents the results obtained for the treatment of 12% (by mass) solid for the Kynoch phosphogypsum and the Omnia phosphogypsum samples with a 0.1% milk of lime solution. These suspensions were stirred for different time periods, after which it was filtered and dried overnight at 45°C.

The Omnia phosphogypsum revealed a significant increase in surface area, and thus reactivity, when treated with milk of lime. This increase in surface area for the Omnia phosphogypsum can possibly be explained by the hydration of calcium sulphate hemihydrate, the main constituent of untreated Batch 1 Omnia phosphogypsum. Because the untreated Kynoch phosphogypsum consists mainly of the dihydrate form of calcium sulphate, no significant increase (due to hydration) was observed in its surface area.

For the Omnia phosphogypsum, an optimum surface area was obtained after approximately 5 minutes of stirring, while it was obtained after 10 minutes for the Kynoch phosphogypsum.

**Figure 7.2** Stirring of 12% (by mass) of solid for the phosphogypsum samples with a 0.1% milk of lime solution, for different time periods



### 7.4.3 Thermal treatment of phosphogypsum

The last step of the process involved the thermal treatment of the Kynoch phosphogypsum, Omnia phosphogypsum and pure  $\text{CaSO}_4 \cdot 2\text{H}_2\text{O}$  at different temperatures for different time periods. The results, given in Figures 7.3, 7.4 and 7.5, indicate that all three species reached a maximum surface area when the samples were treated between 30 - 40 minutes at a temperature of 140°C.

Figure 7.3 The thermal treatment of Omnia phosphogypsum for different time periods at different temperatures

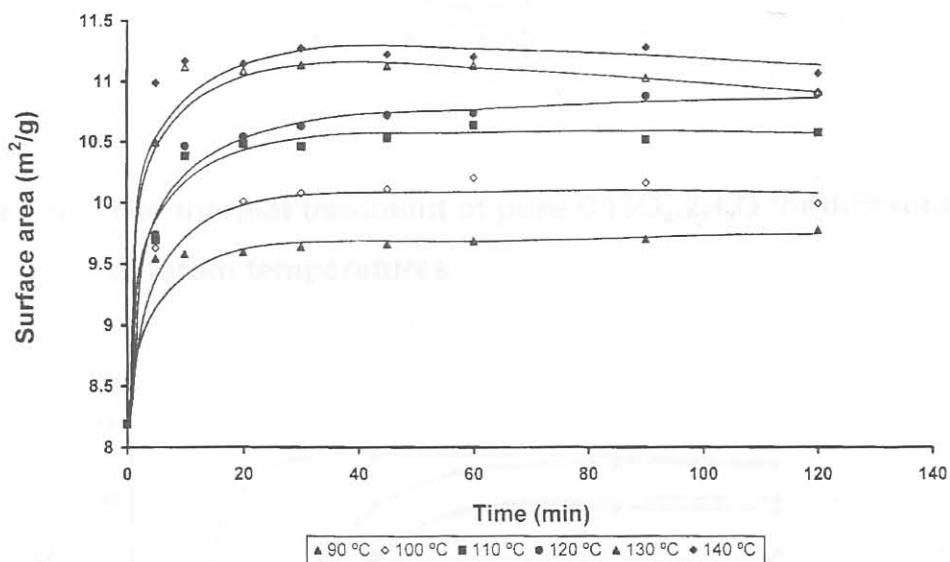




Figure 7.4 The thermal treatment of Kynoch phosphogypsum for different time periods at different temperatures

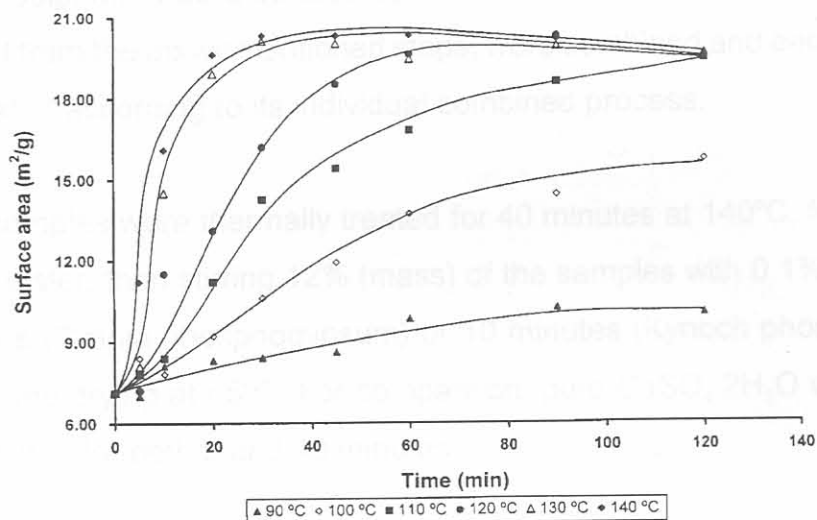
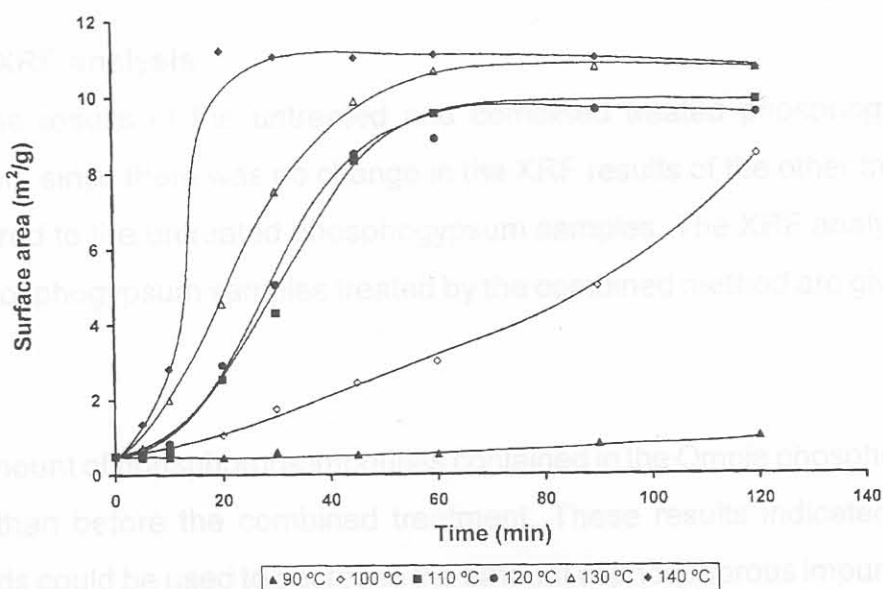


Figure 7.5 The thermal treatment of pure CaSO<sub>4</sub>·2H<sub>2</sub>O for different time periods at different temperatures



#### **7.4.4 Treatment of the different phosphogypsum samples by combining the washing and thermal treatment methods**

The effect of combining the washing and thermal treatment of the respective phosphogypsum samples on the amount of phosphorous impurities and hydrate form of calcium sulphate was also studied. The results of the optimum treatment conditions, obtained from the abovementioned steps, were combined and each of the gypsum species was treated according to its individual combined process.

All the samples were thermally treated for 40 minutes at 140°C, followed by washing with distilled water, then stirring 12% (mass) of the samples with 0.1% milk of lime solution for 5 minutes (Omnia phosphogypsum) or 10 minutes (Kynoch phosphogypsum) and finally filtering and drying at 45°C. For comparison, pure  $\text{CaSO}_4 \cdot 2\text{H}_2\text{O}$  was stirred in the milk of lime solution for both 5 and 10 minutes.

### **7.5 Characterization of the untreated and treated phosphogypsum samples**

#### **7.5.1 XRF analysis**

Only the results of the untreated and combined treated phosphogypsum samples are provided, since there was no change in the XRF results of the other treated samples when compared to the untreated phosphogypsum samples. The XRF analyses of the untreated and phosphogypsum samples treated by the combined method are given in Tables 7.3 and 7.4.

The amount of phosphorous impurities contained in the Omnia phosphogypsum was slightly lower than before the combined treatment. These results indicated that none of these methods could be used to decrease the amount of phosphorous impurities, contained in the South African phosphogypsum, significantly.

Table 7.3 The XRF results of the untreated and treated Batch 1 Omnia phosphogypsum and Kynoch phosphogypsum samples

Compounds (%)	Kynoch phosphogypsum		Omnia phosphogypsum	
	Untreated	Combined treatment	Untreated	Combined treatment
Al <sub>2</sub> O <sub>3</sub>	0.11	0*	0.04	0.02
CaO	33.04	34.57	38.38	39.80
Cr <sub>2</sub> O <sub>3</sub>	0	0.12	0	0
Fe <sub>2</sub> O <sub>3</sub>	0.09	0.25	0.05	0.06
K <sub>2</sub> O	0	0.03	0	0
MgO	0.13	0	0.16	0.09
MnO	0	0	0	0
Na <sub>2</sub> O	0	0	0	0
P <sub>2</sub> O <sub>5</sub>	<b>0.71</b>	<b>0.65</b>	<b>1.68</b>	<b>1.50</b>
SiO <sub>2</sub>	0.16	0.18	0	0
TiO <sub>2</sub>	0	0	0	0
V <sub>2</sub> O <sub>5</sub>	0	0	0	0
ZrO <sub>2</sub>	0	0.04	0	0
Sr	0.28	0.38	0.32	0.33
SO <sub>3</sub>	44.06	46.06	51.24	52.34
Loss on ignition	22.21	19.29	10.06	6.99
<b>Total</b>	100.79	101.57	101.93	101.13

\*0 means that the compound was present in a quantity below the detection limit



**Table 7.4** The XRF results of the untreated and treated Batch 1 Omnia phosphogypsum and Kynoch phosphogypsum samples, normalised to a loss free basis

Compounds (%)	Kynoch phosphogypsum		Omnia phosphogypsum	
	Untreated	Combined treatment	Untreated	Combined treatment
Al <sub>2</sub> O <sub>3</sub>	0.14	0*	0.04	0.02
CaO	42.05	42.02	41.79	41.43
Cr <sub>2</sub> O <sub>3</sub>	0	0.15	0	0
Fe <sub>2</sub> O <sub>3</sub>	0.11	0.30	0.05	0.06
K <sub>2</sub> O	0	0.04	0	0
MgO	0.17	0	0.17	0.10
P <sub>2</sub> O <sub>5</sub>	<b>0.90</b>	<b>0.79</b>	<b>1.83</b>	<b>1.59</b>
SiO <sub>2</sub>	0.20	0.22	0	0
ZrO <sub>2</sub>	0	0.05	0	0
Sr	0.36	0.46	0.35	0.35
SO <sub>3</sub>	56.07	55.98	55.79	55.60

\*0 means that the compound was present in a quantity below the detection limit

### 7.5.2 Thermal analysis

The DSC curves given in Figures 7.6, 7.7, and 7.8, were obtained by encapsulating the samples in hermetic aluminium pans. This method resolved the two peaks, thus separating the two hydration reactions, except for the Omnia phosphogypsum which contains mainly hemihydrate.

Figure 7.6 The DSC curves for treated and untreated Omnia phosphogypsum samples in crimped Al hermetic pans

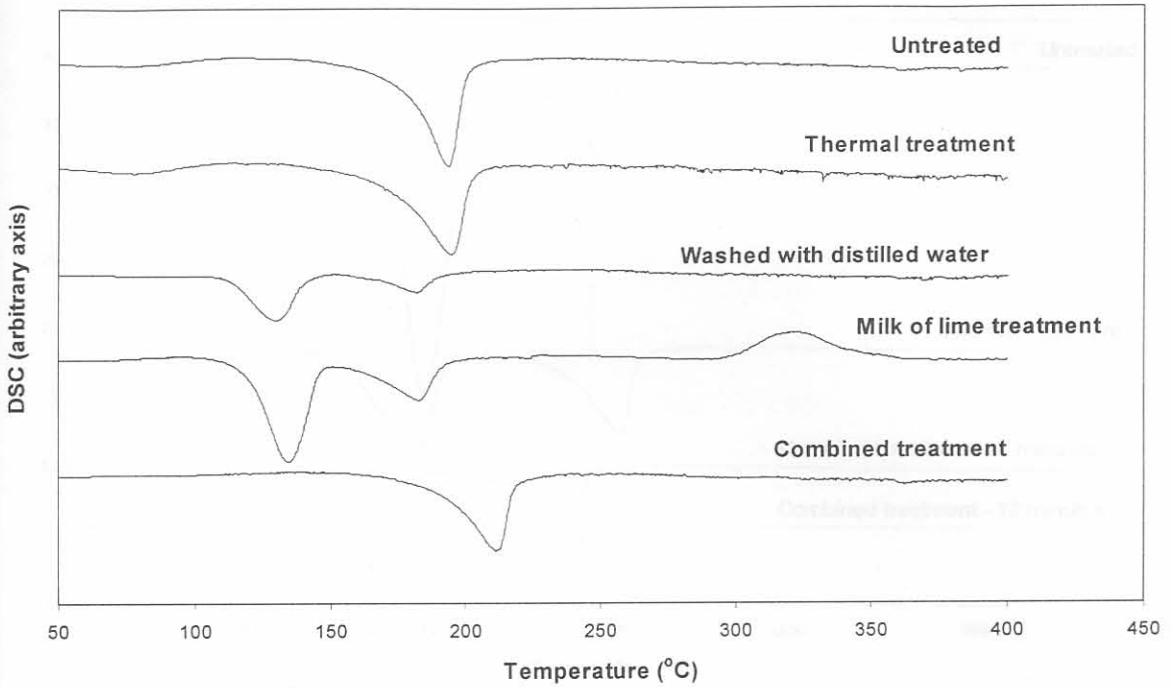
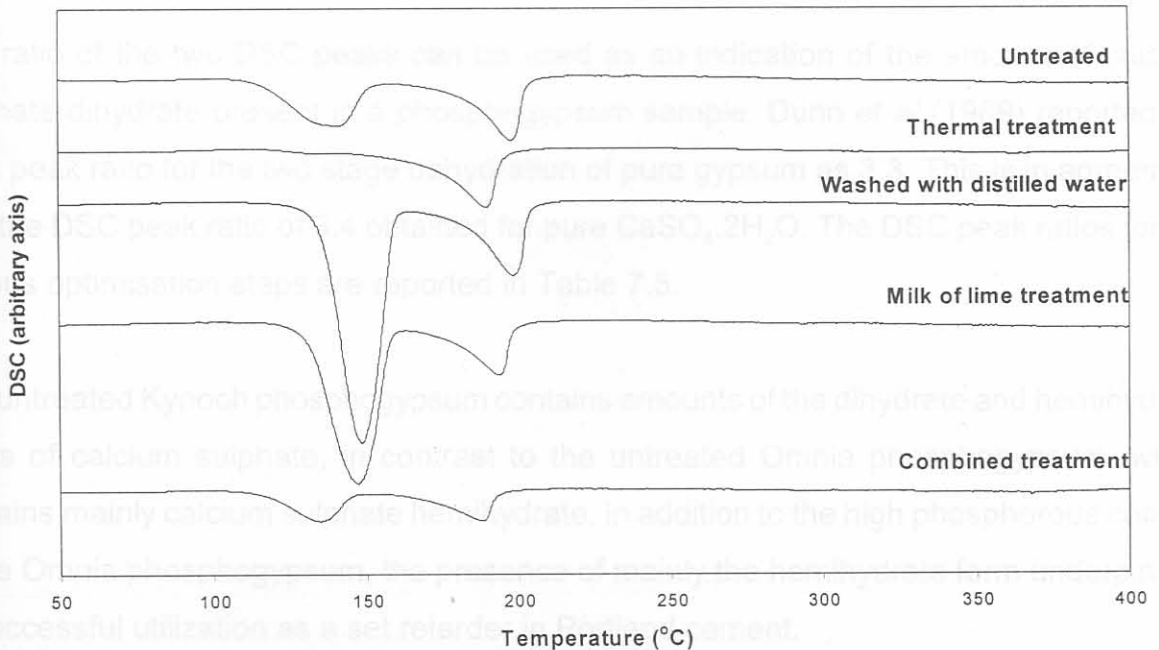
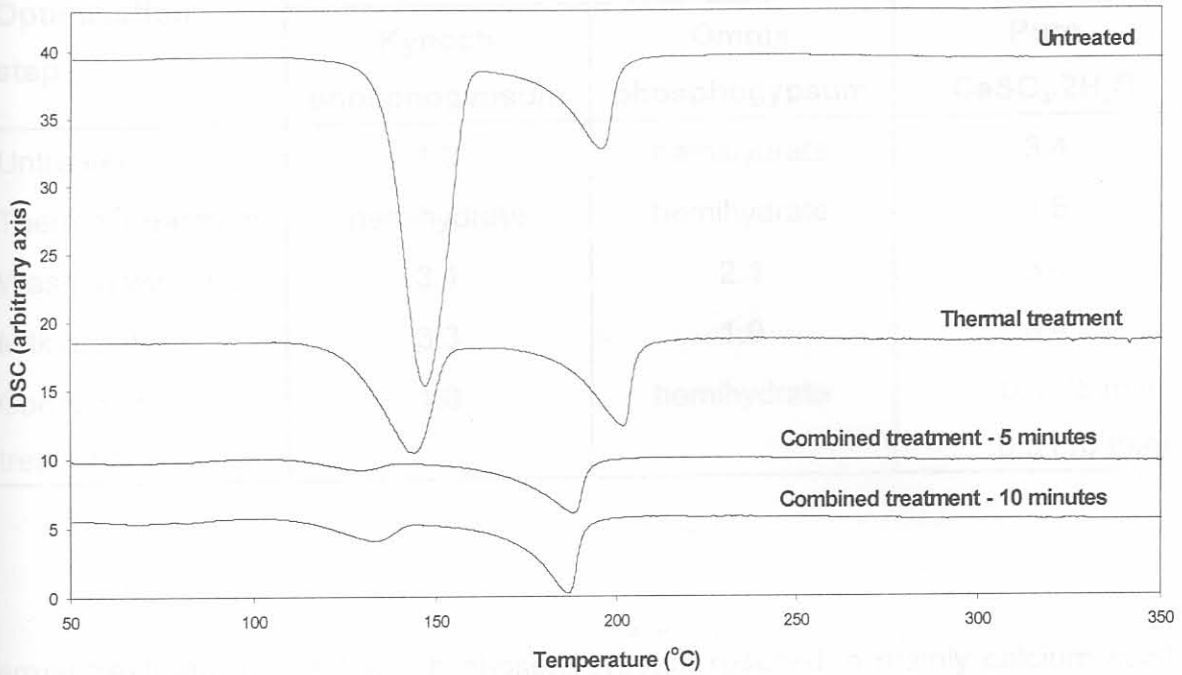


Figure 7.7 The DSC curves for treated and untreated Kynoch phosphogypsum samples in crimped Al hermetic pans



**Figure 7.8** The DSC curves for treated and untreated  $\text{CaSO}_4 \cdot 2\text{H}_2\text{O}$  samples in crimped Al hermetic pans



Pure gypsum and natural gypsum are used successfully as set retarders in Portland cement. The ratio in which the different calcium sulphate species occur in the phosphogypsum, can have a major influence on its behaviour as a set retarder.

The ratio of the two DSC peaks can be used as an indication of the amount of calcium sulphate dihydrate present in a phosphogypsum sample. Dunn *et al* (1989) reported the DSC peak ratio for the two stage dehydration of pure gypsum as 3.3. This is in agreement with the DSC peak ratio of 3.4 obtained for pure  $\text{CaSO}_4 \cdot 2\text{H}_2\text{O}$ . The DSC peak ratios for the various optimisation steps are reported in Table 7.5.

The untreated Kynoch phosphogypsum contains amounts of the dihydrate and hemihydrate forms of calcium sulphate, in contrast to the untreated Omnia phosphogypsum, which contains mainly calcium sulphate hemihydrate. In addition to the high phosphorous content in the Omnia phosphogypsum, the presence of mainly the hemihydrate form underpins its unsuccessful utilization as a set retarder in Portland cement.



Table 7.5 The DSC peak ratios obtained for the different optimisation steps

Optimisation step	DSC peak ratio		
	Kynoch phosphogypsum	Omnia phosphogypsum	Pure $\text{CaSO}_4 \cdot 2\text{H}_2\text{O}$
Untreated	1.0	hemihydrate	3.4
Thermal treatment	hemihydrate	hemihydrate	1.5
Washed with $\text{H}_2\text{O}$	3.1	2.1	3.4
Milk of lime	3.3	1.9	3.4
Combined treatment	1.0	hemihydrate	0.1 (5 min) 0.3 (10 min)

Thermal treatment of the Kynoch phosphogypsum resulted in mainly calcium sulphate hemihydrate being formed, in contrast to pure  $\text{CaSO}_4 \cdot 2\text{H}_2\text{O}$ , which easily rehydrates back to the dihydrate form. As expected, the Omnia phosphogypsum remained mainly in the hemihydrate form.

When washed with distilled water, the Kynoch phosphogypsum was converted to a mixture of calcium sulphate dihydrate and calcium sulphate hemihydrate as the DSC peak ratio of 3.1 indicated. The DSC peak ratio of the hydrates formed for the Omnia phosphogypsum increased to 2.1, indicating the formation of a small amount of calcium sulphate dihydrate.

Stirring with a 0.1% milk of lime solution resulted in an increase in the DSC peak ratio of the Kynoch phosphogypsum to 3.3, which is in good agreement with that obtained for pure gypsum. For the Omnia phosphogypsum a DSC peak ratio of 1.9 was obtained, which indicated that the conversion to the dihydrate form was less successful if compared to washing with distilled water.

For both the Omnia phosphogypsum and the Kynoch phosphogypsum, the DSC curves for the combined treatment are similar to that of the untreated samples. However, when pure

$\text{CaSO}_4 \cdot 2\text{H}_2\text{O}$  was treated by the combined treatment, mainly the hemihydrate form is formed. A longer stirring period seemed to favour the formation of calcium sulphate dihydrate.

### 7.5.3 Infrared analysis

The IR spectra of the untreated phosphogypsum, treated phosphogypsum and pure  $\text{CaSO}_4 \cdot 2\text{H}_2\text{O}$  are given in Figures 7.9 and 7.10. The band characteristics  $832\text{ cm}^{-1}$ , attributed to the water-insoluble phosphorous impurities, could still be observed in all the treated and untreated phosphogypsum samples.

When the IR spectra of the untreated and combined treated Omnia phosphogypsum samples were compared with that of pure  $\text{CaSO}_4 \cdot 2\text{H}_2\text{O}$ , it was clear that these samples did not consist of only calcium sulphate dihydrate. For the treated phosphogypsum samples, a small split in the peaks at  $600\text{ cm}^{-1}$  and  $667\text{ cm}^{-1}$  indicated the presence of calcium sulphate hemihydrate or anhydrite. When the peaks in the region between  $1600 - 1700\text{ cm}^{-1}$  are compared, the untreated and combined treated Omnia phosphogypsum samples showed only a single peak in comparison to the double peak of  $\text{CaSO}_4 \cdot 2\text{H}_2\text{O}$ . This also indicated a decrease in the amount of water of crystallization present in the treated samples. For both phosphogypsum samples, the peaks between  $3400 - 4000\text{ cm}^{-1}$ , due to the presence of water, were much narrower than that of the pure  $\text{CaSO}_4 \cdot 2\text{H}_2\text{O}$  samples. This confirms the results obtained by TG/DSC analyses.

The IR spectra obtained for the treated and untreated Kynoch phosphogypsum samples were similar to that of pure  $\text{CaSO}_4 \cdot 2\text{H}_2\text{O}$ , except for the small peak at  $832\text{ cm}^{-1}$  due to the phosphorous impurities contained in phosphogypsum. This indicated that the untreated and treated Kynoch phosphogypsum samples consisted of mainly the dihydrate form of calcium sulphate.

Figure 7.9 The IR spectra of the untreated and treated Omnia phosphogypsum samples and pure  $\text{CaSO}_4 \cdot 2\text{H}_2\text{O}$

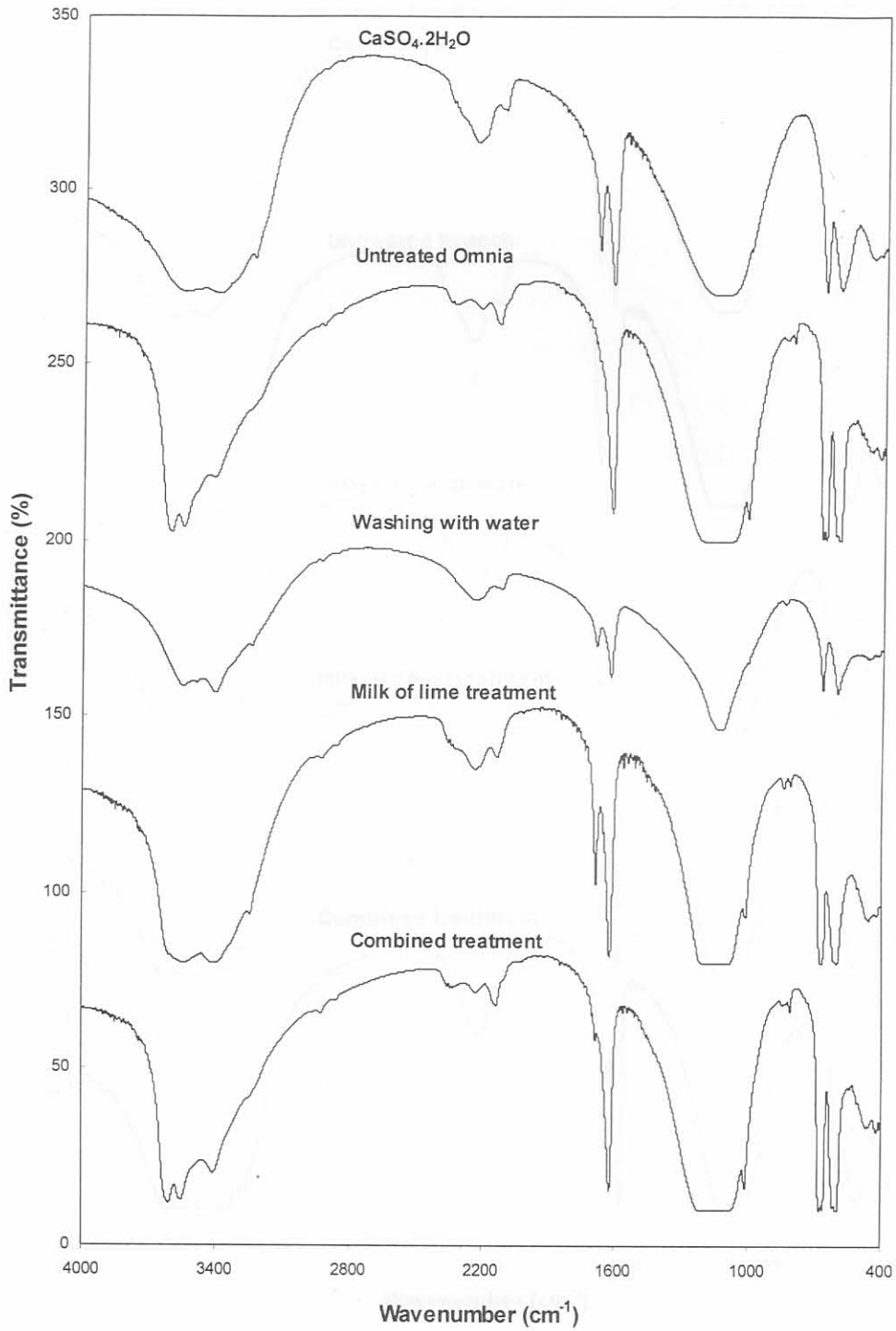
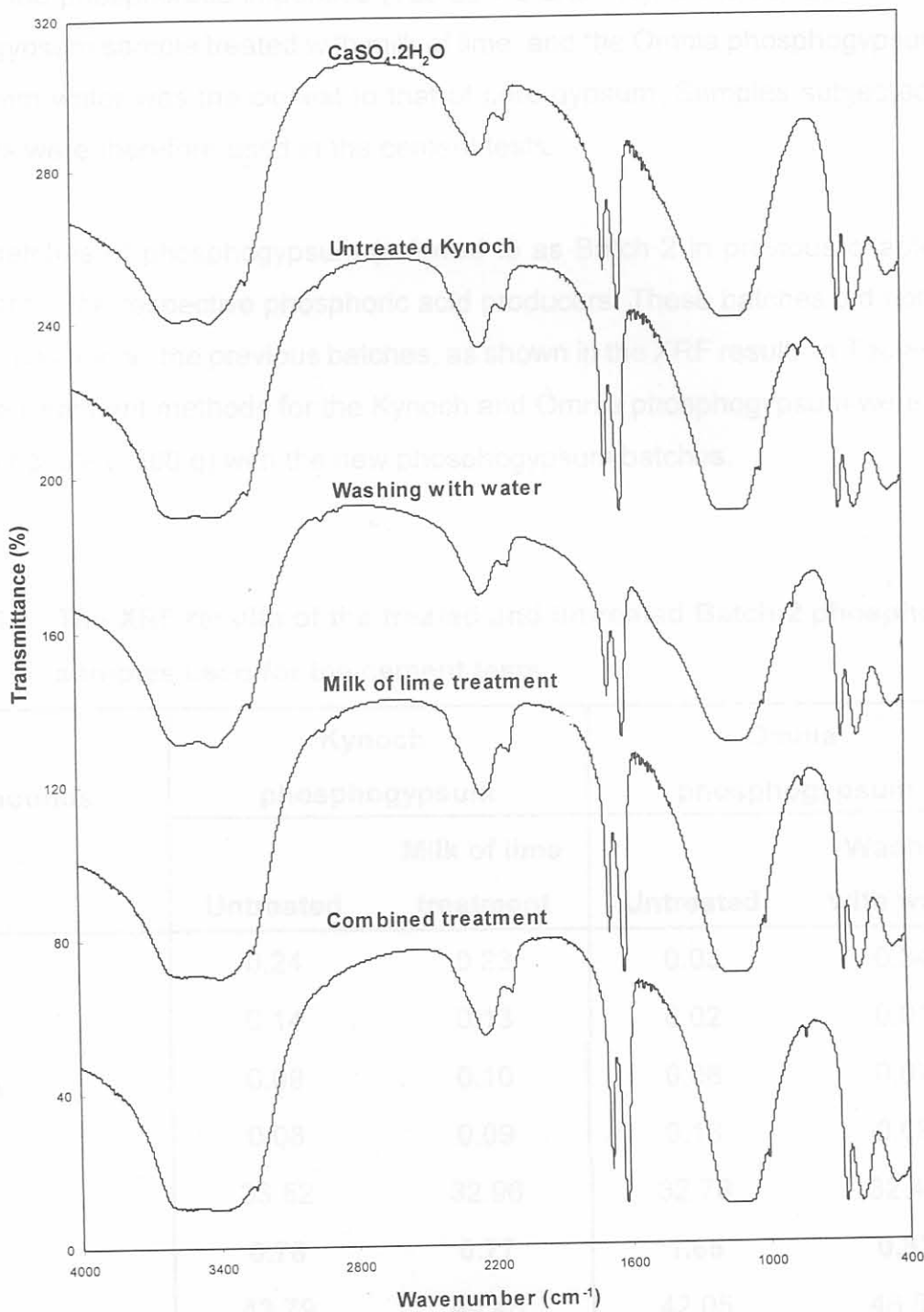




Figure 7.10 The IR spectra of the untreated and treated Kynoch phosphogypsum samples and pure  $\text{CaSO}_4 \cdot 2\text{H}_2\text{O}$



SiO <sub>2</sub>	0.10	0.10	0.09	0.09
Al <sub>2</sub> O <sub>3</sub>	0.02	0.02	0.02	0.02
Fe <sub>2</sub> O <sub>3</sub>	0.08	0.10	0.09	0.09
MgO	0.03	0.09	0.09	0.09
CaO	52.52	32.96	32.78	32.96
P <sub>2</sub> O <sub>5</sub>	0.00	0.00	0.00	0.00
SO <sub>2</sub>	43.79	32.96	42.05	43.50
Loss on ignition	20.96	21.80	22.64	21.72
Total	99.80	100.54	99.62	102.40

### 7.5.4 Cement tests

Although the thermal and washing treatment methods did not prove to be successful in removing the phosphorous impurities (Tables 7.3 and 7.4), the DSC ratio of the Kynoch phosphogypsum sample treated with milk of lime, and the Omnia phosphogypsum sample washed with water was the closest to that of pure gypsum. Samples subjected to these treatments were therefore used in the cement tests.

Second batches of phosphogypsum (referred to as Batch 2 in previous chapters) were obtained from the respective phosphoric acid producers. These batches did not have the same composition as the previous batches, as shown in the XRF results in Tables 7.6. The respective treatment methods for the Kynoch and Omnia phosphogypsum were repeated on a larger scale ( $\pm 300$  g) with the new phosphogypsum batches.

**Table 7.6 The XRF results of the treated and untreated Batch 2 phosphogypsum samples used for the cement tests**

Compounds (%)	Kynoch phosphogypsum		Omnia phosphogypsum	
	Untreated	Milk of lime treatment	Untreated	Washed with water
SiO <sub>2</sub>	0.24	0.23	0.03	0.34
Al <sub>2</sub> O <sub>3</sub>	0.14	0.13	0.02	0.01
Fe <sub>2</sub> O <sub>3</sub>	0.09	0.10	0.08	0.07
MgO	0.08	0.09	0.13	0.08
CaO	33.52	32.96	32.78	32.46
P <sub>2</sub> O <sub>5</sub>	<b>0.78</b>	<b>0.77</b>	<b>1.65</b>	<b>0.87</b>
SO <sub>3</sub>	43.79	44.46	42.05	46.85
Loss on ignition	20.96	21.80	22.88	21.72
<b>Total</b>	99.60	100.54	99.62	102.40

**Table 7.7** The XRF results of the treated and untreated Batch 2 phosphogypsum samples used for the cement tests, normalised to a loss free basis

Compounds (%)	Kynoch phosphogypsum		Omnia phosphogypsum	
	Milk of lime		Washed	
	Untreated	treatment	Untreated	with water
SiO <sub>2</sub>	0.31	0.29	0.04	0.42
Al <sub>2</sub> O <sub>3</sub>	0.18	0.17	0.03	0.01
Fe <sub>2</sub> O <sub>3</sub>	0.11	0.13	0.10	0.09
MgO	0.10	0.11	0.17	0.10
CaO	42.62	41.86	42.72	40.23
P <sub>2</sub> O <sub>5</sub>	<b>0.99</b>	<b>0.98</b>	<b>2.15</b>	<b>1.08</b>
SO <sub>3</sub>	55.68	56.46	54.79	58.07

The XRF results for the untreated and treated phosphogypsum samples, used in the cement tests, are given in Tables 7.6 and 7.7. The amount of phosphorous impurities in the Batch 2 Kynoch phosphogypsum was the same as before treatment. A significant decrease in the amount of phosphorous impurities was observed when the Batch 2 Omnia phosphogypsum sample was washed with water.

The cement test results for the untreated phosphogypsum, treated phosphogypsum and natural gypsum are listed in Table 7.8. The initial and final setting times of cement containing untreated and treated phosphogypsum samples differed significantly from cement containing natural gypsum. The results indicated that both the initial and final setting times of the cement mixes was markedly retarded when the untreated Kynoch and Omnia phosphogypsum samples were used instead of natural gypsum.

This retardation effect of phosphogypsum can be ascribed to the suppression of cement hydration. The liquid phase in the cement paste generally has high alkalinity. Due to the high concentration of lime and alkali, insoluble calcium phosphate salts are produced near



the cement particles soon after phosphorous enters into the alkaline liquid phase, and subsequently, they cover the surface of the cement grains, providing a protective barrier against the attack of water (Singh, 1987).

**Table 7.8 Results of the cement test performed on treated and untreated Kynoch, Omnia phosphogypsum samples and natural gypsum**

Test	O-U <sup>a</sup>	O-T <sup>b</sup>	K-U <sup>c</sup>	K-T <sup>d</sup>	N-G <sup>e</sup>
SO <sub>3</sub> content of gypsum (%)	47.24	46.39	46.68	45.70	42.50
Gypsum added to clinker (%)	3.46	3.52	3.50	3.58	3.85
Specific Surface of cement (cm <sup>2</sup> /g)	3470	3175	3200	3250	3200
Relative density of cement	3.15	3.10	3.10	3.12	3.10
Initial setting time (min)	243	257	354	274	140
Final setting time (h)	5.11	5.25	6.75	5.75	3.25
2-day Compressive strength (MPa)	17.12	17.74	17.35	16.96	20.33
7-day Compressive strength (MPa)	33.91	34.15	34.41	35.36	38.04
28-day Compressive strength (MPa)	46.07	48.01	47.25	44.83	49.10

<sup>a</sup> Untreated Omnia phosphogypsum

<sup>b</sup> Omnia phosphogypsum washed with distilled water

<sup>c</sup> Untreated Kynoch phosphogypsum

<sup>d</sup> Kynoch phosphogypsum treated with Ca(OH)<sub>2</sub>

<sup>e</sup> Natural Gypsum

There was no significant effect on the setting times when Omnia phosphogypsum was treated with water. However, the treated Kynoch phosphogypsum sample, when compared to the untreated sample, revealed a favourable decrease in both the initial and final setting times. The initial and final setting times of the cement samples containing the milk of lime treated Kynoch phosphogypsum possibly decreased due to the inactivation of some of the phosphorous impurities, and also due to the higher amount of calcium sulphate dihydrate present in the treated sample.

## 7.6 Conclusion

From the XRF and IR results it is evident that by applying the method used by Ölmez and Yilmaz (1988), the phosphorous impurities contained in the South African phosphogypsum samples could not be removed successfully, although some of the phosphorous impurities contained in the Batch 2 Omnia phosphogypsum could be removed partially by the washing treatment.

For the Omnia phosphogypsum, Kynoch phosphogypsum and pure  $\text{CaSO}_4 \cdot 2\text{H}_2\text{O}$ , combination of the thermal and washing processes suppressed the formation of the dihydrate form of calcium sulphate. This combined process was therefore unsuitable for treatment of the phosphogypsum samples used.

When washing the Omnia phosphogypsum with distilled water, a DSC peak ratio of 2.1 was obtained, in comparison to the absence of calcium sulphate dihydrate before treatment. Stirring the Kynoch phosphogypsum sample with milk of lime solution resulted in a DSC peak ratio of 3.3, which is similar to that of pure gypsum.

Both the initial and final setting times of the cement mixes was markedly retarded when the untreated Kynoch and Omnia phosphogypsum samples were used instead of natural gypsum. Treatment of the Kynoch phosphogypsum sample with a milk of lime solution resulted in inactivation of some of the water-soluble phosphorous impurities, and to a higher amount of calcium sulphate dihydrate present in the treated sample. This sample revealed a favourable decrease in both the initial and final setting times when compared to the untreated Kynoch phosphogypsum samples. Treatment of Omnia phosphogypsum with water did not improve the performance of the Omnia phosphogypsum as a set retarder in Portland cement. Although the amount of phosphorous impurities contained in Omnia phosphogypsum was reduced by the washing treatment, no significant change in the setting behaviour was observed.

Application of these methods to South African phosphogypsum did not remove the phosphorous impurities successfully. Therefore, alternative methods should be investigated to reduce the harmful impurities contained in phosphogypsum.



## Chapter 8 Sulphuric acid treatment of South African phosphogypsum

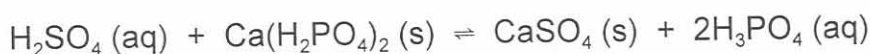
### 8.1 Introduction

Jarosiński (1994) described a method in which he first leached the phosphogypsum sample in a 12% (by mass) sulphuric acid solution to recover rare earth elements, followed by a conversion into the  $\beta$ -anhydrite form of calcium sulphate in a 50% sulphuric acid solution. The purpose of this study was to investigate the properties of anhydrite cement by using  $\beta$ -anhydrite obtained from purified phosphogypsum. The procedure he followed to obtain the purified anhydrite is summarised in Table 8.1.

**Table 8.1 Experimental conditions followed by Jarosiński (1994) to purify and recrystallize anhydrite phosphogypsum**

Parameters	Stage	
	Leaching	Conversion
Temperature ( $^{\circ}\text{C}$ )	40	50
Sulphuric acid concentration (% m/m)	12	50
Solid/liquid mass ratio	1 : 2	1 : 1
Stirring time (min)	45	120
Standardized mechanical agitation, revolution ( $\text{min}^{-1}$ )	150	150

Jarosiński found this method to be successful in removing the undesirable impurities such as compounds of phosphorous, fluorine and sodium. He claimed that the following equilibrium process takes place in the direction of  $\text{CaSO}_4$  during the conversion:





In this chapter, the application of this method to South African phosphogypsum is discussed. However, the final product to be obtained for use in Portland cement is preferred to be  $\text{CaSO}_4 \cdot 2\text{H}_2\text{O}$  and not the anhydrite form as required by Jarosiński's method.

## 8.2 Experimental

### 8.2.1 Samples

Phosphogypsum samples were obtained from two South-African phosphoric acid producers, Omnia and Kynoch. Batch 1 of both the Kynoch and Omnia phosphogypsum was used for the initial small scale treatment, while Batch 2 of both phosphogypsums were used for the large scale treatments and optimization of the method. The samples were dried overnight at  $45^\circ\text{C}$ .

### 8.2.2 Instrumental analysis

Thermal analysis, Infrared analysis and X-ray fluorescence analysis were done as described in Chapter 5.2.

### 8.2.3 Jarosiński's method applied to South African phosphogypsum

The method followed by Jarosiński was adapted for the Kynoch phosphogypsum and Omnia phosphogypsum samples. Batch 1 of both of the Kynoch and Omnia phosphogypsum was used. A heater stirrer was used to perform the leaching and conversion steps. A solid:liquid mass ratio of 1:2 for the Omnia phosphogypsum formed a paste which could not be stirred by the stirrer. This resulted in using a solid:liquid ratio of 1:4 for the Omnia phosphogypsum and 1:2 for the Kynoch phosphogypsum. The experimental conditions followed, are summarised in Table 8.2.

**Table 8.2 Adapted experimental conditions used to purify and recrystallize Omnia and Kynoch phosphogypsum**

Parameters	Leaching		Conversion
	Kynoch	Omnia	(Omnia and Kynoch)
Temperature (°C)	40	40	50
Sulphuric acid concentration (% m/m)	12	12	50
Solid:liquid mass ratio	1 : 2	1 : 4	1 : 1
Stirring time (min)	45	45	120
Sample mass (g)	15.0 g	15.0 g	-

#### 8.2.4 Sulphuric acid treatment of phosphogypsum at a larger scale

Batch 2 of both of the Kynoch and Omnia phosphogypsum was used in this study. To be able to perform cement tests, the above method had to be repeated on a larger scale so that enough gypsum could be obtained. The method was performed, starting with 300 g of each of the phosphogypsums.

#### 8.2.5 Optimisation of the sulphuric acid method

Batch 2 of both of the Kynoch and Omnia phosphogypsum was used to optimize the sulphuric acid treatment method. Optimisation of the method was performed on the following parameters: temperature, concentration of sulphuric acid, time and solid:liquid ratio. The optimisation was measured in terms of the least amount of phosphorous impurities present in the treated samples, as well as the highest amount of calcium sulphate dihydrate. The aim was also to combine the leaching and conversion stages into one purification step, since this would be more cost-effective and less time consuming. Table 8.3 describes the experimental method followed during optimisation.

**Table 8.3 Experimental parameters used for optimisation of the sulphuric acid treatment of phosphogypsum**

Order of Optimisation	Temperature (°C)	H <sub>2</sub> SO <sub>4</sub> concentration (% m/m)	Time (min)	Solid:liquid ratio
1	23, 27, 40, 51, 60, 69	12	60	1:4
2	23	5, 10, 20, 30, 40, 50	60	1:4
3	23	5 (Omnia) 20 (Kynoch)	15, 30, 45, 60, 90, 120, 180, 360	1:4
4	23	5 (Omnia) 20 (Kynoch)	30	1:1, 1:2, 1:3, 1:4

### 8.2.6 The optimized sulphuric acid method on a large scale

Batch 2 of both of the Kynoch and Omnia phosphogypsum was used in this study. The untreated phosphogypsum samples were dried overnight at 45°C. Sample masses of 300 g were used. The samples were stirred in sulphuric acid (5% m/m for Omnia phosphogypsum and 20% m/m for the Kynoch phosphogypsum) for 30 minutes at room temperature, at a solid:liquid mass ratio of 1:4. Samples were then filtered and washed with a saturated milk of lime solution and deionised water, and dried overnight at 45°C.

### 8.2.7 Sulphuric acid treatment combined with thermal treatment

Batch 2 of both of the Kynoch and Omnia phosphogypsum was used in this study. The sulphuric acid treatment was combined with thermal treatment by heating the phosphogypsum samples at 160°C until a constant mass was obtained after approximately 3 hours (i.e. until all the calcium sulphate dihydrate and hemihydrate was converted to the anhydrite). The samples were then treated in sulphuric acid according to the optimum method obtained in the optimisation discussed in Chapter 8.2.5. A solid:liquid mass ratio of 1:4 formed a paste which could not be stirred by the stirrer. It was found that by using a solid:liquid ratio of approximately 1:10, a manageable paste was formed.



Therefore, the samples were thermally treated at 160°C for 3 hours, followed by the acid treatment at a solid:liquid ratio of 1:10 at room temperature for 30 minutes in a 5% (m/m) H<sub>2</sub>SO<sub>4</sub> solution for Omnia phosphogypsum and a 20% (m/m) H<sub>2</sub>SO<sub>4</sub> solution for the Kynoch phosphogypsum.

### **8.2.8 Optimisation of the combined thermal and acid treating method**

Batch 2 of both of the Kynoch and Omnia phosphogypsum was used to study the effect of sulphuric acid concentration in the combined thermal and acid treating method. Sulphuric acid concentrations used were 1, 5, 10, 20 and 50% m/m. The optimisation was measured in terms of the least amount of phosphorous impurities present in the treated samples, as well as the highest amount of calcium sulphate dihydrate.

### **8.2.9 The combined thermal and acid treatment of phosphogypsum at a larger scale**

Batch 2 of both of the Kynoch and Omnia phosphogypsum was used in this study. To be able to perform cement tests, the above method had to be repeated on a larger scale so that enough gypsum can be obtained.

The method was performed, starting with 300 g of each of the phosphogypsums. To ensure that the samples were completely converted to anhydrite, the samples were thermally treated overnight at 160°C. This was then followed by the acid treatment at a solid:liquid ratio of 1:10 at room temperature for 45 minutes in a 5% (m/m) H<sub>2</sub>SO<sub>4</sub> solution for both phosphogypsum samples. The samples were then filtered and repeatedly washed with milk of lime and water, and was then dried overnight at 45°C.

### **8.2.10 Cement tests**

All cement control tests were performed according to standard methods described by the South African Bureau of Standards (SABS EN 196-1). The phosphogypsum samples as well as natural gypsum (used as reference) were interground with Hercules clinker. The SO<sub>3</sub> contents of the clinker and of each gypsum sample was first determined by a wet chemical

analysis method as described in Chapter 7.3.4, and each of the gypsum samples was then interground with the clinker to achieve a final  $\text{SO}_3$  content of 2.3% in the cement. The sample was then milled to a fineness of approximately  $3200 \text{ cm}^2/\text{g}$  Blaine surface area. The relative density, initial and final setting time and compressive strength of the cement after 2, 7 and 28 days were then determined.

### 8.3 Results and discussion of the sulphuric acid treatment of South African phosphogypsum

#### 8.3.1 Application of Jarosiński's method to South African phosphogypsum

Results of the XRF analyses of Batch 1 phosphogypsum samples treated by Jarosiński's method are summarised in Table 8.4.

For both phosphogypsum samples, the amount of phosphorous was decreased significantly in the leaching step, and after conversion to the anhydrite in 50% sulphuric acid almost no phosphorous was left in the samples.

The results of the FT IR measurements for the different testing steps are presented in Figures 8.1 and 8.2. When the IR spectra of the respective untreated and fully acid-treated phosphogypsum samples were compared, it was observed that the small peak at  $832 \text{ cm}^{-1}$ , due to the presence of phosphate impurities, was only present in the untreated phosphogypsum samples. This confirmed the results obtained by XRF analysis.

**Table 8.4 XRF analysis of Batch 1 phosphogypsum samples treated with H<sub>2</sub>SO<sub>4</sub>, normalised to a loss free basis**

Compounds (%)	Kynoch phosphogypsum			Omnia phosphogypsum		
	Untreated	Leaching	Conversion	Untreated	Leaching	Conversion
Al <sub>2</sub> O <sub>3</sub>	0.36	0.30	0.58	0.35	0.30	0.30
CaO	38.46	39.73	38.75	38.80	38.31	40.03
Cr <sub>2</sub> O <sub>3</sub>	0*	0	0	0	0	0.01
Fe <sub>2</sub> O <sub>3</sub>	0.09	0.07	0.06	0.08	0.04	0.04
K <sub>2</sub> O	0	0	0	0	0	0
MgO	0.08	0.10	0.06	0.14	0.07	0.06
MnO	0	0	0	0	0	0
Na <sub>2</sub> O	0	0	0	0	0	0
<b>P<sub>2</sub>O<sub>5</sub></b>	<b>0.92</b>	<b>0.10</b>	<b>0.02</b>	<b>1.79</b>	<b>0.14</b>	<b>0.04</b>
SiO <sub>2</sub>	0.17	0	0	0	0	0
TiO <sub>2</sub>	0	0	0	0	0	0
V <sub>2</sub> O <sub>5</sub>	0	0	0	0	0	0
ZrO <sub>2</sub>	0	0	0	0	0	0
Sr	0.29	0.26	0.23	0.33	0.25	0.18
SO <sub>3</sub>	59.63	59.45	60.25	58.50	60.89	59.34

\*0 means that the compound was present in a quantity below the detection limit

The results of the FT-IR measurements for the different treating steps are presented in Figures 8.1 and 8.2. When the IR spectra of the respective untreated and sulphuric acid treated phosphogypsum samples were compared, it was observed that the small peak at 832 cm<sup>-1</sup>, due to the presence of phosphate impurities, was only present in the untreated phosphogypsum samples. This confirmed the results obtained by XRF analysis.



Figure 8.1 The IR spectra of the untreated and acid treated Batch 1 Kynoch phosphogypsum samples and pure  $\text{CaSO}_4 \cdot 2\text{H}_2\text{O}$

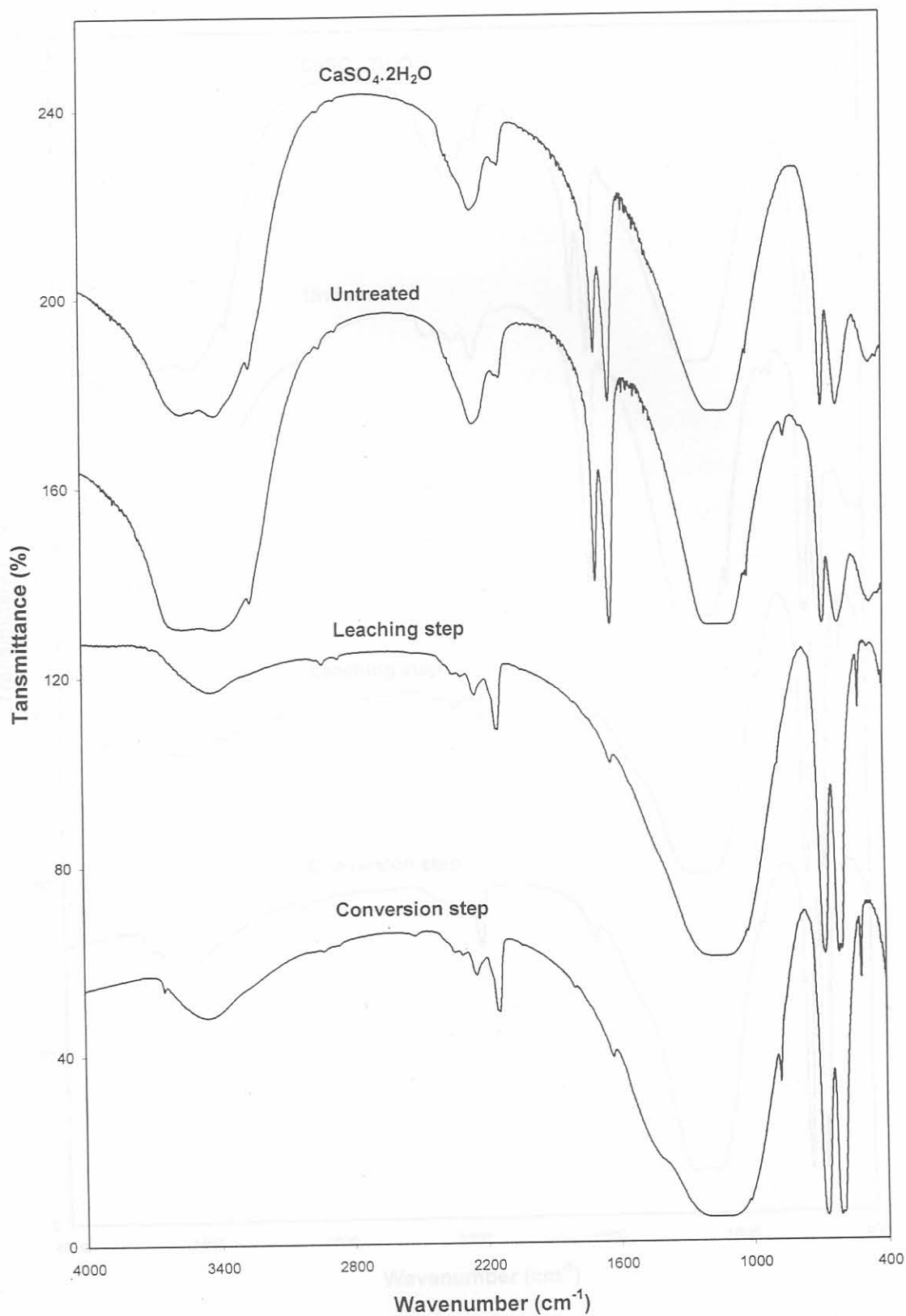
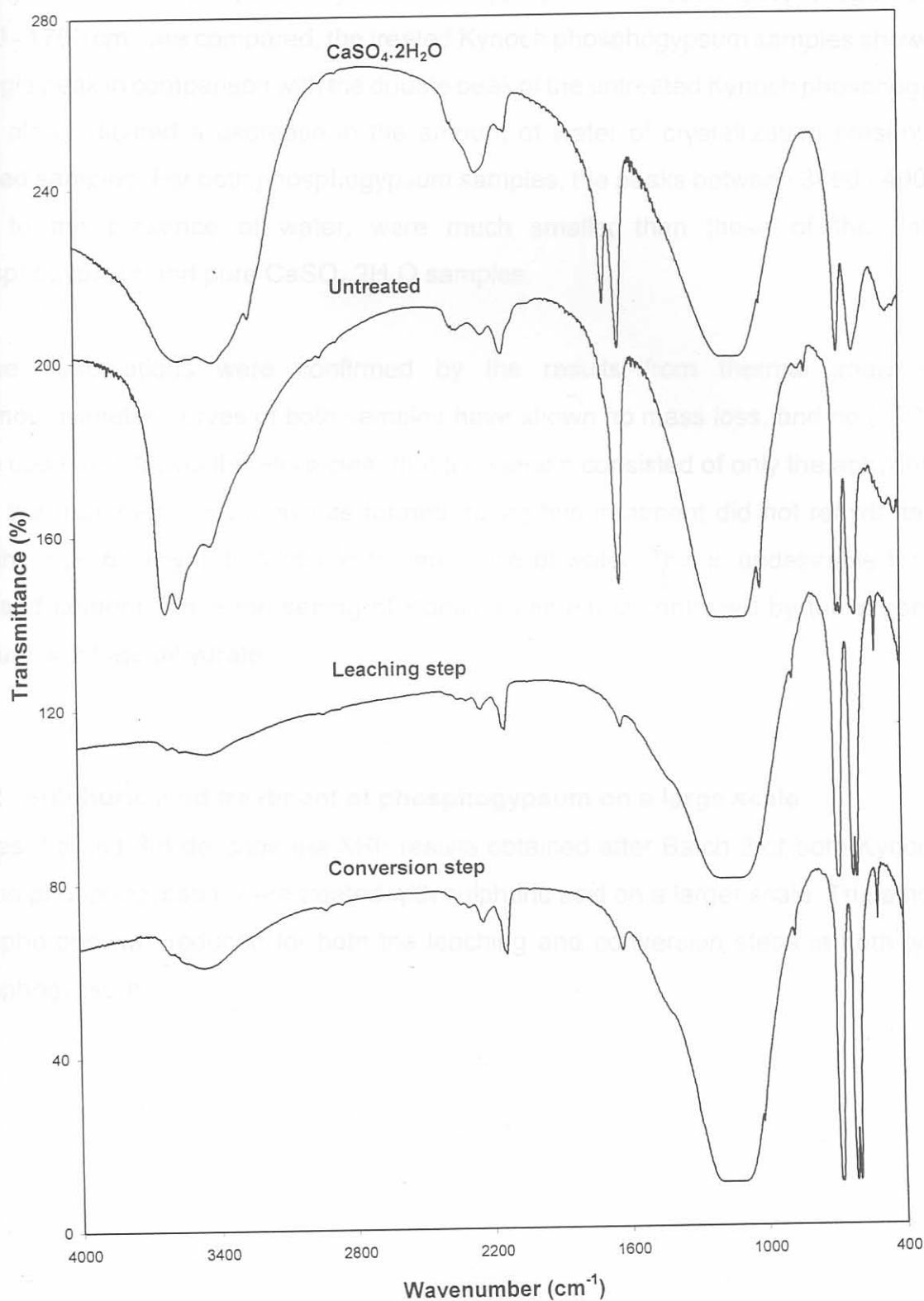


Figure 8.2 The IR spectra of the untreated and acid treated Batch 1 Omnia phosphogypsum samples and pure  $\text{CaSO}_4 \cdot 2\text{H}_2\text{O}$



For the treated phosphogypsum samples, a split in the peaks at  $600\text{ cm}^{-1}$  and  $667\text{ cm}^{-1}$  indicated that the phosphogypsum samples were not in the dihydrate form, but consisted mainly of calcium sulphate hemihydrate or anhydrite. When the peaks in the region between  $1600 - 1700\text{ cm}^{-1}$  are compared, the treated Kynoch phosphogypsum samples showed only a single peak in comparison with the double peak of the untreated Kynoch phosphogypsum. This also indicated a decrease in the amount of water of crystallization present in the treated samples. For both phosphogypsum samples, the peaks between  $3400 - 4000\text{ cm}^{-1}$ , due to the presence of water, were much smaller than those of the untreated phosphogypsum and pure  $\text{CaSO}_4 \cdot 2\text{H}_2\text{O}$  samples.

These observations were confirmed by the results from thermal analysis. The thermogravimetric curves of both samples have shown no mass loss, and no DSC peaks were observed. It was therefore clear that the sample consisted of only the anhydrite form after the treatment. The anhydrite formed during this treatment did not rehydrate to the hemihydrate or dihydrate forms in the presence of water. This is undesirable for use in Portland cement, since the setting of Portland cement is controlled by the presence of calcium sulphate dihydrate.

### 8.3.2 Sulphuric acid treatment of phosphogypsum on a large scale

Tables 8.5 and 8.6 describe the XRF results obtained after Batch 2 of both Kynoch and Omnia phosphogypsum were treated with sulphuric acid on a larger scale. The amount of phosphorous was reduced for both the leaching and conversion steps in both types of phosphogypsum.



Table 8.5 XRF analysis of Batch 2 phosphogypsum samples, treated with sulphuric acid on a larger scale *normalised to a loss free basis*

Compounds (%)	Kynoch phosphogypsum (Batch2)			Omnia phosphogypsum (Batch 2)		
	Untreated	Leaching	Conversion	Untreated	Leaching	Conversion
Al <sub>2</sub> O <sub>3</sub>	0.08	0*	0	0	0	0
CaO	33.16	33.44	33.89	33.94	33.46	34.59
Cr <sub>2</sub> O <sub>3</sub>	0	0	0	0	0.01	0
Fe <sub>2</sub> O <sub>3</sub>	0.04	0.05	0.05	0.09	0.06	0.08
K <sub>2</sub> O	0	0	0	0	0	0
MgO	0.07	0.06	0.08	0.10	0.10	0.06
MnO	0	0	0	0	0	0
Na <sub>2</sub> O	0	0	0	0	0	0
<b>P<sub>2</sub>O<sub>5</sub></b>	<b>0.77</b>	<b>0.60</b>	<b>0.53</b>	<b>1.34</b>	<b>0.81</b>	<b>0.65</b>
SiO <sub>2</sub>	0.03	0	0	0	0	0
TiO <sub>2</sub>	0	0	0	0	0	0
V <sub>2</sub> O <sub>5</sub>	0	0	0	0	0	0
ZrO <sub>2</sub>	0	0	0	0	0	0
Sr	0.27	0.26	0.24	0.30	0.29	0.27
SO <sub>3</sub>	45.76	44.83	45.90	45.72	44.70	45.76
Loss on ignition	21.29	21.87	20.96	20.02	21.57	19.04
<b>Total</b>	<b>101.47</b>	<b>101.11</b>	<b>101.65</b>	<b>101.51</b>	<b>100.97</b>	<b>100.45</b>

\*0 means that the compound was present in a quantity below the detection limit

**Table 8.6 XRF analysis of Batch 2 phosphogypsum samples, treated with sulphuric acid on a larger scale, normalised to a loss free basis**

Compounds (%)	Kynoch phosphogypsum (Batch2)			Omnia phosphogypsum (Batch 2)		
	Untreated	Leaching	Conversion	Untreated	Leaching	Conversion
Al <sub>2</sub> O <sub>3</sub>	0.10	0*	0	0	0	0
CaO	41.36	42.20	42.00	41.65	42.14	42.68
Cr <sub>2</sub> O <sub>3</sub>	0	0	0	0	0.01	0
Fe <sub>2</sub> O <sub>3</sub>	0.05	0.06	0.06	0.11	0.08	0.10
MgO	0.09	0.08	0.10	0.12	0.13	0.07
P <sub>2</sub> O <sub>5</sub>	<b>0.96</b>	<b>0.76</b>	<b>0.66</b>	<b>1.64</b>	<b>1.02</b>	<b>0.80</b>
SiO <sub>2</sub>	0.04	0	0	0	0	0
Sr	0.34	0.33	0.30	0.37	0.37	0.33
SO <sub>3</sub>	57.07	56.57	56.88	56.11	56.30	56.46

\*0 means that the compound was present in a quantity below the detection limit

The conversion step was then extended to 4 hours, to test the effect of time on the amount of phosphorous. The XRF results are summarised in Tables 8.7 and 8.8. There was not a significant decrease in the amount of phosphorous in any of the phosphogypsum samples after the extended time period.

**Table 8.7 XRF analysis of sulphuric acid treatment on large scale with an extended time period of 4 hours for the conversion step**

Compounds (%)	Kynoch phosphogypsum		Omnia phosphogypsum	
	Untreated	Conversion	Untreated	Conversion
Al <sub>2</sub> O <sub>3</sub>	0.08	0*	0	0
CaO	33.16	35.21	33.94	33.83
Cr <sub>2</sub> O <sub>3</sub>	0	0.01	0	0.01
Fe <sub>2</sub> O <sub>3</sub>	0.04	0.04	0.09	0.07
K <sub>2</sub> O	0	0	0	0
MgO	0.07	0.06	0.10	0.09
MnO	0	0	0	0
Na <sub>2</sub> O	0	0	0	0
<b>P<sub>2</sub>O<sub>5</sub></b>	<b>0.77</b>	<b>0.55</b>	<b>1.34</b>	<b>0.66</b>
SiO <sub>2</sub>	0.03	0	0	0
Sr	0.27	0.26	0.30	0.27
SO <sub>3</sub>	45.76	48.40	45.72	47.04
Loss on ignition	21.29	17.22	20.02	20.29
<b>Total</b>	<b>101.47</b>	<b>101.75</b>	<b>101.51</b>	<b>102.26</b>

\*0 means that the compound was present in a quantity below the detection limit



**Table 8.8 XRF analysis of sulphuric acid treatment on large scale with an extended time period of 4 hours for the conversion step, normalised to a loss free basis**

Compounds (%)	Kynoch phosphogypsum		Omnia phosphogypsum	
	Untreated	Conversion	Untreated	Conversion
Al <sub>2</sub> O <sub>3</sub>	0.10	0*	0	0
CaO	41.36	41.65	41.65	41.27
Cr <sub>2</sub> O <sub>3</sub>	0	0.01	0	0.01
Fe <sub>2</sub> O <sub>3</sub>	0.05	0.05	0.11	0.09
MgO	0.09	0.07	0.12	0.11
<b>P<sub>2</sub>O<sub>5</sub></b>	<b>0.96</b>	<b>0.65</b>	<b>1.64</b>	<b>0.81</b>
SiO <sub>2</sub>	0.04	0	0	0
Sr	0.34	0.31	0.37	0.33
SO <sub>3</sub>	57.07	57.26	56.11	57.39

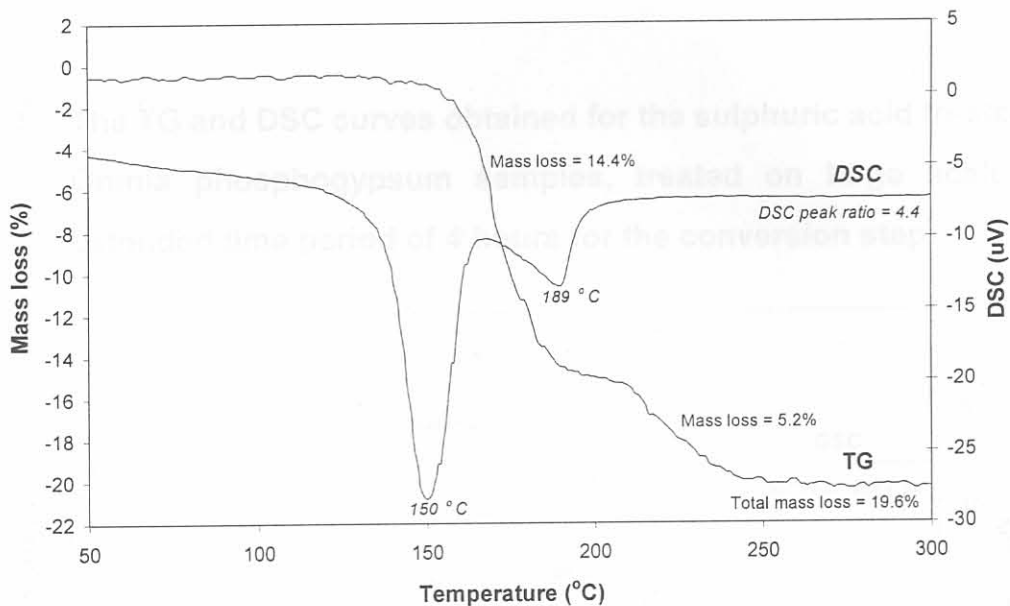
\*0 means that the compound was present in a quantity below the detection limit

The inability to remove the phosphorous impurities from these phosphogypsum samples can possibly be ascribed to problems regarding upscaling of the experimental method. The method seemed to be less effective when repeated on a larger scale, due to constraints posed by the laboratory scale apparatus used to conduct these large scale experiments.

When the TG and DSC curves of Figure 8.3 are compared with that of the untreated Batch 2 phosphogypsum samples from Figures 5.6 and 5.7, it can be seen that there was no significant difference in the TG and DSC curves of the treated and untreated Kynoch phosphogypsum samples. The obtained total mass loss of 19.6% is close to the theoretical value of 20.9%, which indicates that the treated phosphogypsum sample contained mainly calcium sulphate dihydrate. The high value obtained for the DSC peak ratio could not be of any use, since the separation of the two dehydration peaks was not satisfactory. Furthermore, the peak for the first dehydration reaction did not return to the baseline before

the second dehydration reaction started. The temperatures at which the respective maximums occurred were the same as for the untreated Kynoch phosphogypsum sample.

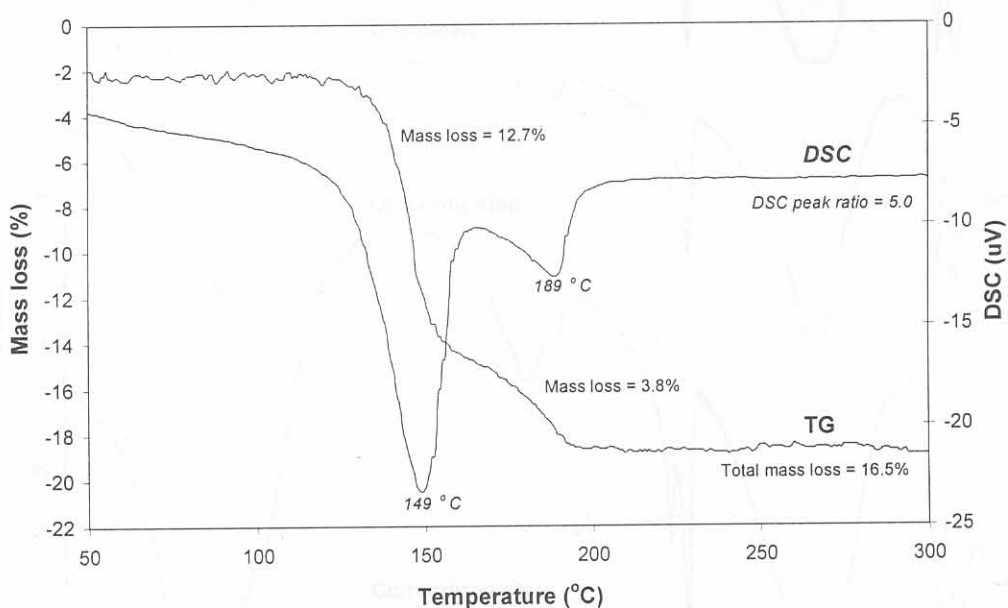
**Figure 8.3** The TG and DSC curves obtained for the sulphuric acid treated Batch 2 Kynoch phosphogypsum samples, treated on large scale with an extended time period of 4 hours for the conversion step



When the DSC curves of Figure 8.4 are compared with that of the untreated Omnia phosphogypsum samples, no significant change was observed. However, the TG curve revealed a lower total mass loss of 16.5% when compared to 20.2% for the untreated Omnia phosphogypsum samples (given in Figure 5.5). This indicated that the treated sample contained some calcium sulphate hemihydrate or anhydrite which did not rehydrate during treatment. It seems as if it is the anhydrite form that is present in this samples, due to the small second mass loss of only 3.8%. The presence of calcium sulphate hemihydrate will result in a higher second mass loss due its dehydration. This hemihydrate originates from both dehydrated dihydrate as well as some hemihydrate that was originally present in the sample.

The DSC peak ratio could again not be useful, for the same reason as stated for Kynoch phosphogypsum above. The temperature at which the peak maximum for the first dehydration occur shifted from 118°C for the untreated Omnia phosphogypsum sample, to 149°C for the treated sample. As explained in Chapter 5.3.3, this indicates that the untreated Omnia phosphogypsum forms the  $\alpha$ -hemihydrate when dehydrated, while after the sample was treated with sulphuric acid, dehydration results in the formation of the  $\beta$ -hemihydrate.

**Figure 8.4** The TG and DSC curves obtained for the sulphuric acid treated Batch 2 Omnia phosphogypsum samples, treated on large scale with an extended time period of 4 hours for the conversion step



The respective infrared spectra for the untreated and treated Kynoch and Omnia phosphogypsum samples are given in Figures 8.5 and 8.6. The results obtained from IR measurements confirmed the XRF and TG/DSC results, that indicated that the dihydrate form of calcium sulphate was mainly formed in all instances. The small peak at  $\sim 832\text{ cm}^{-1}$  due to phosphorous impurities was still present. No difference in the IR spectra for the leaching and conversion steps was observed for any of the phosphogypsum samples.



Figure 8.5 The IR spectra of the untreated and acid treated Batch 2 Kynoch phosphogypsum samples, treated on large scale with an extended time period of 4 hours for the conversion step

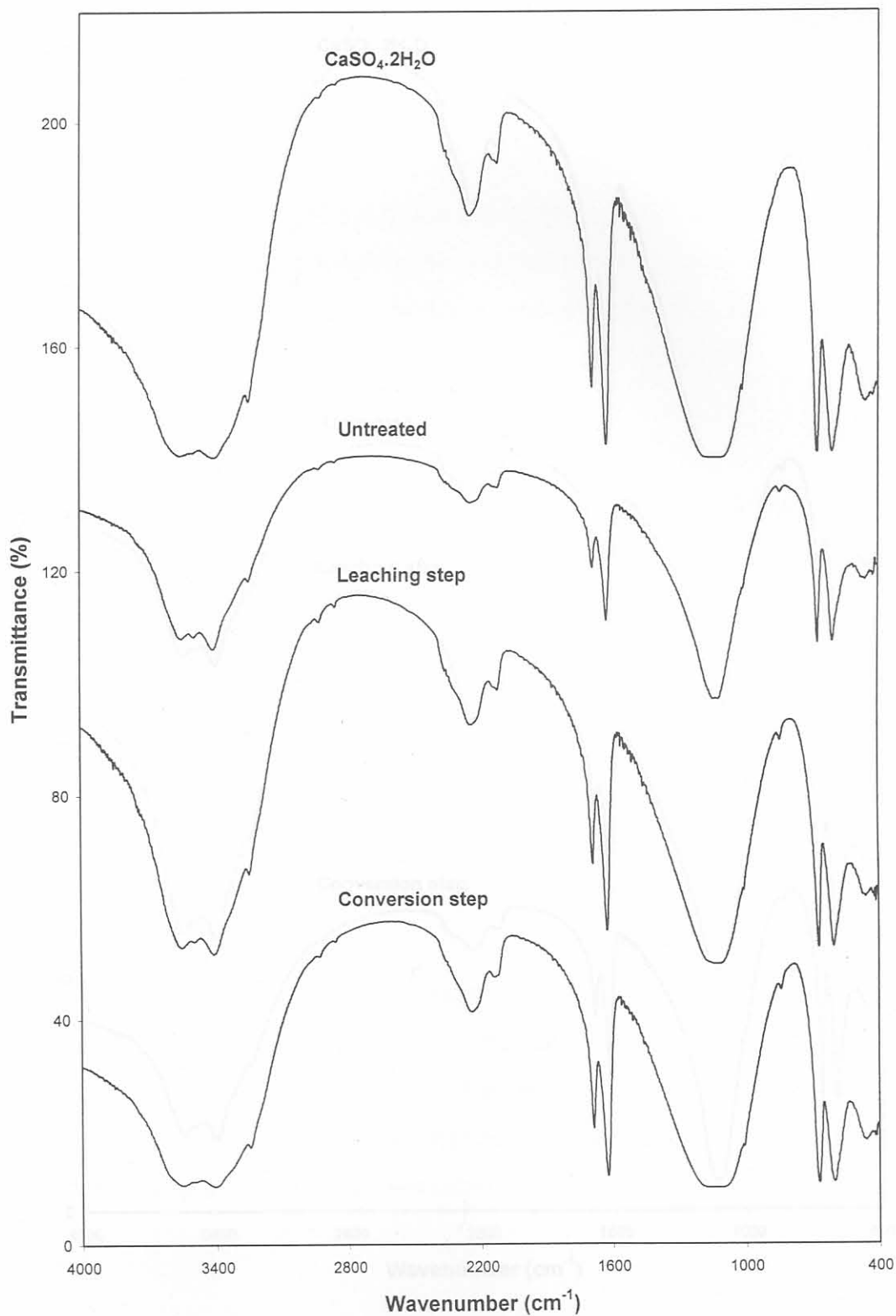
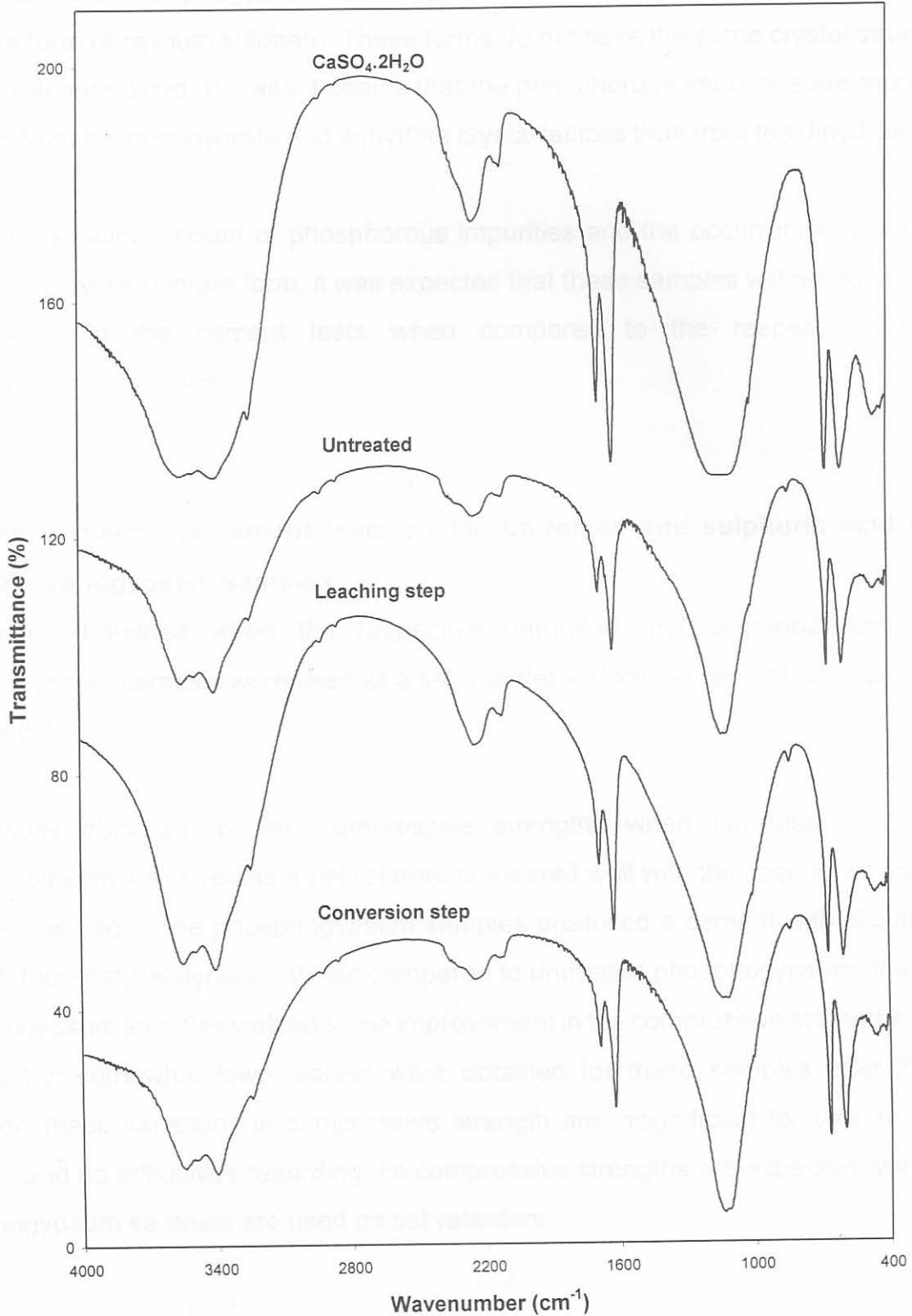


Figure 8.6 The IR spectra of the untreated and acid treated Batch 2 Omnia phosphogypsum samples, treated on large scale with an extended time period of 4 hours for the conversion step



The presence of mainly the dihydrate form of calcium sulphate during the course of the treatment was probably the reason for the unsuccessfulness of this method. To be able to remove the phosphorous impurities by reacting it with sulphuric acid, the dihydrate present in the untreated phosphogypsum samples had to be converted to the hemihydrate or anhydrite form of calcium sulphate. These forms do not have the same crystal structure as calcium sulphate dihydrate, and it seems that the phosphorous impurities are more easily removed from the hemihydrate and anhydrite crystal lattices than from the dihydrate lattice.

Due to the smaller amount of phosphorous impurities and the occurrence of mainly the calcium sulphate dihydrate form, it was expected that these samples will render increased performance in the cement tests when compared to the respective untreated phosphogypsum samples.

### **8.3.3 Performance of cement tests on the untreated and sulphuric acid treated phosphogypsum samples**

The results obtained when the respective untreated and sulphuric acid treated phosphogypsum samples were used as a set retarder in Portland cement, are summarised in Table 8.9.

The results obtained for the compressive strengths when untreated and treated phosphogypsum was used as a set retarder compared well with the case in which natural gypsum was used. The phosphogypsum samples produced a cement with slightly lower strength than natural gypsum. When compared to untreated phosphogypsum, the treated phosphogypsum samples yielded some improvement in the compressive strengths at 2 and 7 days, but somewhat lower values were obtained for these samples after 28 days. However, these variations in compressive strength are insignificant for use in Portland cement, and no difficulties regarding the compressive strengths are expected when these phosphogypsum samples are used as set retarders.



**Table 8.9 Results of the cement test performed on sulphuric acid treated and untreated Kynoch, Omnia phosphogypsum samples and natural gypsum**

Test	O-U <sup>a</sup>	O-ST <sup>b</sup>	K-U <sup>c</sup>	K-ST <sup>d</sup>	N-G <sup>e</sup>
SO <sub>3</sub> content of gypsum (%)	47.24	45.59	46.68	46.96	42.50
Gypsum added to clinker (%)	3.46	3.59	3.50	3.48	3.85
Specific Surface of cement (cm <sup>2</sup> /g)	3470	3225	3200	3275	3200
Relative density of cement	3.15	3.10	3.10	3.12	3.10
Initial setting time (min)	243	160	354	184	140
Final setting time (h)	5.11	4.75	6.75	4.25	3.25
2-day Compressive Strength (MPa)	17.12	18.36	17.35	18.89	20.33
7-day Compressive Strength (MPa)	33.91	35.60	34.41	36.97	38.04
28-day Compressive Strength (MPa)	46.07	45.50	47.25	44.01	49.10

<sup>a</sup> Untreated Omnia phosphogypsum

<sup>b</sup> Omnia phosphogypsum treated with H<sub>2</sub>SO<sub>4</sub>

<sup>c</sup> Untreated Kynoch phosphogypsum

<sup>d</sup> Kynoch phosphogypsum treated with H<sub>2</sub>SO<sub>4</sub>

<sup>e</sup> Natural Gypsum

### 3.3.4 Comparison to the sulphuric acid treatment method

The initial and final setting times of cement containing untreated phosphogypsum samples varied significantly from cement containing natural gypsum. By using untreated phosphogypsum instead of natural gypsum as a set retarder, the initial setting time for the cement containing Kynoch phosphogypsum was delayed from 140 minutes to 354 minutes, and that containing Omnia phosphogypsum to 243 minutes. Furthermore, the final setting time of the cement containing untreated Kynoch phosphogypsum, was delayed from 3.25 hours to 6.75 hours, and that for Omnia phosphogypsum to 5.11 hours.

When comparing cement containing treated Kynoch phosphogypsum to the cement containing untreated Kynoch phosphogypsum, the initial setting time improved from 354 minutes to 184 minutes. For the cement containing treated Omnia phosphogypsum, the initial setting time improved from 243 minutes to 160 minutes, when compared to the sample

containing untreated Omnia phosphogypsum. This indicates that, when the treated Kynoch and Omnia phosphogypsum samples were used in cement, similar initial setting times were produced, when compared to the initial setting time of 140 minutes obtained when natural gypsum was used.

Similarly, the final setting time for the cement containing treated Kynoch phosphogypsum improved from 6.75 hours to 4.25 hours, and that for the treated Omnia phosphogypsum from 5.11 hours to 4.75 hours. The values obtained when the treated phosphogypsum samples were used, compared better to the final setting time of 3.25 hours obtained for cement containing natural gypsum, than for the cement containing untreated phosphogypsum.

A significant decrease in both the initial and final setting times could be observed when the results of the untreated and treated phosphogypsum samples were compared. These results proved that by decreasing the amount of phosphorous impurities, combined with the presence of mainly calcium sulphate dihydrate in the treated phosphogypsum samples, the performance of phosphogypsum as a set retarder in cement is improved.

#### **8.3.4 Optimisation of the sulphuric acid treatment method**

The sulphuric acid treatment method was optimized in terms of the amount of phosphorous removed from the phosphogypsum and the thermogravimetric results which yields the highest amount of calcium sulphate dihydrate. This means that the optimum condition will be when there is the least amount of phosphorous in the gypsum, combined with a TG mass loss of about 20.9% (which is the theoretical amount for pure  $\text{CaSO}_4 \cdot 2\text{H}_2\text{O}$ ). Because phosphorous was the only impurity of concern in the optimisation, only the values of  $\text{P}_2\text{O}_5$  from the XRF analyses were considered and reported.

The mass loss percentages and percentage  $\text{P}_2\text{O}_5$  in the respective untreated phosphogypsum samples differ for the different optimization steps. The amount of phosphogypsum necessary for a specific optimization was taken from the large batch, dried overnight and mixed with a mortar and pestle to homogenise the sample. This sample was



then used for the optimization of a specific parameter. Both the mass loss percentage and %  $P_2O_5$  of the homogenised untreated phosphogypsum was determined before optimization. This explains the difference in mass loss percentages and amount of phosphorous impurities for the untreated phosphogypsum samples between the respective optimisation steps.

The results of the effect of reaction temperature are summarised in Table 8.10. The XRF results were normalised to a loss free basis.

**Table 8.10 XRF and thermogravimetric results for the optimisation of temperature for the sulphuric acid method**

Temperature (°C)	Kynoch phosphogypsum		Omnia phosphogypsum	
	$P_2O_5$ (%)	Mass loss (%)	$P_2O_5$ (%)	Mass loss (%)
Untreated	1.09	19.5	2.15	14.3
23	0.77	19.9	0.73	18.7
27	0.75	19.1	0.79	18.7
40	0.78	19.0	0.72	19.5
51	0.72	19.5	0.68	17.4
60	0.73	19.9	0.73	18.8
69	0.80	21.4	0.64	18.8

From the results in Table 8.10, it was clear that by using a sulphuric acid concentration of 12%, the effect of temperature on the amount of phosphorous contained in the treated samples, was insignificant for both the Kynoch and Omnia phosphogypsum. Except for the Omnia phosphogypsum treated at 51°C, all other samples contained mainly dihydrate. Based on these results, it was decided to use room temperature (20 - 25°C) for the following optimization steps.



The effect of acid concentration on the amount of phosphorous impurities and dihydrate at constant room temperature of 23°C is given in Table 8.11. The XRF results were normalised to a loss free basis.

**Table 8.11 XRF and thermogravimetric results for the optimisation of concentration H<sub>2</sub>SO<sub>4</sub> for the sulphuric acid method**

Concentration H <sub>2</sub> SO <sub>4</sub> (% m/m)	Kynoch phosphogypsum		Omnia phosphogypsum	
	P <sub>2</sub> O <sub>5</sub> (%)	Mass loss (%)	P <sub>2</sub> O <sub>5</sub> (%)	Mass loss (%)
Untreated	0.99	19.5	1.97	14.3
5	0.63	13.7	0.49	19.0
10	0.83	17.2	0.43	18.3
20	0.54	18.7	0.43	19.0
30	0.56	15.5	1.04	17.1
40	0.57	17.7	0.95	19.1
50	0.58	16.0	1.09	20.7

For the Kynoch phosphogypsum, the amount of dihydrate in the treated samples was reduced for all sulphuric acid concentrations. The highest amount of phosphorous impurities was removed when the Kynoch phosphogypsum was treated in H<sub>2</sub>SO<sub>4</sub> solutions with concentrations of more than 20% by mass. The highest mass loss, and therefore the most dihydrate, was obtained by stirring in a 20% H<sub>2</sub>SO<sub>4</sub> solution. Consequently, the optimum H<sub>2</sub>SO<sub>4</sub> concentration for treating Kynoch phosphogypsum was chosen as 20%.

For the Omnia phosphogypsum, the amount of dihydrate increased when the samples were treated with sulphuric acid. Treatment of Omnia phosphogypsum in 5%, 10% or 20% H<sub>2</sub>SO<sub>4</sub> solutions removed the highest amount of phosphorous impurities, while more dihydrate was obtained by treatment in a 50% H<sub>2</sub>SO<sub>4</sub> solution. However, treatment in a 50% H<sub>2</sub>SO<sub>4</sub> solution removed far less impurities than the other concentrations, while treatment in the 5%

and 20%  $H_2SO_4$  solutions produced mainly dihydrate. It was therefore decided to use a sulphuric acid concentration of 5% in further optimization steps, due to economical aspects.

The phosphogypsum samples were then treated at room temperature in a 20%  $H_2SO_4$  solution for the Kynoch phosphogypsum, and 5% for Omnia phosphogypsum. The effect of different stirring times at constant room temperature is shown in Table 8.12. The XRF results were normalised to a loss free basis.

**Table 8.12 XRF and thermogravimetric results for the optimisation of reaction time for the sulphuric acid method**

Time (min)	Kynoch phosphogypsum		Omnia phosphogypsum	
	$P_2O_5$ (%)	Mass loss (%)	$P_2O_5$ (%)	Mass loss (%)
Untreated	1.04	19.5	2.25	14.3
15	0.82	19.0	1.05	19.3
30	0.77	18.9	0.77	19.5
45	0.77	18.0	1.04	18.6
60	0.78	20.8	1.02	18.0
90	0.81	18.5	0.72	19.2
120	0.76	17.8	0.70	19.4
180	0.71	16.2	1.10	19.6
360	0.74	18.9	1.06	17.5

The effect of reaction time was not significant for the treatment of Kynoch phosphogypsum. The same quantity of impurities was removed, regardless of the reaction time. The samples treated for 180 minutes revealed a lower mass loss than the other treated samples, which can possibly be ascribed to experimental error.

For the treated Omnia phosphogypsum samples, fewer phosphorous impurities were present in the samples treated for 30, 90 and 120 minutes. For all Omnia samples, an improvement in the amount of dihydrate was observed due to the higher mass losses. It was decided to choose the optimum time for both Omnia and Kynoch phosphogypsum as 30 minutes.

The phosphogypsum samples were then treated for 30 minutes at room temperature in a 20% H<sub>2</sub>SO<sub>4</sub> solution for the Kynoch phosphogypsum, and 5% for Omnia phosphogypsum. The effect of varying the solid:liquid ratio is shown in Table 8.13. The XRF results were normalised to a loss free basis.

**Table 8.13 XRF and thermogravimetric results for the optimisation of the solid : liquid ratio for the sulphuric acid method**

Ratio (s:l)	Kynoch phosphogypsum		Omnia phosphogypsum	
	P <sub>2</sub> O <sub>5</sub> (%)	Mass loss (%)	P <sub>2</sub> O <sub>5</sub> (%)	Mass loss (%)
Untreated	0.95	17.2	2.08	15.1
1:1	0.82	18.8	0.85	20.0
1:2	0.76	20.1	0.83	20.6
1:3	0.77	18.7	0.82	19.2
1:4	0.77	19.4	0.75	20.2

Contrary to what was observed for the Batch 1 Omnia phosphogypsum sample, the Batch 2 samples of both the Kynoch and Omnia phosphogypsum formed a manageable paste when a solid:liquid ratio of 1:1 was used. It was therefore decided to vary the solid:liquid ratio between 1:1 and 1:4.

For both Kynoch and Omnia phosphogypsum, the treated samples showed an improvement in the amount of calcium sulphate dihydrate, when compared to the untreated samples. The



treated samples contained mainly calcium sulphate dihydrate. The difference in the amount of phosphorous impurities between the different treated samples was insignificant. A solid:liquid ratio of 1:4 was chosen as the optimum, because this produced a paste that could be stirred more easily.

When all optimisation steps were combined, the phosphogypsum samples were treated for 30 minutes at room temperature at a solid:liquid ratio of 1:4 in a 20% H<sub>2</sub>SO<sub>4</sub> solution for the Kynoch phosphogypsum, and 5% for Omnia phosphogypsum.

**8.3.5 The optimum sulphuric acid treatment of phosphogypsum on a large scale for performance of cement tests**

The Kynoch and Omnia phosphogypsum samples were treated on a large scale for use in the performance of cement tests, according the optimum sulphuric acid method as discussed above. The results of the XRF analyses are summarised in Tables 8.14 and 8.15. For both types of phosphogypsum, the amount of phosphorous impurities was reduced by the optimum sulphuric acid treatment.

**Table 8.14 XRF analysis of Batch 2 phosphogypsum samples, treated on a large scale for the performance of cement tests by the optimum sulphuric acid treatment method**

Compounds (%)	Kynoch phosphogypsum		Omnia phosphogypsum	
	Untreated	Optimum acid treatment	Untreated	Optimum acid treatment
SiO <sub>2</sub>	0.22	0.11	0.14	0.05
Al <sub>2</sub> O <sub>3</sub>	0.11	0.01	0.01	0
Fe <sub>2</sub> O <sub>3</sub>	0*	0	0	0
MnO	0	0	0	0
MgO	0	0	0	0
CaO	32.75	32.88	32.21	33.68
Cr <sub>2</sub> O <sub>3</sub>	0	0	0	0
K <sub>2</sub> O	0	0	0	0
Na <sub>2</sub> O	0	0	0	0
<b>P<sub>2</sub>O<sub>5</sub></b>	<b>0.81</b>	<b>0.57</b>	<b>1.21</b>	<b>0.64</b>
SO <sub>3</sub>	42.85	44.80	45.75	44.68
LOI	21.38	20.55	20.35	20.68
<b>TOTAL</b>	<b>98.12</b>	<b>98.92</b>	<b>99.67</b>	<b>99.73</b>

\*0 means that the compound was present in a quantity below the detection limit

**Table 8.15** XRF analysis of Batch 2 phosphogypsum samples, treated on a large scale for the performance of cement tests by the optimum sulphuric acid treatment method, normalised to a loss free basis

Compounds (%)	Kynoch phosphogypsum		Omnia phosphogypsum	
	Untreated	Optimum acid treatment	Untreated	Optimum acid treatment
SiO <sub>2</sub>	0.29	0.14	0.18	0.06
Al <sub>2</sub> O <sub>3</sub>	0.14	0.01	0.01	0*
CaO	42.68	41.95	40.59	42.61
P <sub>2</sub> O <sub>5</sub>	<b>1.06</b>	<b>0.73</b>	<b>1.53</b>	<b>0.81</b>
SO <sub>3</sub>	55.84	57.16	57.67	56.52

\*0 means that the compound was present in a quantity below the detection limit

The thermogravimetric curves for the optimum sulphuric acid treated phosphogypsum samples are presented in Figures 8.7 and 8.8.

**Figure 8.7** The TG and DSC curves obtained for the optimum sulphuric acid treated Batch 2 Kynoch phosphogypsum samples, treated on a large scale for the performance of cement tests

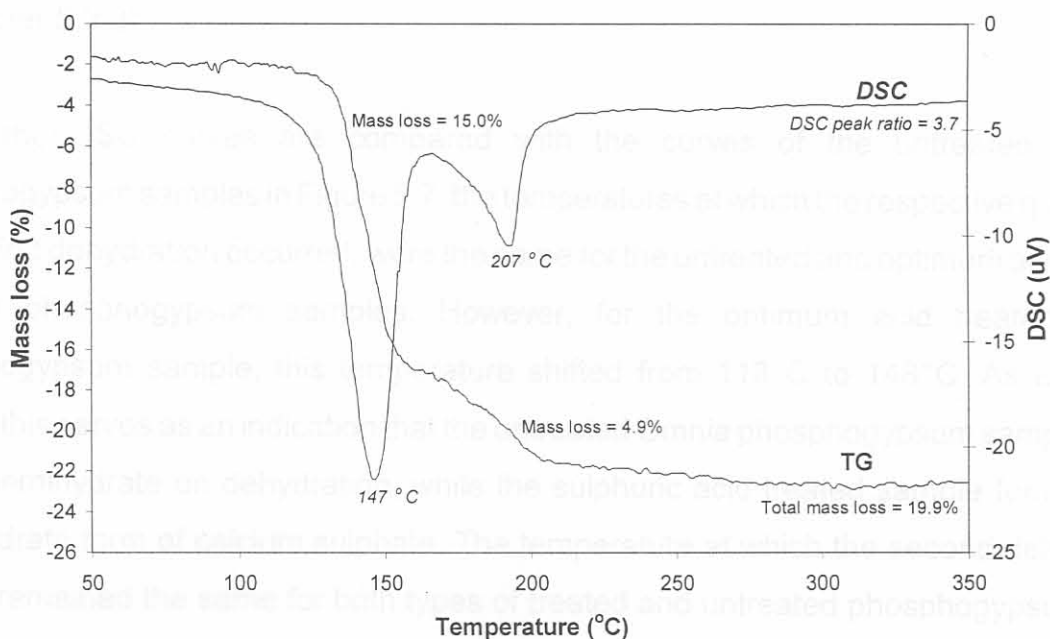
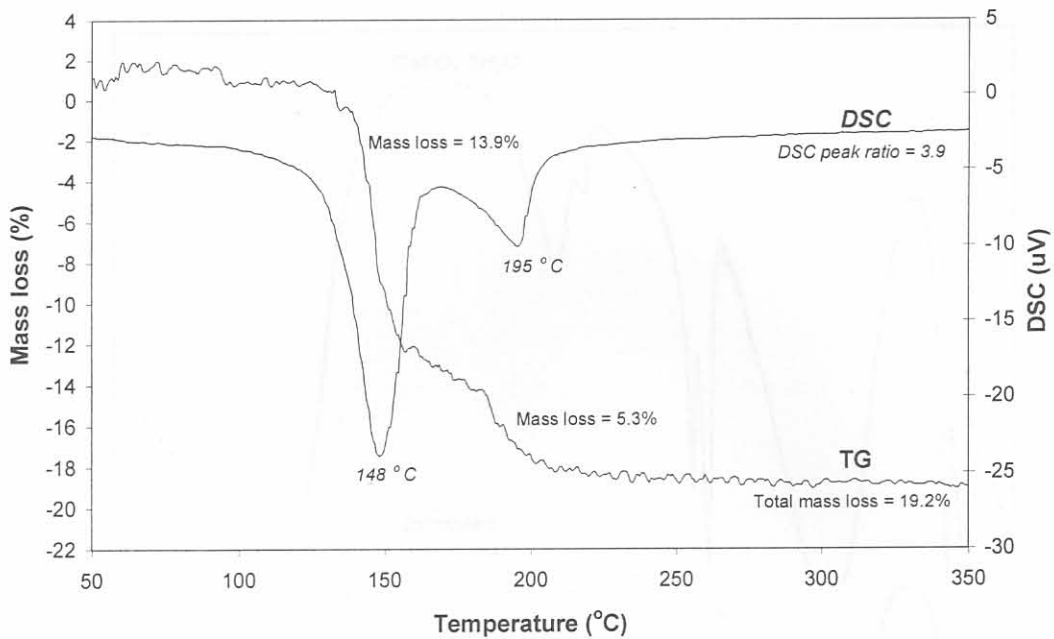




**Figure 8.8** The TG and DSC curves obtained for the optimum sulphuric acid treated Batch 2 Omnia phosphogypsum samples, treated on a large scale for the performance of cement tests



Both the Kynoch and Omnia phosphogypsum samples contained mainly the dihydrate form of calcium sulphate after the optimum treatment, as can be seen from the total mass losses which are in both cases close to the theoretical value of 20.9%. This is confirmed by the values of the DSC peak ratios, which are close to the theoretical value of 3.3 (as discussed in Chapter 5.3.3).

When the DSC curves are compared with the curves of the untreated Batch 2 phosphogypsum samples in Figure 5.7, the temperatures at which the respective maximums for the first dehydration occurred, were the same for the untreated and optimum acid treated Kynoch phosphogypsum samples. However, for the optimum acid treated Omnia phosphogypsum sample, this temperature shifted from 118 °C to 148 °C. As explained before, this serves as an indication that the untreated Omnia phosphogypsum sample forms the  $\alpha$ -hemihydrate on dehydration, while the sulphuric acid treated sample forms the  $\beta$ -hemihydrate form of calcium sulphate. The temperature at which the second dehydration occurs remained the same for both types of treated and untreated phosphogypsum.

**Figure 8.9** The IR spectra of the untreated and optimum sulphuric acid treated Batch 2 Kynoch phosphogypsum samples, used for the performance of cement tests

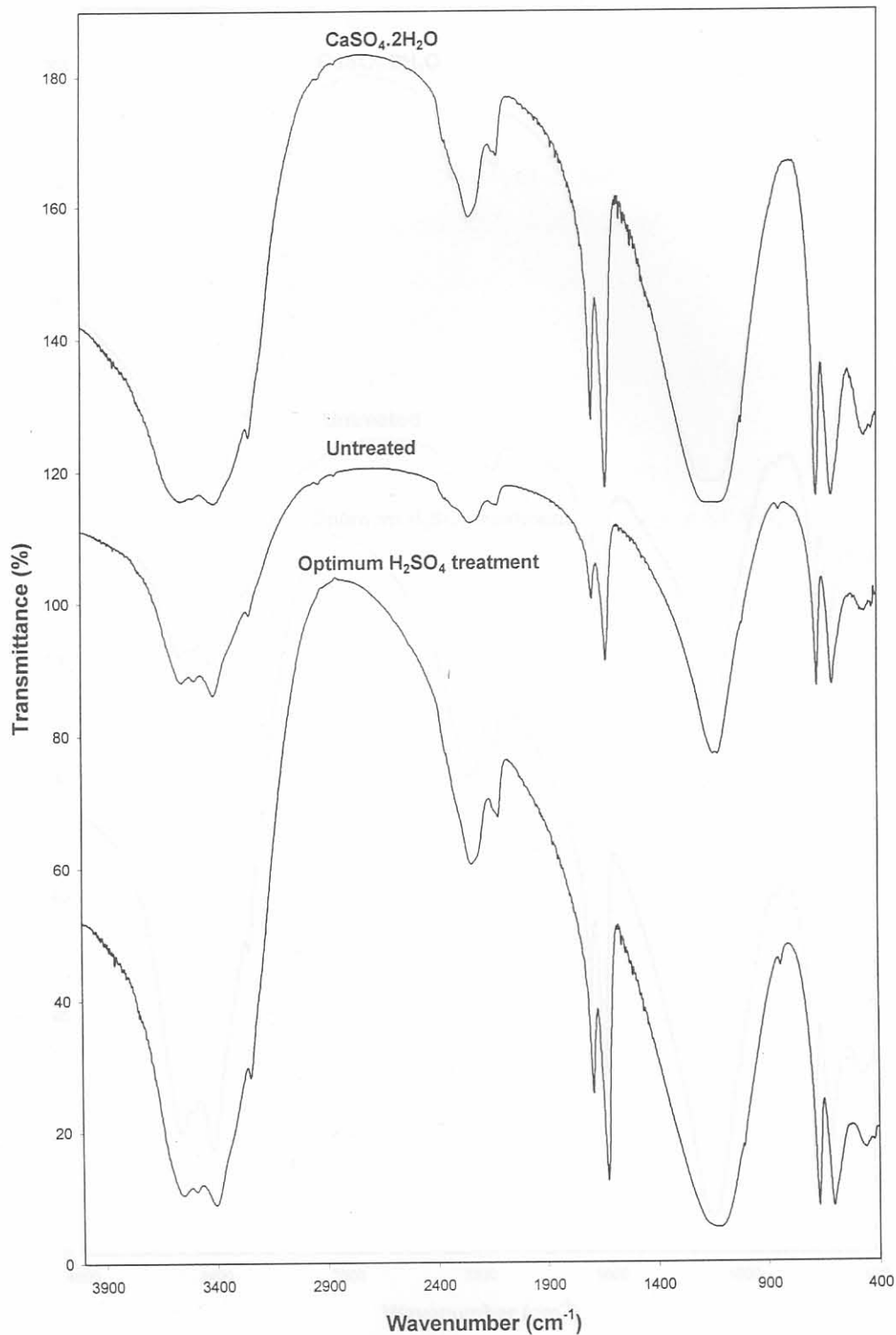
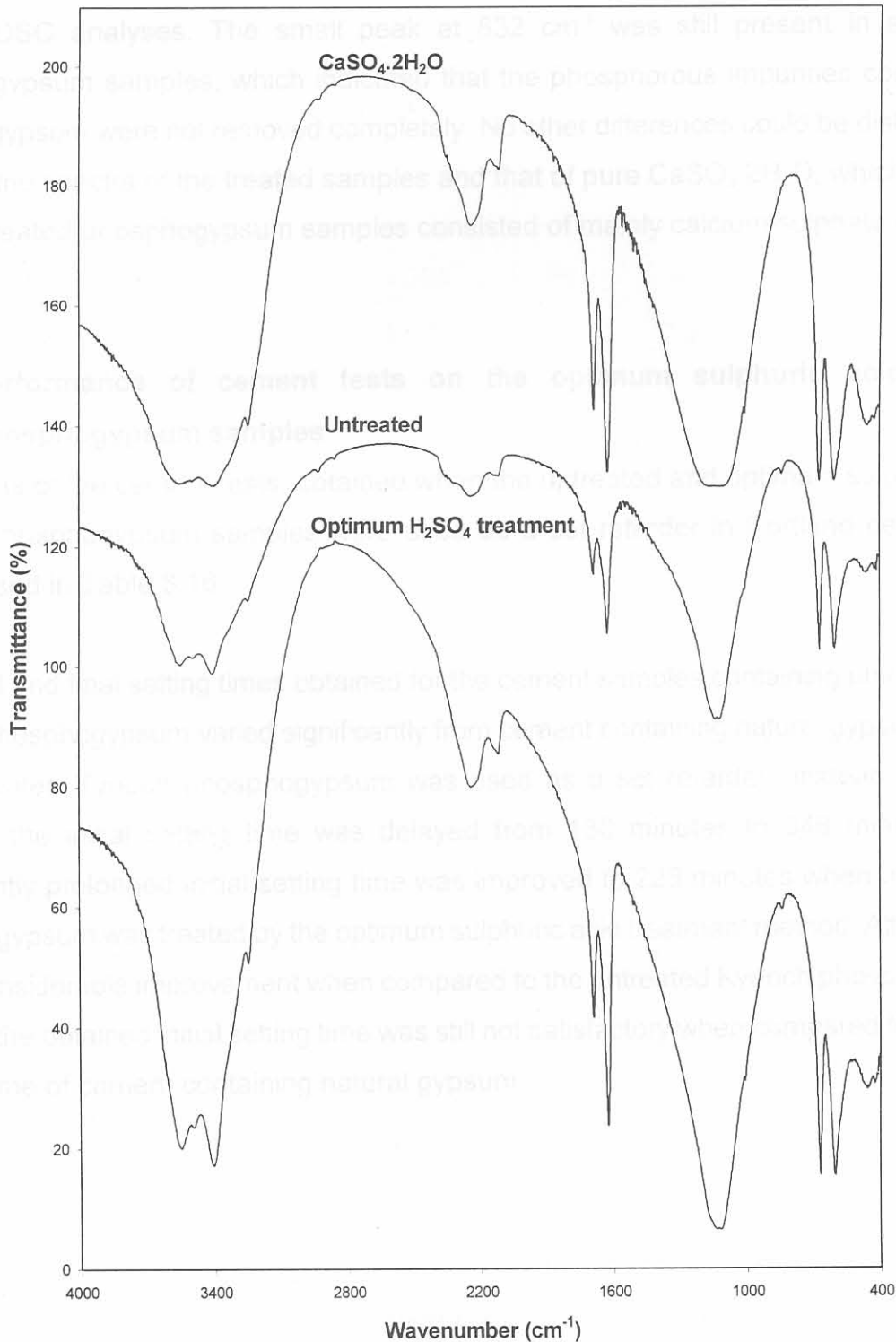


**Figure 8.10** The IR spectra of the untreated and optimum sulphuric acid treated Batch 2 Omnia phosphogypsum samples, used for the performance of cement tests





The results of the FT-IR analyses of the untreated and optimum sulphuric acid treated phosphogypsum samples are given in Figures 8.9 and 8.10.

The results obtained from the IR analyses supported the conclusions made from the XRF and TG/DSC analyses. The small peak at  $832\text{ cm}^{-1}$  was still present in all treated phosphogypsum samples, which indicated that the phosphorous impurities contained in phosphogypsum were not removed completely. No other differences could be distinguished between the spectra of the treated samples and that of pure  $\text{CaSO}_4 \cdot 2\text{H}_2\text{O}$ , which confirms that the treated phosphogypsum samples consisted of mainly calcium sulphate dihydrate.

### **8.3.6 Performance of cement tests on the optimum sulphuric acid treated phosphogypsum samples**

The results of the cement tests, obtained when the untreated and optimum sulphuric acid treated phosphogypsum samples were used as a set retarder in Portland cement, are summarised in Table 8.16.

The initial and final setting times obtained for the cement samples containing untreated and treated phosphogypsum varied significantly from cement containing natural gypsum. When the untreated Kynoch phosphogypsum was used as a set retarder instead of natural gypsum, the initial setting time was delayed from 130 minutes to 348 minutes. This significantly prolonged initial setting time was improved to 228 minutes when the Kynoch phosphogypsum was treated by the optimum sulphuric acid treatment method. Although this was a considerable improvement when compared to the untreated Kynoch phosphogypsum sample, the obtained initial setting time was still not satisfactory when compared to the initial setting time of cement containing natural gypsum.

**Table 8.16 Results of the cement test performed when untreated and optimum sulphuric acid treated Kynoch and Omnia phosphogypsum samples, and natural gypsum was used as a set retarder in Portland cement**

Test	O-U <sup>a</sup>	O-OST <sup>b</sup>	K-U <sup>c</sup>	K-OST <sup>d</sup>	N-G <sup>e</sup>
SO <sub>3</sub> content of gypsum (%)	47.06	45.98	45.76	45.78	42.50
Gypsum added to clinker (%)	3.47	3.56	3.57	3.57	3.85
Specific Surface of cement (cm <sup>2</sup> /g)	3159	3457	3180	3258	3314
Relative density of cement	3.15	3.15	3.14	3.14	3.14
Initial setting time (min)	265	189	348	228	130
Final setting time (h)	5.8	4.2	7.2	4.9	3.0
2-day Compressive Strength (MPa)	14.17	17.35	14.67	15.07	19.27
7-day Compressive Strength (MPa)	31.17	33.47	34.40	33.13	32.37
28-day Compressive Strength (MPa)	38.28	45.47	41.43	39.10	47.90

<sup>a</sup> Untreated Omnia phosphogypsum

<sup>b</sup> Omnia phosphogypsum treated by the optimum H<sub>2</sub>SO<sub>4</sub> treatment method

<sup>c</sup> Untreated Kynoch phosphogypsum

<sup>d</sup> Kynoch phosphogypsum treated by the optimum H<sub>2</sub>SO<sub>4</sub> treatment method

<sup>e</sup> Natural Gypsum

The initial setting time of cement containing untreated Omnia phosphogypsum was delayed from 130 minutes to 265 minutes, when compared to cement containing natural gypsum. The retardation effect was smaller than in the case of untreated Kynoch phosphogypsum. When the Omnia phosphogypsum was treated by the optimum sulphuric acid treatment method, the initial setting time was improved to 189 minutes. Although this was still not comparable to the initial setting time of 130 minutes obtained for the cement samples containing natural gypsum, the Omnia phosphogypsum sample treated by the optimum sulphuric acid treatment method yielded an initial setting time closest to the desired value. This indicates that the optimum sulphuric acid treatment method has been successful in improving the initial setting times of cement containing phosphogypsum as a set retarder.



The final setting time of cement containing untreated Kynoch phosphogypsum was significantly impeded from 3.0 hours to 7.2 hours, but was improved to 4.9 hours when the Kynoch phosphogypsum sample was treated by the optimum sulphuric acid treatment method. Similarly, the final setting time of cement containing untreated Omnia phosphogypsum was delayed from 3.0 hours to 5.8 hours, with an improvement to 4.2 hours when the treated Omnia phosphogypsum was used.

The prolonged setting times of cement containing phosphogypsum can again be ascribed to the fact that all the treated and untreated phosphogypsum samples still contained a considerable amount of phosphorous impurities.

The 2-day compressive strength was in all instances lower when treated and untreated Kynoch phosphogypsum samples were used as a set retarder instead of natural gypsum. However, some improvement was observed in the 2-day compressive strength of the cement sample containing the optimum sulphuric acid treated Omnia phosphogypsum sample. The cement samples containing both the treated and untreated phosphogypsum have shown similar performance in the 7-day compressive strengths when compared to the cement sample containing natural gypsum.

For both Kynoch and Omnia phosphogypsum, the 28-day compressive strengths of cement containing the untreated phosphogypsum samples were lower than that of the cement sample containing natural gypsum. Treatment of these samples by the optimized sulphuric acid treatment method improved the performance of the cement sample containing the treated Omnia phosphogypsum, but had no significant effect on the 28-day compressive strength of cement containing treated Kynoch phosphogypsum.

CaO	72.85	33.07	33.78	33.45
H <sub>2</sub> O	0.76	0.03	1.60	0.07
SO <sub>3</sub>	48.27	48.86	49.35	48.83
LOI	21.31	18.25	18.78	18.74
TOTAL	101.84	101.33	99.73	101.14

<sup>10</sup> means that the compound was present in a quantity below the detection limit



## 8.4 Results and discussion of the combined thermal and sulphuric acid treatment method, applied to South African phosphogypsum

A new method was developed in which the South African phosphogypsum samples were subjected to thermal treatment, followed by treatment in sulphuric acid. The aim of this method was to change the hydrated form of calcium sulphate contained in phosphogypsum, and subsequently study the effect of a change in the amount of water of crystallization on the purification of phosphogypsum.

### 8.4.1 The combined thermal and sulphuric acid treatment method

Tables 8.17 and 8.18 describe the XRF results obtained after Batch 2 of both Kynoch and Omnia phosphogypsum were treated by the combined thermal and sulphuric acid method. The treated samples contained almost no  $P_2O_5$ , which implies that this method was successful in removing the harmful phosphorous impurities from the phosphogypsum samples.

**Table 8.17 XRF analysis of Batch 2 phosphogypsum samples, treated by the combined thermal and sulphuric acid treatment method**

Compounds (%)	Kynoch phosphogypsum		Omnia phosphogypsum	
	Untreated	Treated	Untreated	Treated
SiO <sub>2</sub>	0.23	0.12	0.05	0
Al <sub>2</sub> O <sub>3</sub>	0.12	0	0	0
Fe <sub>2</sub> O <sub>3</sub>	0*	0	0	0
MgO	0	0	0.07	0
CaO	32.58	33.07	33.79	33.45
<b>P<sub>2</sub>O<sub>5</sub></b>	<b>0.76</b>	<b>0.03</b>	<b>1.69</b>	<b>0.07</b>
SO <sub>3</sub>	46.22	48.86	45.35	48.83
LOI	21.31	19.25	18.78	18.79
TOTAL	101.64	101.33	99.73	101.14

\*0 means that the compound was present in a quantity below the detection limit

**Table 8.18 XRF analysis of Batch 2 phosphogypsum samples, treated by the combined thermal and sulphuric acid treatment method, normalised to a loss free basis**

Compounds (%)	Kynoch phosphogypsum		Omnia phosphogypsum	
	Untreated	Treated	Untreated	Treated
SiO <sub>2</sub>	0.29	0.15	0.06	0*
Al <sub>2</sub> O <sub>3</sub>	0.15	0	0	0
MgO	0	0	0.09	0
CaO	40.46	40.29	41.74	40.56
<b>P<sub>2</sub>O<sub>5</sub></b>	<b>0.95</b>	<b>0.04</b>	<b>2.09</b>	<b>0.09</b>
SO <sub>3</sub>	57.54	59.53	56.02	59.30

\*0 means that the compound was present in a quantity below the detection limit

The results obtained from the thermogravimetric analyses of the phosphogypsum samples, treated by the combined thermal and sulphuric acid method, are given in Figures 8.11 and 8.12.

The treated Kynoch phosphogypsum revealed a total mass loss of 19.5%, which is close to the theoretical value of 20.9%. This indicates that the sample consisted mainly of calcium sulphate dihydrate. However, the treated Omnia phosphogypsum sample showed a total mass loss of only 15.4%, which means that this sample contained a mixture of calcium sulphate dihydrate and one or both of the hemihydrate and anhydrite forms. The DSC peak ratio obtained for the treated Omnia phosphogypsum could not be of any help to solve this, since the first dehydration peak did not return to the baseline before the second peak started, which makes the value of the peak ratio unusable.

**Figure 8.11** TG and DSC curves obtained for the Batch 2 Kynoch phosphogypsum sample, treated by the combined thermal and H<sub>2</sub>SO<sub>4</sub> treatment method

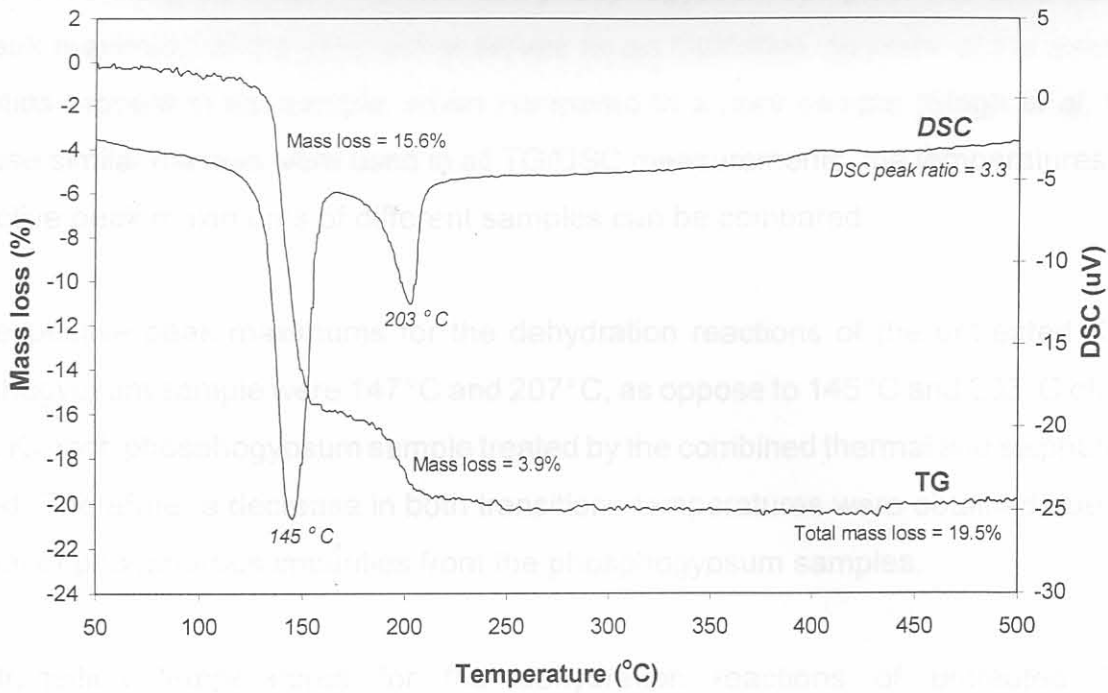
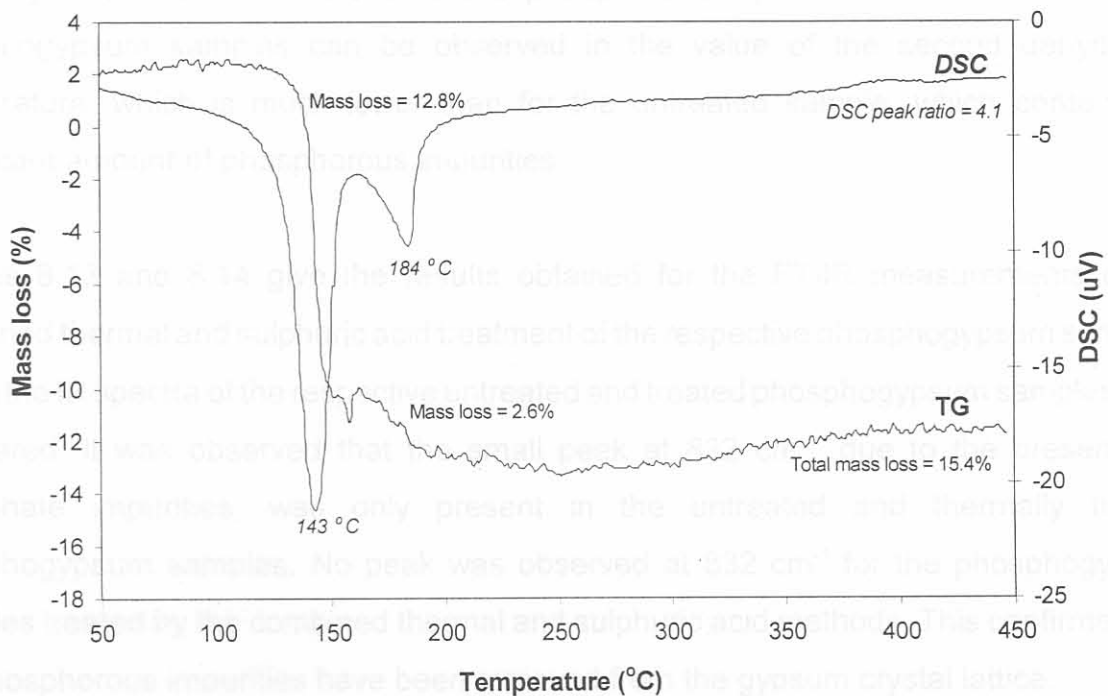


**Figure 8.12** TG and DSC curves obtained for the Batch 2 Omnia phosphogypsum sample, treated by the combined thermal and H<sub>2</sub>SO<sub>4</sub> treatment method





When the DSC curves are compared with the curves of the untreated Batch 2 phosphogypsum samples in Figure 5.7, the maximum temperatures for both dehydration reactions were slightly lower for the treated phosphogypsum samples. The temperature at the peak maximum of the DSC curve serves as an indicative measure of the amount of impurities present in the sample, when compared to a pure sample (Singh *et al*, 1996). Because similar masses were used in all TG/DSC measurements, the temperatures of the respective peak maximums of different samples can be compared.

The respective peak maximums for the dehydration reactions of the untreated Kynoch phosphogypsum sample were 147°C and 207°C, as oppose to 145°C and 203°C obtained for the Kynoch phosphogypsum sample treated by the combined thermal and sulphuric acid method. Therefore, a decrease in both transitions temperatures were obtained due to the removal of phosphorous impurities from the phosphogypsum samples.

The transition temperatures for the dehydration reactions of untreated Omnia phosphogypsum were 118°C and 194°C, compared to 143°C and 184°C for the combined thermal and sulphuric acid treated samples. The much lower value of the first transition can again be explained by the formation of the  $\alpha$ -hemihydrate on dehydration of the untreated Omnia phosphogypsum, while the treated Omnia phosphogypsum samples formed the  $\beta$ -hemihydrate. The effect of the removal of phosphorous impurities from the treated Omnia phosphogypsum samples can be observed in the value of the second dehydration temperature, which is much lower than for the untreated sample, which contained a significant amount of phosphorous impurities.

Figures 8.13 and 8.14 give the results obtained for the FT-IR measurements of the combined thermal and sulphuric acid treatment of the respective phosphogypsum samples. When the IR spectra of the respective untreated and treated phosphogypsum samples were compared, it was observed that the small peak at 832  $\text{cm}^{-1}$ , due to the presence of phosphate impurities, was only present in the untreated and thermally treated phosphogypsum samples. No peak was observed at 832  $\text{cm}^{-1}$  for the phosphogypsum samples treated by the combined thermal and sulphuric acid methods. This confirmed that the phosphorous impurities have been removed from the gypsum crystal lattice.

Figure 8.13 The IR spectra of  $\text{CaSO}_4 \cdot 2\text{H}_2\text{O}$ , the untreated and treated Batch 2 Kynoch phosphogypsum samples, treated by the combined thermal and  $\text{H}_2\text{SO}_4$  treatment method

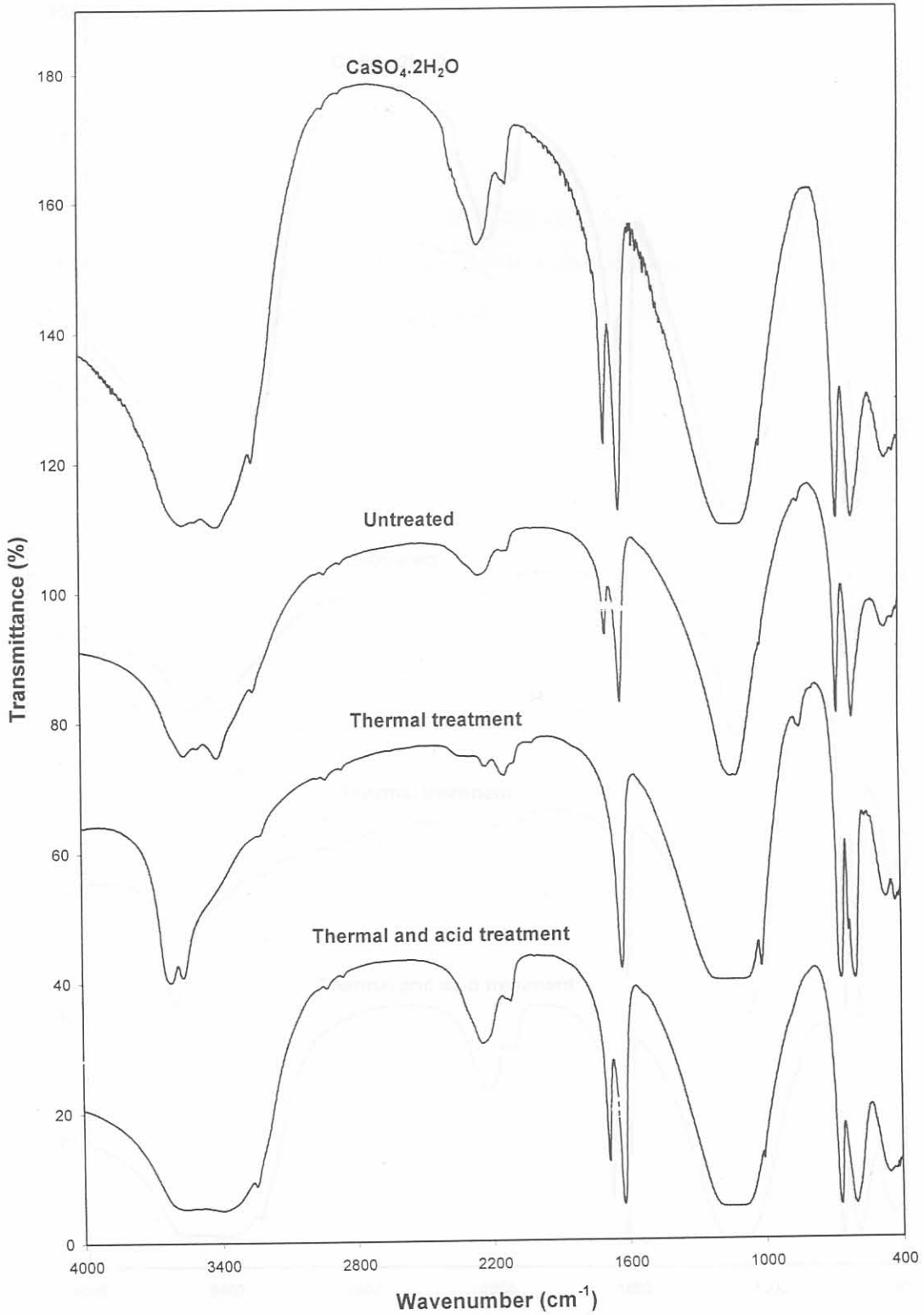
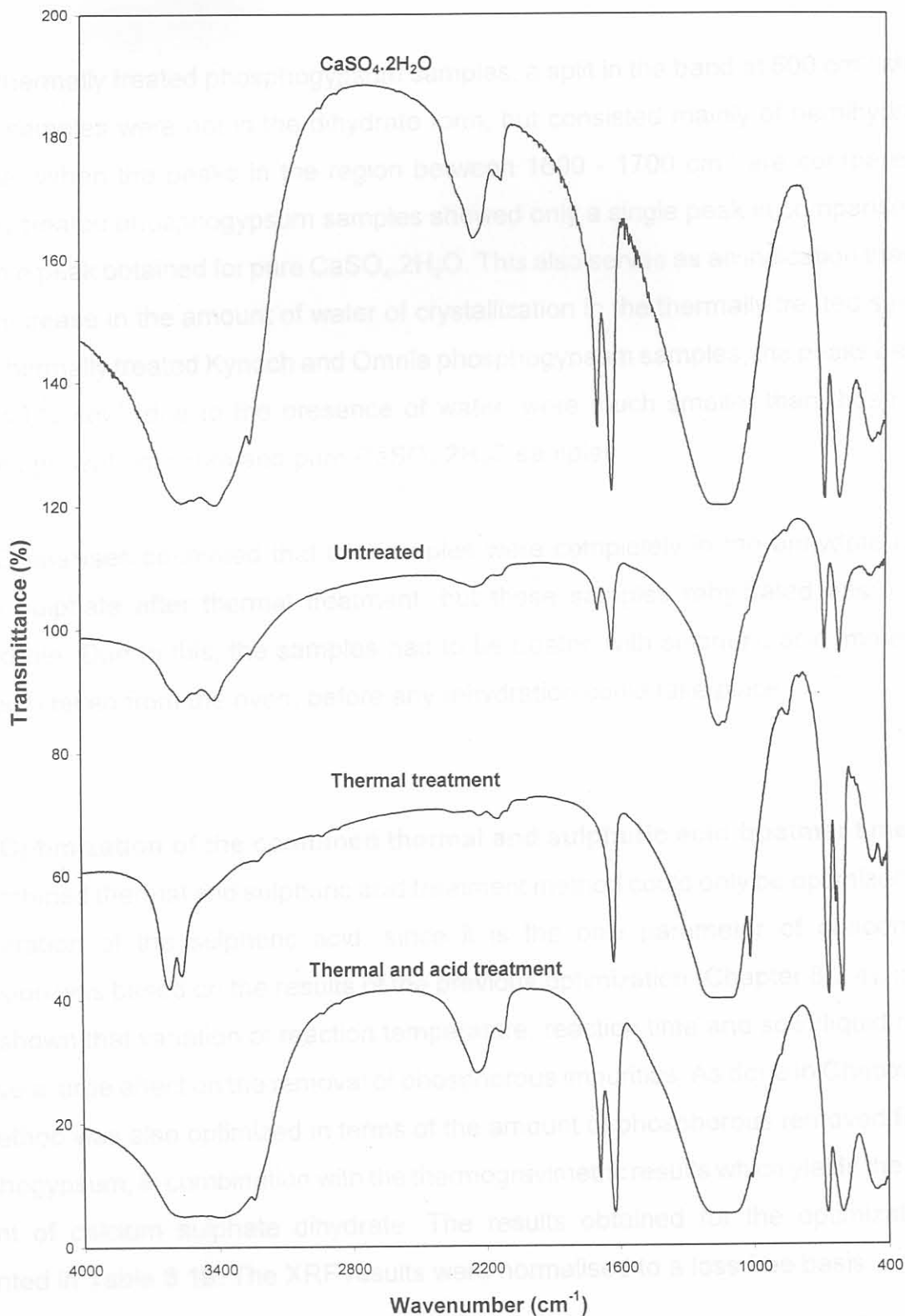


**Figure 8.14** The IR spectra of  $\text{CaSO}_4 \cdot 2\text{H}_2\text{O}$ , the untreated and treated Batch 2 Omnia phosphogypsum samples, treated by the combined thermal and  $\text{H}_2\text{SO}_4$  treatment method





The IR spectra of the phosphogypsum samples treated by the combined thermal and sulphuric acid method was the same as that obtained for pure  $\text{CaSO}_4 \cdot 2\text{H}_2\text{O}$ , which also confirms the TG/DSC results in that the samples consisted of the dihydrate form of calcium sulphate.

For the thermally treated phosphogypsum samples, a split in the band at  $600\text{ cm}^{-1}$  showed that the samples were not in the dihydrate form, but consisted mainly of hemihydrate or anhydrite. When the peaks in the region between  $1600 - 1700\text{ cm}^{-1}$  are compared, the thermally treated phosphogypsum samples showed only a single peak in comparison with the double peak obtained for pure  $\text{CaSO}_4 \cdot 2\text{H}_2\text{O}$ . This also serves as an indication that there was a decrease in the amount of water of crystallization in the thermally treated samples. For the thermally treated Kynoch and Omnia phosphogypsum samples, the peaks between  $3400 - 4000\text{ cm}^{-1}$ , due to the presence of water, were much smaller than those of the untreated phosphogypsum and pure  $\text{CaSO}_4 \cdot 2\text{H}_2\text{O}$  samples.

TG/DSC analyses confirmed that the samples were completely in the anhydrite form of calcium sulphate after thermal treatment, but these samples rehydrated easily to the hemihydrate. Due to this, the samples had to be treated with sulphuric acid immediately after being taken from the oven, before any rehydration could take place.

#### **8.4.2 Optimization of the combined thermal and sulphuric acid treatment method**

The combined thermal and sulphuric acid treatment method could only be optimized for the concentration of the sulphuric acid, since it is the only parameter of concern. This conclusion was based on the results of the previous optimization (Chapter 8.3.4), in which it was shown that variation of reaction temperature, reaction time and solid:liquid ratio did not have a large effect on the removal of phosphorous impurities. As done in Chapter 8.3.4, this method was also optimized in terms of the amount of phosphorous removed from the phosphogypsum, in combination with the thermogravimetric results which yields the highest amount of calcium sulphate dihydrate. The results obtained for the optimization are presented in Table 8.19. The XRF results were normalised to a loss free basis.

**Table 8.19 XRF and TG results for the optimization of the concentration of sulphuric acid for the combined thermal and acid treatment method**

Concentration $H_2SO_4$ (% m/m)	Kynoch phosphogypsum		Omnia phosphogypsum	
	$P_2O_5$ (%)	Mass loss (%)	$P_2O_5$ (%)	Mass loss (%)
Untreated	1.05	17.2	1.86	15.1
1	0.14	19.1	0.20	18.1
5	0.08	18.4	0.09	19.9
10	0.06	16.8	0.06	19.1
20	0.05	20.4	0.06	19.9
50	0.04	19.5	0.63	15.8

For the Kynoch phosphogypsum sample treated in a 1%  $H_2SO_4$  solution there were still some phosphorous impurities present. All other samples contained almost no phosphorous impurities, and produced mainly calcium sulphate dihydrate, as can be observed from the high mass losses. The sample treated in a 10%  $H_2SO_4$  solution yielded a lower amount of calcium sulphate dihydrate than the other samples.

The phosphorous impurities contained in Omnia phosphogypsum were removed in the samples treated in 5%, 10% and 20%  $H_2SO_4$ . Fewer phosphorous impurities were removed when the Omnia phosphogypsum samples were treated in a 50%  $H_2SO_4$  solution, and the percentage mass loss for this sample was smaller than that of the other treated Omnia phosphogypsum samples. This indicates that treatment of the Omnia phosphogypsum in a 50%  $H_2SO_4$  solution resulted in the formation of a smaller amount of the dihydrate form of calcium sulphate when compared to the other samples.

Based on the abovementioned remarks, a sulphuric acid concentration of 5% (by mass) was chosen as the optimum concentration. Although other concentrations produced similar results, it is more economical for industrial purposes, to use an acid concentration as low as possible.



### 8.4.3 The combined thermal and sulphuric acid treatment on a large scale for the performance of cement tests

After optimization of the concentration of sulphuric acid, the combined thermal and acid treatment method was used to treat the Kynoch and Omnia phosphogypsum samples on a large scale for use in cement tests. The results of the XRF analyses are summarised in Tables 8.20 and 8.21. For both types of phosphogypsum, the phosphorous impurities were almost completely removed, which means that the samples consisted of mainly pure calcium sulphate.

**Table 8.20 XRF analysis of Batch 2 phosphogypsum samples, treated on a large scale by the combined thermal and H<sub>2</sub>SO<sub>4</sub> method, for the performance of cement tests**

Compounds (%)	Kynoch phosphogypsum		Omnia phosphogypsum	
	Untreated	Thermal and acid treatment	Untreated	Thermal and acid treatment
SiO <sub>2</sub>	0.22	0.15	0.14	0.07
Al <sub>2</sub> O <sub>3</sub>	0.11	0*	0.01	0
Fe <sub>2</sub> O <sub>3</sub>	0	0	0	0
MnO	0	0	0	0
MgO	0	0	0	0
CaO	32.75	32.56	32.21	33.24
Cr <sub>2</sub> O <sub>3</sub>	0	0	0	0
K <sub>2</sub> O	0	0	0	0
Na <sub>2</sub> O	0	0	0	0
<b>P<sub>2</sub>O<sub>5</sub></b>	<b>0.81</b>	<b>0.03</b>	<b>1.21</b>	<b>0.05</b>
SO <sub>3</sub>	42.85	46.34	45.75	45.79
LOI	21.38	21.01	20.35	20.90
<b>TOTAL</b>	<b>98.12</b>	<b>100.13</b>	<b>99.67</b>	<b>100.05</b>

\*0 means that the compound was present in a quantity below the detection limit



**Table 8.21** XRF analysis of Batch 2 phosphogypsum samples, treated on a large scale by the combined thermal and H<sub>2</sub>SO<sub>4</sub> method, for the performance of cement tests

Compounds (%)	Kynoch phosphogypsum		Omnia phosphogypsum	
	Untreated	Thermal and acid treatment	Untreated	Thermal and acid treatment
SiO <sub>2</sub>	0.29	0.19	0.18	0.09
Al <sub>2</sub> O <sub>3</sub>	0.14	0*	0.01	0
CaO	42.68	41.15	40.61	42.00
P <sub>2</sub> O <sub>5</sub>	<b>1.06</b>	<b>0.04</b>	<b>1.53</b>	<b>0.06</b>
SO <sub>3</sub>	55.84	58.57	57.68	57.85

\*0 means that the compound was present in a quantity below the detection limit

The results obtained from the thermogravimetric analysis of these samples are summarised in Figures 8.15 and 8.16.

**Figure 8.15** The TG and DSC curves obtained for the untreated and treated Batch 2 Kynoch phosphogypsum samples, treated on a large scale by the combined thermal and H<sub>2</sub>SO<sub>4</sub> method, for the performance of cement tests

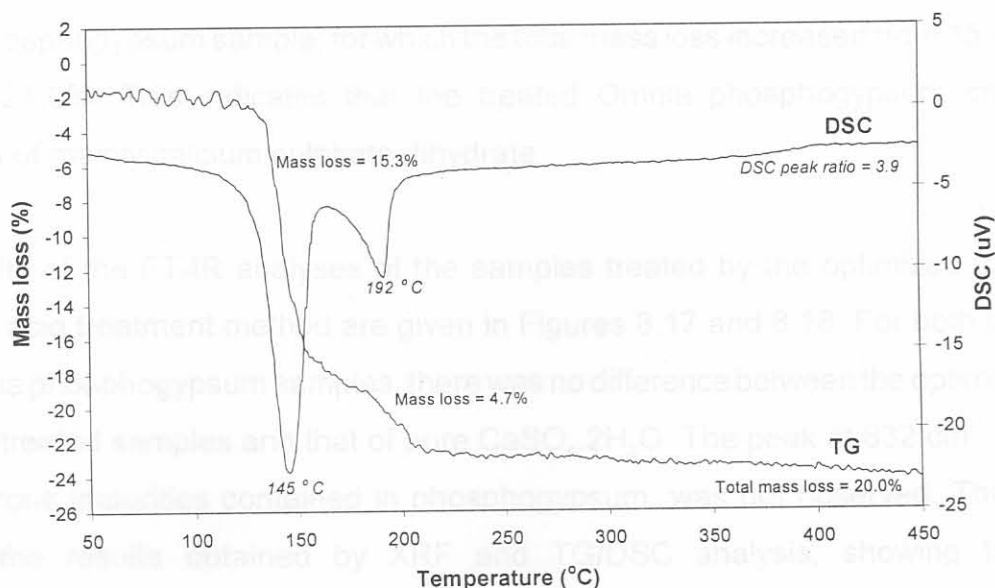
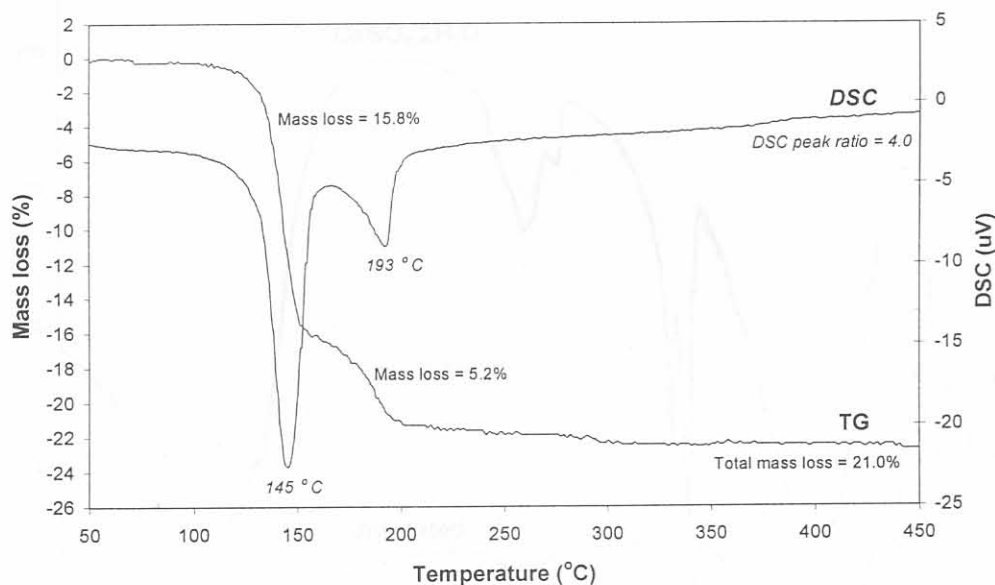


**Figure 8.16** The TG and DSC curves obtained for the untreated and treated Batch 2 Omnia phosphogypsum samples, treated on a large scale by the combined thermal and H<sub>2</sub>SO<sub>4</sub> method, for the performance of cement tests



The DSC curves are similar to the results obtained when the phosphogypsum samples were treated by this method on a small scale, as discussed in Chapter 8.3.7. After optimization of the concentration of H<sub>2</sub>SO<sub>4</sub>, the TG curve obtained for Kynoch shows that the treated Kynoch phosphogypsum sample, which revealed a total mass loss of 20.0%, was still in the preferred dihydrate form. The optimization had a significant effect on the treatment of the Omnia phosphogypsum sample, for which the total mass loss increased from 15.4% (Figure 8.12) to 21.0%. This indicates that the treated Omnia phosphogypsum sample also consisted of mainly calcium sulphate dihydrate.

The results of the FT-IR analyses of the samples treated by the optimized thermal and sulphuric acid treatment method are given in Figures 8.17 and 8.18. For both the Kynoch and Omnia phosphogypsum samples, there was no difference between the optimum thermal and acid treated samples and that of pure CaSO<sub>4</sub>·2H<sub>2</sub>O. The peak at 832 cm<sup>-1</sup>, due to the phosphorous impurities contained in phosphogypsum, was not observed. These results confirm the results obtained by XRF and TG/DSC analysis, showing the treated phosphogypsum samples consisted mainly of pure CaSO<sub>4</sub>·2H<sub>2</sub>O.

Figure 8.17 The IR spectra of the untreated and treated Batch 2 Kynoch phosphogypsum samples, treated on a large scale by the combined thermal and sulphuric acid method, for the performance of cement tests

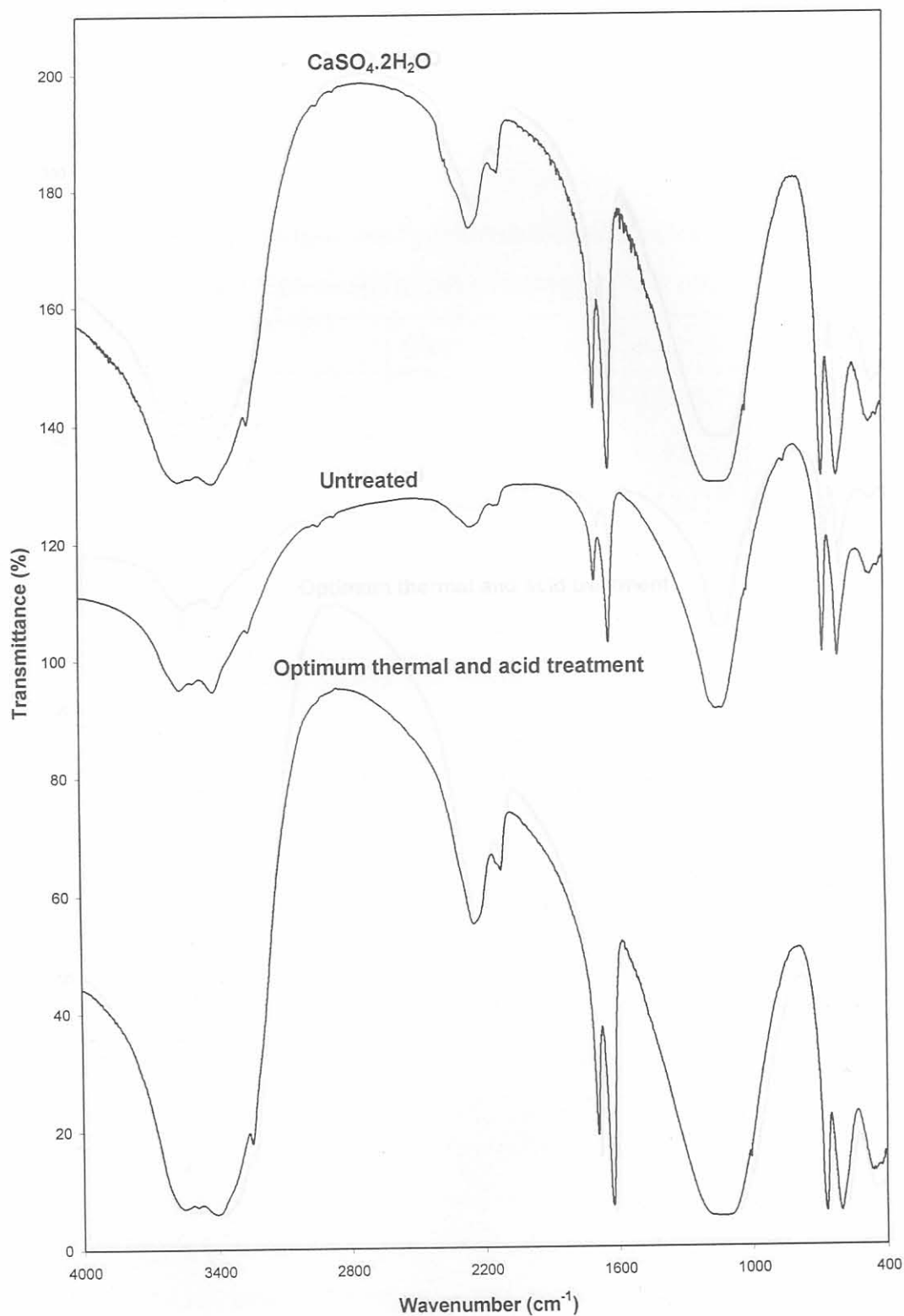
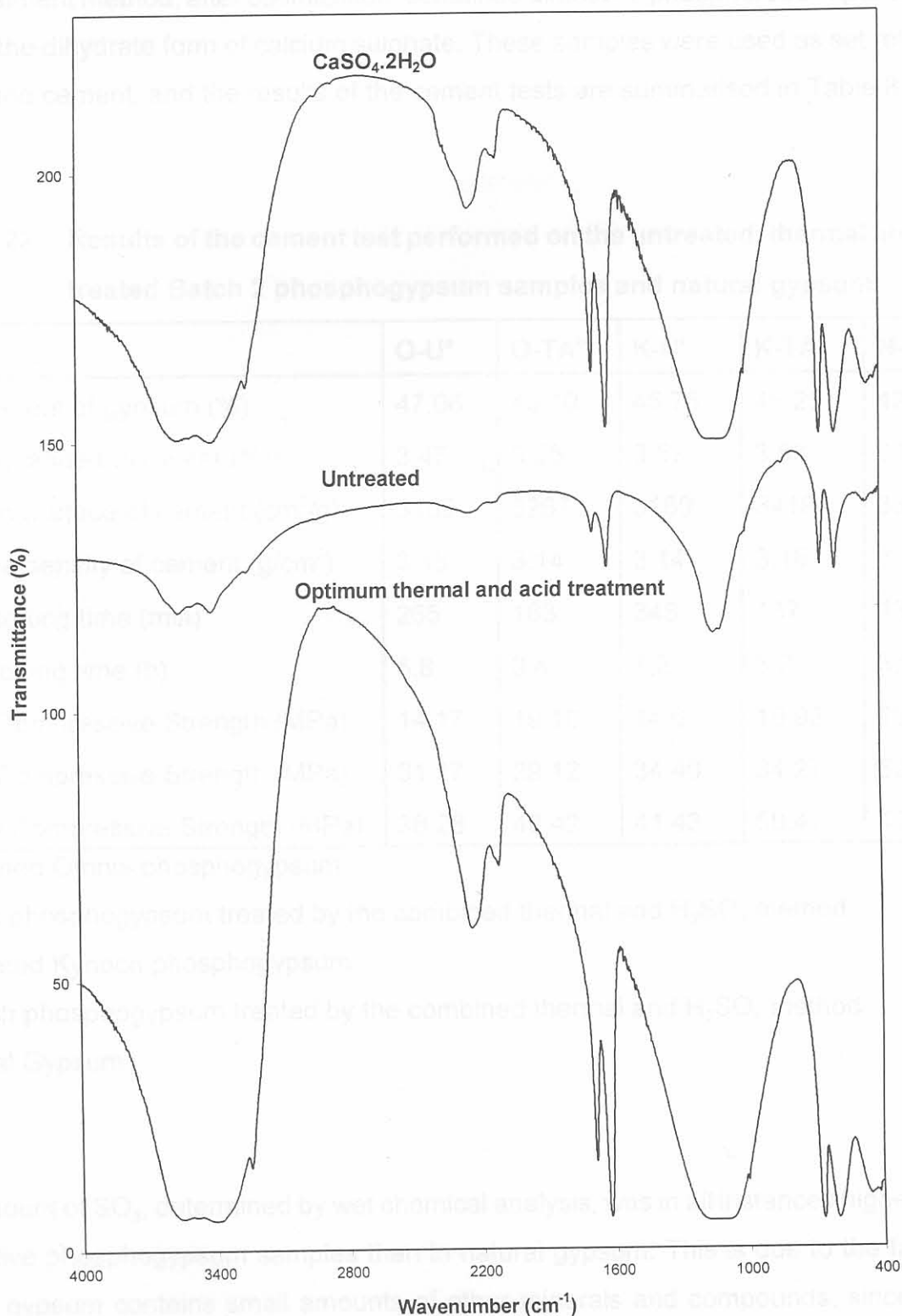




Figure 8.18 The IR spectra of the untreated and treated Batch 2 Omnia phosphogypsum samples, treated on a large scale by the combined thermal and sulphuric acid method, for the performance of cement tests



#### 8.4.4 Performance of cement tests on the combined thermal and sulphuric acid treated phosphogypsum samples

The treated phosphogypsum samples obtained from the combined thermal and sulphuric acid treatment method, after optimization, contained almost no phosphorous impurities and were in the dihydrate form of calcium sulphate. These samples were used as set retarders in Portland cement, and the results of the cement tests are summarised in Table 8.22.

**Table 8.22 Results of the cement test performed on the untreated, thermal and acid treated Batch 2 phosphogypsum samples and natural gypsum**

Test	O-U <sup>a</sup>	O-TA <sup>b</sup>	K-U <sup>c</sup>	K-TA <sup>d</sup>	N-G <sup>e</sup>
SO <sub>3</sub> content of gypsum (%)	47.06	46.10	45.76	46.25	42.50
Gypsum added to clinker (%)	3.47	3.55	3.57	3.53	3.85
Specific Surface of cement (cm <sup>2</sup> /g)	3159	3267	3180	3419	3314
Relative density of cement (g/cm <sup>3</sup> )	3.15	3.14	3.14	3.16	3.14
Initial setting time (min)	265	163	348	137	130
Final setting time (h)	5.8	3.4	7.2	3.2	3.0
2-day Compressive Strength (MPa)	14.17	19.10	14.67	19.93	19.27
7-day Compressive Strength (MPa)	31.17	29.12	34.40	34.27	32.37
28-day Compressive Strength (MPa)	38.28	46.42	41.43	50.47	47.90

<sup>a</sup> Untreated Omnia phosphogypsum

<sup>b</sup> Omnia phosphogypsum treated by the combined thermal and H<sub>2</sub>SO<sub>4</sub> method

<sup>c</sup> Untreated Kynoch phosphogypsum

<sup>d</sup> Kynoch phosphogypsum treated by the combined thermal and H<sub>2</sub>SO<sub>4</sub> method

<sup>e</sup> Natural Gypsum

The amount of SO<sub>3</sub>, determined by wet chemical analysis, was in all instances higher in the respective phosphogypsum samples than in natural gypsum. This is due to the fact that natural gypsum contains small amounts of other minerals and compounds, since it is a naturally mined product. The specific surface area and relative density of the cement

containing the respective treated and untreated phosphogypsum samples was similar to that containing natural gypsum.

The 2-day compressive strength of the cement containing untreated Kynoch and Omnia phosphogypsum was lower than cement containing natural gypsum. However, after the phosphogypsum samples were treated by the combined thermal and sulphuric acid treatment method, the respective 2-day strengths were improved to values similar to that obtained for the cement sample containing natural gypsum. The 7-day compressive strengths of cement samples containing the untreated and treated Kynoch and Omnia phosphogypsum compared well to the compressive strength value obtained for the cement sample containing natural gypsum.

The 28-day compressive strength of cement containing untreated Kynoch and Omnia phosphogypsum was lower than that of cement containing natural gypsum. After treatment of the respective phosphogypsum samples by the combined thermal and sulphuric acid treatment method, the 28-day compressive strength of cement containing the treated phosphogypsum samples improved to values similar to that for cement containing natural gypsum.

The initial setting time of the cement containing untreated Omnia phosphogypsum sample was delayed from 130 minutes to 265 minutes, when compared to the sample containing natural gypsum. This was improved to 163 minutes after the Omnia phosphogypsum was treated by the combined thermal and sulphuric acid treatment method. This sample contained 0.06%  $P_2O_5$ , and was mainly in the dihydrate form of calcium sulphate.

For the untreated Kynoch phosphogypsum, an initial setting time of 348 minutes was obtained when used as a set retarder in cement. The initial setting time for cement containing Kynoch phosphogypsum treated by the combined thermal and sulphuric acid treatment method, was considerably improved to 137 minutes, which compares well to the value of 130 minutes obtained for cement containing natural gypsum. The treated Kynoch phosphogypsum sample contained 0.04%  $P_2O_5$ , and was also mainly in the dihydrate form of calcium sulphate.



The final setting time of cement containing untreated Omnia phosphogypsum was 5.8 hours, and 7.2 hours for cement containing untreated Kynoch phosphogypsum. These samples produced final setting times that were significantly longer than the value of 3.0 hours obtained when natural gypsum was used as a set retarder. After treatment of the phosphogypsum samples by the combined thermal and sulphuric acid treatment method, the final setting time of cement containing treated Omnia phosphogypsum, was improved to 3.4 hours, and that for Kynoch phosphogypsum to 3.2 hours. These values correspond well to the value obtained when natural gypsum is used as a set retarder.

According to Jackson (Hewlett, 1998b), the retarding action of phosphorous impurities can only be eliminated if the water-soluble content of  $P_2O_5$  is reduced to below 0.02%. The effect of the amount of phosphorous impurities has been demonstrated clearly in this study, and the total amount of phosphorous impurities contained in phosphogypsum should preferably be kept below 0.06%.

## 8.5 Conclusion

When Jarosiński's method was applied to Batch 1 of both types of South African phosphogypsum, the phosphorous impurities were removed completely. However, the final products consisted of only calcium sulphate anhydrite. Although these treated samples were free of phosphorous impurities, they could not be applied as a set retarder in Portland cement, because the dihydrate form of calcium sulphate is required. Rehydration of these samples was not possible since the insoluble anhydrite, which shows no reaction with water, was formed.

This method was repeated on new batches of both types of phosphogypsum. Fewer phosphorous impurities were removed, when compared to the first batches, but the obtained products contained mainly calcium sulphate dihydrate. Treatment of Batch 2 phosphogypsum samples removed about 32% of the phosphorous impurities contained in Kynoch phosphogypsum, and 51% from the Omnia phosphogypsum. The respective total mass losses obtained by TG analysis were 19.6% for the Kynoch phosphogypsum sample

and 16.5% for the Omnia phosphogypsum. This indicated that the treated Omnia phosphogypsum sample contained some calcium sulphate hemihydrate and/or anhydrite. After optimization of this method, the total mass loss for the Omnia phosphogypsum sample increased to 19.2%, which means that this sample also contained mainly calcium sulphate dihydrate.

A possible explanation for the difference in behaviour of these different batches of phosphogypsum can be found from the FT-IR analyses. These analyses have shown that, after the leaching step, the respective Batch 1 phosphogypsum samples were in the anhydrite form, while the corresponding samples for the Batch 2 phosphogypsum were in the dihydrate form. This shows that the phosphorous impurities are more easily removed from the anhydrite crystal lattice than from the dihydrate lattice. The Batch 1 phosphogypsum samples possibly formed the anhydrite due to different physical properties of these samples, or due to the fact that this treatment was done on a smaller scale than treatment of the Batch 2 phosphogypsum samples.

The results obtained for the cement tests when sulphuric acid treated phosphogypsum samples were used instead of natural gypsum as a set retarder in Portland cement have shown that the compression strengths of cement containing untreated and treated phosphogypsum compared well with the case in which natural gypsum was used.

When compared to the cement containing untreated phosphogypsum, the initial and final setting times of the cement samples containing the sulphuric acid treated phosphogypsum samples improved significantly. However, this improvement was not satisfactory when compared to the performance of the cement tests when natural gypsum is used as a set retarder in Portland cement.

Treating the respective Batch 2 phosphogypsum samples by the combined thermal and sulphuric acid treatment method removed 96% of the phosphorous impurities for both the Kynoch and Omnia phosphogypsum. A total mass loss of 19.5% was obtained for the dehydration reaction of the treated Kynoch phosphogypsum sample, while a mass loss of 15.4% was obtained for the Omnia phosphogypsum sample. After optimization of the



concentration of sulphuric acid, the total mass loss obtained for Omnia phosphogypsum was increased to 21.0%.

The combined thermal and sulphuric acid treatment method was successful in removing the harmful phosphorous impurities from the gypsum crystal lattice, and the obtained products consisted of the required dihydrate form of calcium sulphate. These samples produced FT-IR curves that were the same as that of pure  $\text{CaSO}_4 \cdot 2\text{H}_2\text{O}$ .

The initial setting time of the cement containing Omnia phosphogypsum treated by the combined thermal and sulphuric acid treatment method improved to from 265 minutes to 163 minutes. This sample contained 0.06%  $\text{P}_2\text{O}_5$ , and was mainly in the dihydrate form of calcium sulphate. The initial setting time for cement containing Kynoch phosphogypsum treated by the same treatment method was considerably improved from 348 minutes to 137 minutes, which compares well to the value of 130 minutes obtained for cement containing natural gypsum. The treated Kynoch phosphogypsum sample contained 0.04%  $\text{P}_2\text{O}_5$ , and was also mainly in the dihydrate form of calcium sulphate.

After treatment of the phosphogypsum samples by the combined thermal and sulphuric acid treatment method, the final setting time of cement containing treated Omnia phosphogypsum was improved to 3.4 hours, and that for Kynoch phosphogypsum to 3.2 hours. These values correspond well to the value obtained when natural gypsum is used as a set retarder.

These results have proved that the combined thermal and sulphuric acid treatment method was successful in removing most of the phosphorous impurities from the phosphogypsum crystal lattice, as well as in converting the samples to the dihydrate form of calcium sulphate. Portland cement containing phosphogypsum samples treated by the combined thermal and sulphuric acid treatment method revealed setting times and compressive strength values similar to values obtained when natural gypsum was used as a set retarder.



## Chapter 9 Conclusion

Phosphogypsum has to be purified of the harmful phosphorous impurities before it can replace natural gypsum as a set retarder in Portland cement. The amount of impurities contained in phosphogypsum depend upon the purity of the raw materials used in the production of phosphoric acid, the operating conditions of the phosphoric acid process and the age of the disposed phosphogypsum stockpile. These impurities tend in an unpredictable way to delay the setting time, and decrease the mechanical strength development of cement.

The calcium sulphate phase present in the Portland cement mixture will also affect the setting time considerably, due to the difference in solubility of the different phases. The calcium sulphate dihydrate form,  $\text{CaSO}_4 \cdot 2\text{H}_2\text{O}$ , is preferred for use in Portland cement.

The different South African phosphogypsum samples used during this study were found to contain a significant amount of phosphorous impurities, substituted in the gypsum crystal lattice. The presence of considerable amounts of calcium sulphate hemihydrate or anhydrite in some of the untreated phosphogypsum samples could also limit the effectiveness of phosphogypsum as a set retarder in Portland cement.

The particle size distribution in the South African phosphogypsum samples plays an important role when the phosphorous impurities are considered, which indicates that sieving can be applied to remove some of the phosphorous impurities. However, this is not effective for the purification of phosphogypsum for use in Portland cement, since the amount of phosphorous impurities, contained in the sieved fractions with fewer phosphorous impurities, was still too large.

In order to remove more of the phosphorous impurities, a combined thermal and washing treatment was performed on the respective phosphogypsum samples. A similar method was

described by Ölmez and Yilmaz (1988) as being successful in removing most of the impurities in Turkish phosphogypsum. Application of this method to South African phosphogypsum proved not to remove the phosphorous impurities contained in the phosphogypsum crystal lattice, but was successful in removing some of the water-soluble impurities. The phosphorous impurities contained in South African phosphogypsum seemed to consist mainly of phosphorous combined in the gypsum crystal lattice and not water-soluble compounds.

Jarosiński (1994) described a sulphuric acid treatment method for the recovery of rare earths from phosphogypsum. Treatment of the South African phosphogypsum samples by a similar sulphuric acid treatment method removed more phosphorous impurities than the previous washing treatments, and the treated samples contained mainly the dihydrate form of calcium sulphate.

The sulphuric acid treatment method was then combined with thermal treatment, and this method proved to be successful in removing most of the harmful phosphorous impurities from the gypsum crystal lattice. The obtained gypsum products consisted mainly of the required dihydrate form of calcium sulphate. This treatment method proved to be the best for the South African phosphogypsum samples, and a possible explanation for its mechanism will be discussed.

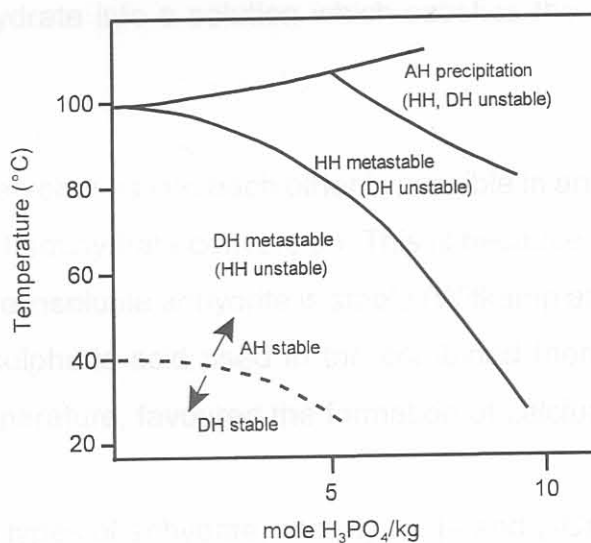
The amount of foreign ions incorporated in the gypsum crystal lattice largely depends on the operating conditions of the phosphoric acid process, given by the  $\text{H}_3\text{PO}_4$  and  $\text{H}_2\text{SO}_4$  content of the reaction solution, the temperature, and the supersaturation. The nature of the precipitated calcium sulphate phase also influences the uptake of foreign ions. Depending on the temperature and the  $\text{H}_3\text{PO}_4$  and  $\text{H}_2\text{SO}_4$  content of the solution, either calcium sulphate dihydrate, hemihydrate or insoluble anhydrite ( $\beta\text{-CaSO}_4$ ) will be formed, as shown in Figure 9.1 (van der Sluis *et al*, 1986).

The solid lines in Figure 9.1 represent equilibrium curves, but since some of the modifications are metastable under the given conditions, these lines merely indicate which phase will initially precipitate. The broken line separates the regions where either dihydrate



or anhydrite is stable. The dihydrate and insoluble anhydrite are the only thermodynamically stable forms of calcium sulphate, as the hemihydrate form only exists as a metastable phase. The influence of  $H_2SO_4$  on the position of the curves in Figure 9.1 can be taken into account by assuming 1 mol of  $H_2SO_4$  is equivalent to about 1.5 mol of  $H_3PO_4$  (van der Sluis *et al*, 1986).

**Figure 9.1** The precipitated calcium sulphate phase as a function of the  $H_3PO_4$  content and temperature of the solution (van der Sluis *et al*, 1986; Witkamp and van Rosmalen; 1990)



The role of  $H_2SO_4$  and  $H_3PO_4$  in the formation of the different calcium sulphate phases can be explained by the activity of water, as the determining factor in the stability of the three phases (Witkamp and van Rosmalen, 1986). The three phases contain different percentages of water, leading to a dependency of their stability on the activity of water. At higher acid concentrations, the amount of free water, and therefore the activity of water, is lower. This favours the formation of a more dehydrated phase, namely anhydrite or hemihydrate with respect to the dihydrate phase. At higher temperatures, water tends to form looser bonds in the crystal and also in the solution, thus favouring the vapour phase. This makes calcium sulphate forms which contain less water of crystallization stable at high temperatures.



From the diagram it is observed that insoluble anhydrite ( $\beta$ - $\text{CaSO}_4$ ) appears to be stable in the largest part of the diagram, that is above  $40^\circ\text{C}$  in pure water, and above lower temperature levels at increasing acid concentrations. Up to high temperatures and acid concentrations, however, metastable dihydrate and hemihydrate can be formed in the stable anhydrite region. This results from the fact that anhydrite growth proceeds very slowly in a large part of the diagram. Eventually, the metastable dihydrate or hemihydrate phases will be transformed into anhydrite, but this only occurs with measurable speed at high temperatures and acid concentrations (Witkamp and van Rosmalen, 1986). It can further be seen that hemihydrate only exists as a metastable phase. Conversion of hemihydrate into dihydrate and vice versa can occur by crossing the dihydrate-hemihydrate equilibrium line, or by bringing dihydrate into a solution which satisfies the metastable hemihydrate conditions.

Any transition of the three phases into each other is possible in an acid solution, except the insoluble anhydrite into hemihydrate conversion. This is because hemihydrate can only be formed in a region where insoluble anhydrite is stable (Witkamp and van Rosmalen, 1986). The concentration of sulphuric acid used in the combined thermal and acid treatment, performed at room temperature, favoured the formation of calcium sulphate dihydrate.

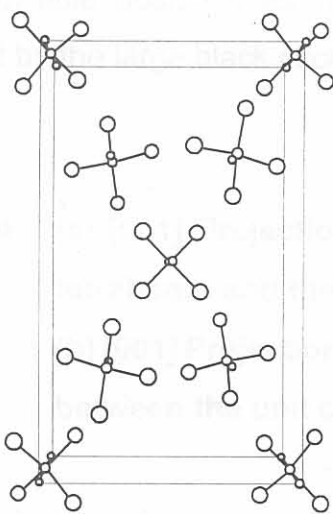
There are three distinct types of anhydrite, namely  $\alpha$ -,  $\beta$ - and  $\gamma$ - $\text{CaSO}_4$ . The first,  $\alpha$ - $\text{CaSO}_4$  only exists at temperatures above  $1180^\circ\text{C}$ , and is therefore not relevant to this discussion. The  $\gamma$ - $\text{CaSO}_4$  form, also called soluble anhydrite readily absorbs vapour or liquid water to convert to the hemihydrate form. Instead,  $\beta$ - $\text{CaSO}_4$  or insoluble anhydrite, converts to the dihydrate form through a solution process (i.e. recrystallization). The rate of conversion of insoluble anhydrite to gypsum is relatively slow and depends on the particle size and temperature at which it was formed as well as the temperature, composition and pH of the hydrated solution.

During the combined thermal and sulphuric acid treatment method, phosphogypsum in the dihydrate form is first changed, in a laboratory oven at  $160^\circ\text{C}$ , into the soluble anhydrite ( $\gamma$ - $\text{CaSO}_4$ ) form. When this soluble anhydrite is added to the sulphuric acid solution, immediate uptake of water in the crystal lattice of the  $\gamma$ - $\text{CaSO}_4$ , to form calcium sulphate hemihydrate

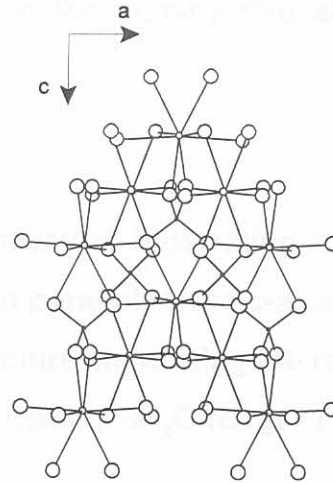
takes place. The calcium sulphate hemihydrate formed has a similar crystal structure as  $\gamma\text{-CaSO}_4$ , with the main difference the presence of water of crystallization in the hemihydrate structure, which causes the unit cell volume of the hemihydrate to be twice that of  $\gamma\text{-CaSO}_4$ , due to elongation of the c-axis (Bezou *et al*, 1995).

The crystal structures of  $\gamma\text{-CaSO}_4$  and  $\text{CaSO}_4 \cdot \frac{1}{2}\text{H}_2\text{O}$  are given in Figures 9.2 and 9.3 respectively. The basic structural unit of both these crystal structures is a chain of edge-sharing sulphate tetrahedra and  $\text{CaO}_8$  polyhedra (Lager *et al*, 1984). In  $\gamma\text{-CaSO}_4$  these chains are related by a six-fold screw axis to form one-dimensional channels. These channels make the uptake of water into the anhydrite structure possible, resulting in its hydration to the hemihydrate form.

**Figure 9.2** Crystal structure of  $\gamma\text{-CaSO}_4$  (Bezou *et al*, 1995; Lager *et al*, 1984)



[001] projection of the  $\gamma\text{-CaSO}_4$  structure.  
The b-axis is along the page.



[010] projection of the  $\gamma\text{-CaSO}_4$  structure illustrating the chains of sulphate tetrahedra and  $\text{CaO}_8$  polyhedra parallel to the c-axis.

**Figure 9.3** Projection of the crystal structure of  $\text{CaSO}_4 \cdot \frac{1}{2}\text{H}_2\text{O}$  along [001]. The b-axis is along the page (Bezou *et al*, 1995)

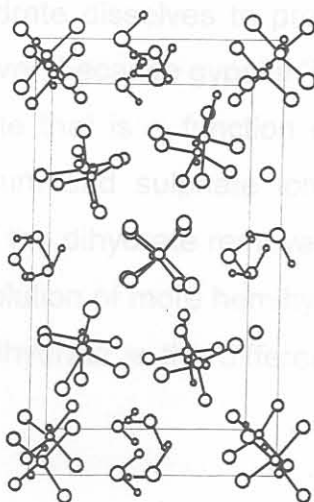
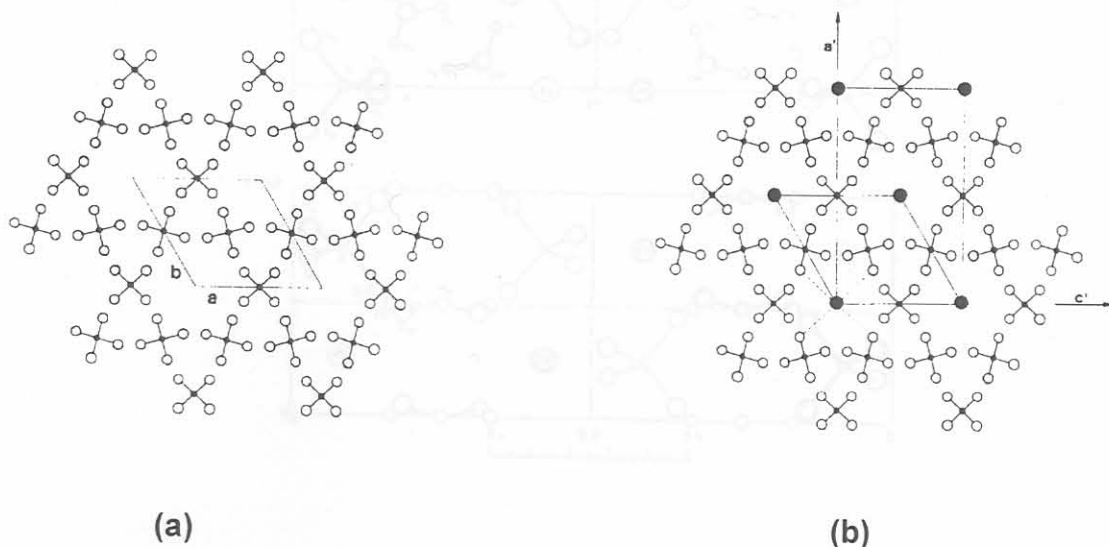


Figure 9.4 illustrates the sulphate tetrahedra and the channels developed parallel to the c-axis. Possible positions for the water molecules in the hemihydrate structure are presented by the large black circles.

**Figure 9.4** (a) [001] Projection of the  $\gamma\text{-CaSO}_4$  structure illustrating the sulphate tetrahedra and the channels developed parallel to the c-axis, and (b) [001] Projection of the  $\gamma\text{-CaSO}_4$  structure illustrating the relationship between the unit cells of  $\gamma\text{-CaSO}_4$  and  $\text{CaSO}_4 \cdot \frac{1}{2}\text{H}_2\text{O}$  (Lager *et al*, 1984)

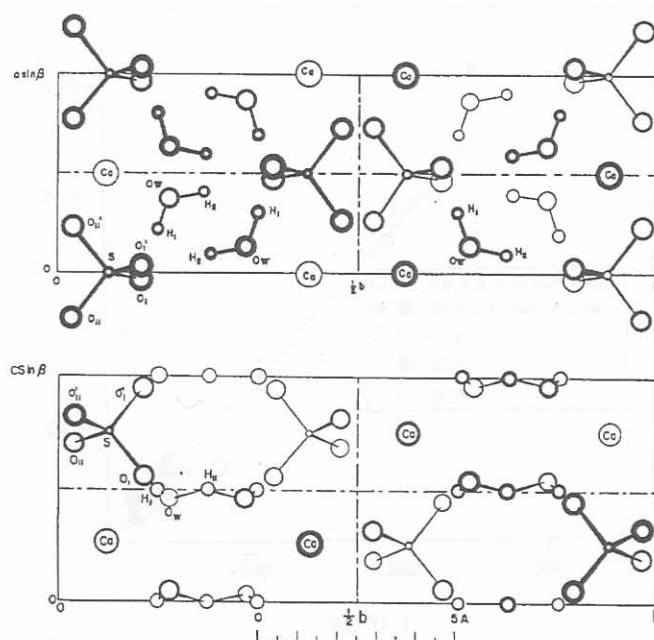




The next step will be the rehydration of calcium sulphate hemihydrate to the dihydrate, a process which is relatively rapid and occurs through a recrystallization process. Upon dispersion in water, the hemihydrate dissolves to produce a liquid phase saturated in calcium and sulphate ions. However, because gypsum is less soluble than hemihydrate, it immediately precipitates at a rate that is a function of slurry conditions, the solubility product, the availability of calcium and sulphate ions and the available surface for precipitation. The precipitation of the dihydrate removes calcium and sulphate ions from solution which promotes the dissolution of more hemihydrate. Therefore, the driving force of the hydration reaction of hemihydrate is the difference in solubility product between hemihydrate and dihydrate.

The crystal structure of  $\text{CaSO}_4 \cdot 2\text{H}_2\text{O}$  is given in Figure 9.5. In the structure of gypsum, pairs of adjacent layers which contain  $\text{Ca}^{2+}$  and  $\text{SO}_4^{2-}$  ions exist. Between successive pairs of layers the water molecules are located in such a way that they are hydrogen bonded to the oxygen atoms of the sulphate groups. Each  $\text{Ca}^{2+}$  ion is coordinated by six oxygen atoms of  $\text{SO}_4^{2-}$  groups and by two water molecules.

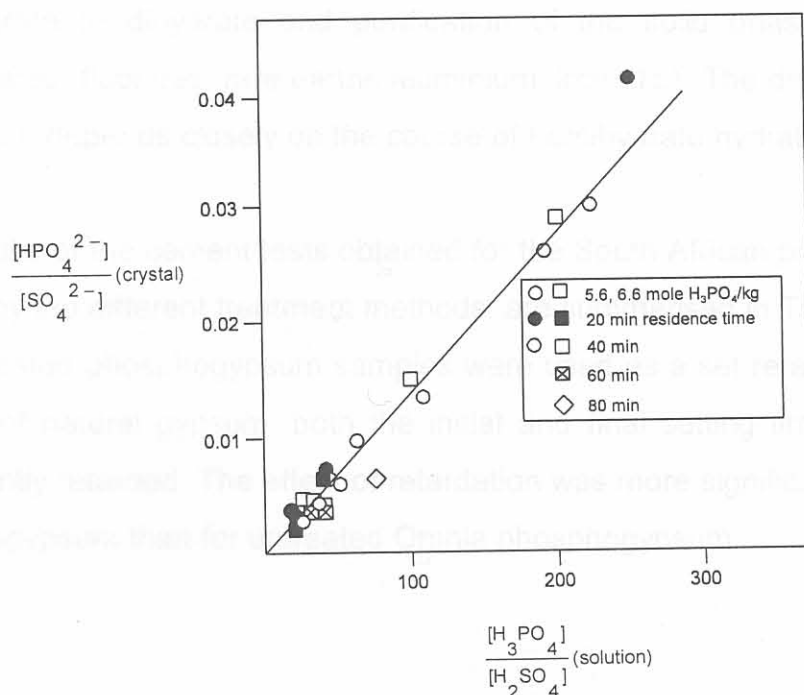
Figure 9.5 The crystal structure of gypsum (Atoji and Rundle, 1958)



In the crystal structure of phosphogypsum, small amounts of  $\text{HPO}_4^{2-}$  ions replace  $\text{SO}_4^{2-}$  ions. The  $\text{HPO}_4^{2-}$  ion can easily substitute a sulphate ion, since these two ions are similar in size and share the same affinity towards calcium ions. The similarity of these anions is also reflected by the existence of two comparable salts:  $\text{CaHPO}_4 \cdot 2\text{H}_2\text{O}$  and  $\text{CaSO}_4 \cdot 2\text{H}_2\text{O}$ , which are both sparingly soluble in water and have the same molar volume (van der Sluis *et al*, 1986).

In Figure 9.6 the  $\text{HPO}_4^{2-}$  incorporation in hemihydrate crystals, expressed as the molar concentration of  $\text{HPO}_4^{2-}$  over  $\text{SO}_4^{2-}$  ratio in the crystals, is given versus the molar concentration of  $\text{H}_3\text{PO}_4$  over  $\text{H}_2\text{SO}_4$  ratio in the solution (van der Sluis *et al*, 1986). The phosphate ion uptake decreases with increasing concentration of  $\text{H}_2\text{SO}_4$  and a linear dependence between the molar phosphate concentration over sulphate concentration ratios in the crystals and in the solution appears to exist. This linearity points to a competition between the two anions for the available adsorption sites at the crystal surface.

**Figure 9.6** The phosphate incorporation in  $\text{CaSO}_4 \cdot \frac{1}{2}\text{H}_2\text{O}$  crystals, expressed as the molar phosphate over sulphate concentration ratio in the crystals, as a function of the same ratio in the solution for various residence times (van der Sluis *et al*, 1986)



Similar results were obtained for the uptake of phosphate in calcium sulphate dihydrate (Witkamp and van Rosmalen, 1990). The phosphate uptake in dihydrate and anhydrite is lower at higher  $H_2SO_4$  concentrations and temperatures. The  $H_3PO_4$  concentration in the solution plays a less important role in the uptake of phosphate impurities with relation to the concentration of  $H_2SO_4$  (Witkamp and van Rosmalen, 1986).

Therefore, it seems that during rehydration of the calcium sulphate hemihydrate to dihydrate through recrystallization, the uptake of  $HPO_4^{2-}$  ions are suppressed by the relatively high concentration of  $SO_4^{2-}$  ions. This process produces a gypsum with a very low percentage of phosphorous impurities contained in the gypsum crystal lattice.

$H_2SO_4$  has not only an effect as an acid, like phosphoric acid, in affecting the solubility of the calcium sulphate, but also as a constituent ion of the calcium sulphate, influencing the molar  $Ca^{2+}/SO_4^{2-}$  ratio in the solution. The presence of sulphate ions, even at concentrations as low as a few weight percentage, generally enhances the conversion rate of any of the calcium sulphate phase transitions.

Jarosiński *et al* (1993) confirmed that in the process of hemihydrate phosphogypsum leaching with sulphuric acid, two simultaneous processes occur; i.e. the conversion of hemihydrate to dihydrate and purification of the solid phase from initial impurities (phosphates, fluorides, rare earths aluminium, iron etc.). The degree of phosphogypsum purification depends closely on the course of hemihydrate hydration.

The results of the cement tests obtained for the South African phosphogypsum samples, treated by the different treatment methods, are summarised in Tables 9.1 and 9.2. When the untreated phosphogypsum samples were used as a set retarder in Portland cement instead of natural gypsum, both the initial and final setting times of the cement were significantly retarded. The effect of retardation was more significant for untreated Kynoch phosphogypsum than for untreated Omnia phosphogypsum.



**Table 9.1** Combination of the results of the cement test performed on Kynoch phosphogypsum, treated by the respective treatment methods. The amount of phosphorous impurities contained in the samples is also included in the table

Test	Untreated (1)	Untreated (2)	Ca(OH) <sub>2</sub> treatment	H <sub>2</sub> SO <sub>4</sub> treatment before optimization	H <sub>2</sub> SO <sub>4</sub> treatment after optimization	Combined thermal and sulphuric acid treatment	Natural gypsum (1)	Natural gypsum (2)
Phosphorous impurities in gypsum (% P <sub>2</sub> O <sub>5</sub> )	0.99	1.06	0.98	0.65	0.73	0.04	-	-
SO <sub>3</sub> content of gypsum (%)	46.68	45.76	45.70	46.96	45.78	46.25	42.50	42.50
Gypsum added to clinker (%)	3.50	3.57	3.58	3.48	3.57	3.53	3.85	3.85
Specific surface of cement (cm <sup>2</sup> /g)	3200	3180	3250	3275	3258	3419	3200	3314
Relative density of cement (g/cm <sup>3</sup> )	3.10	3.14	3.12	3.12	3.14	3.16	3.10	3.14
Initial setting time (min)	354	348	274	184	228	137	140	130
Final setting time (h)	6.8	7.2	5.8	4.3	4.9	3.2	3.3	3.0
2-day Compressive strength (MPa)	17.35	14.67	16.96	18.89	15.07	19.93	20.33	19.27
7-day Compressive strength (MPa)	34.41	34.40	35.36	36.97	33.13	34.27	38.04	32.37
28-day Compressive strength (MPa)	47.25	41.43	44.83	44.01	39.10	50.47	49.10	47.90

**Table 9.2** Combination of the results of the cement test performed on Omnia phosphogypsum, treated by the respective treatment methods. The amount of phosphorous impurities contained in the samples is also included in the table

Test	Untreated (1)	Untreated (2)	Washed with distilled H <sub>2</sub> O	H <sub>2</sub> SO <sub>4</sub> treatment before optimization	H <sub>2</sub> SO <sub>4</sub> treatment after optimization	Combined thermal and sulphuric acid treatment	Natural gypsum (1)	Natural gypsum (2)
Phosphorous impurities in gypsum (% P <sub>2</sub> O <sub>5</sub> )	2.15	1.53	1.08	0.81	0.81	0.06	-	-
SO <sub>3</sub> content of gypsum (%)	47.24	47.06	46.39	45.59	45.98	46.10	42.50	42.50
Gypsum added to clinker (%)	3.46	3.47	3.52	3.59	3.56	3.55	3.85	3.85
Specific surface of cement (cm <sup>2</sup> /g)	3470	3159	3175	3225	3457	3267	3200	3314
Relative density of cement (g/cm <sup>3</sup> )	3.15	3.15	3.10	3.10	3.15	3.14	3.10	3.14
Initial setting time (min)	243	265	257	160	189	163	140	130
Final setting time (h)	5.1	5.8	5.3	4.8	4.2	3.4	3.3	3.0
2-day Compressive strength (MPa)	17.12	14.17	17.74	18.36	17.35	19.10	20.33	19.27
7-day Compressive strength (MPa)	33.91	31.17	34.15	35.60	33.47	29.12	38.04	32.37
28-day Compressive strength (MPa)	46.07	38.28	48.01	45.50	45.47	46.42	49.10	47.90

After treatment of the Kynoch phosphogypsum samples by the respective treatment methods, the best results for both the initial and final setting times were obtained for the Kynoch phosphogypsum sample treated by the combined thermal and sulphuric acid treatment method. The setting times, obtained when this sample was used as a set retarder, were in the same range as the values obtained when natural gypsum was used.

For the Omnia phosphogypsum sample, similar results were obtained for the initial setting times of cement, containing phosphogypsum treated by the combined thermal and sulphuric acid treatment method, and the sample treated by the sulphuric acid treatment method before optimization. However, an improved result, in terms of the comparison with natural gypsum, was obtained for the final setting time when the phosphogypsum sample was treated by the combined thermal and sulphuric acid treatment method. Therefore, the combined thermal and sulphuric acid treatment method also proved to be the best for the Omnia phosphogypsum.

The compressive strength of the cement containing the respective phosphogypsum samples treated by the combined thermal and sulphuric acid treatment method was in the same range as the compressive strengths obtained for the cement samples containing natural gypsum.

It seemed as if the optimization of the sulphuric acid treatment method was not successful in improving the results of the setting times of the cement obtained before optimization. For both Kynoch and Omnia phosphogypsum, the initial setting times increased after optimization of the method. Only the cement containing optimum treated Omnia phosphogypsum has shown some improvement in its final setting time.

These results show that the impurities contained in South African phosphogypsum as well as the occurrence of the anhydrite and hemihydrate forms of calcium sulphate have a greater influence on the setting times of Portland cement than on its strength development. However, treatment of the phosphogypsum samples by the combined thermal and sulphuric acid treatment method removes most of the phosphorous impurities contained in the phosphogypsum samples, and convert the sample to mainly the dihydrate form of calcium



sulphate. These samples have proved to yield results similar to that of natural gypsum when used as a set retarder in Portland cement.

On a worldwide basis phosphogypsum is produced as a by-product from the wet phosphoric acid process, and its rate of utilization remains low. Consequently there is a strong need to widen the field of application of this by-product. The purified South African phosphogypsum was found suitable for use in Portland cement manufacture, and the cement produced revealed compressive strength and setting time characteristics similar to cement produced using mineral gypsum.

- WILFORD, C.H. and TIPPER, C.F.H. (ed) (1969). "Comprehensive Chemical Kinetics" volume 2 "The theory of kinetics", Elsevier, Amsterdam, pp 380-387.
- WILFORD, C.H. (1972). "Early hydration behaviour of cements containing chemical by-product gypsum". *Cem. Res.*, 10(10), 424-431.
- WILFORD, C.H. (1995). "Cements containing by-product gypsum". From the Construction Materials Group Symposium held at London on 25 November 1995. SCI research paper series, Paper no. 9905-1-10.
- DE ZEEG, C., HONAT, A., MUJIB, U. S., NARFIJNO, CHRISTENSEN, A. and CHIAN, M.S. (1995). "Investigation of the Crystal Structure of  $\gamma$ - $\text{CaSO}_4$ ,  $\text{CaSO}_4$ ,  $\text{CaSO}_4 \cdot 2\text{H}_2\text{O}$ , and  $\text{CaSO}_4 \cdot \text{H}_2\text{O}$  by Powder Diffraction Methods". *J. S. Afr. State Chem.*, 117, 165-176.
- BROWN, W.T. (1968). "Introduction to Thermal Methods - Techniques and applications", Chapman & Hall, New York, pp 1-20.
- BYE, G.C. (1963). "Portland Cement - Composition, Production and Properties", 1<sup>st</sup> Edition, Pergamon Press, Oxford, pp 1-132.

## Appendix A                      References

- AL-JABBARI, S., FAISAL, F., ALI, F., NASIR, S. (1988), *Journal of Building Research, Scientific Research Council, Baghdad*, **7**, 49.
- ATOJI, M. and RUNDLE, R.E. (1958), "Neutron Diffraction Study of Gypsum,  $\text{CaSO}_4 \cdot 2\text{H}_2\text{O}$ " *J. Chem. Phys.*, **29(6)**, 1306-1311.
- BAMFORD, C.H. and TIPPER, C.F.H. (ed) (1969), "Comprehensive Chemical Kinetics, Volume 2: The theory of kinetics", Elsevier, Amsterdam, pp 380-387.
- BENSTEDT, J. ( 1979), "Early hydration behaviour of Portland cement containing chemical by-product gypsum", *Cem. Tech.*, **10(10)**, 404-410.
- BENSTED, J. (1995), "Cements containing by-product gypsums", From the Construction Materials Group Symposium held in London on 23 November 1995, SCI Lecture paper series, Paper no. 0069, 1-10.
- BEZOU, C., NONAT, A., MUTIN, J.-C., NØRLUND CHRISTENSEN, A. and LEHMAN, M.S. (1995), "Investigation of the Crystal Structure of  $\gamma\text{-CaSO}_4$ ,  $\text{CaSO}_4 \cdot 0.5\text{H}_2\text{O}$ , and  $\text{CaSO}_4 \cdot 0.6\text{H}_2\text{O}$  by Powder Diffraction Methods", *J. Solid State Chem.*, **117**, 165-176.
- BROWN, M.E. (1988), "Introduction to Thermal Methods - Techniques and applications", Chapman & Hall, New York, pp 1-20.
- BYE, G.C. (1983), "Portland Cement - Composition, Production and Properties", 1<sup>st</sup> Edition, Pergamon Press, Oxford, pp 1-132.

- BYE, G.C. (1999), "Portland Cement - Composition, Production and Properties", 2<sup>nd</sup> Edition, Thomas Telford Publishing, London, pp 1-78.
- CHARSLEY, E.L. and WARRINGTON, S.B. (1992) "Thermal Analysis", The Royal Society of Chemistry, pp 1-16, 31-58.
- COBURN, A., DUDLEY, E. and SPENCE, R. (1989), "Gypsum Plaster - Its manufacture and use", Intermediate Technology Publications, London, pp 5-7.
- DE FREITAS, B.J. and ALBUQUERQUE, P.C.W. (1991), "Alternatives to industrial recycling of phosphogypsum in Brazil", *Wat. Sci. Tech.*, **24(12)**, 245-254.
- DE JAGER, D.H. (1989), "Phosphate resources in the Palabora Igneous Complex, Transvaal, South Africa", *Phosphate deposits of the world*, Notholt, A.J.G., Sheldon, R.P. and Davidson, D.F. (eds), Volume 2: Phosphate rock resources, Cambridge University Press, pp 267-272.
- DODD, J.W., TONGE, K.H. and CURREL, B.R. (1987), "Thermal Methods", John Wiley & Sons, London, pp 1-96.
- DUNN, J.G., OLIVER, K., NGUYEN, G. and SILLS, I. (1987), "The quantitative determination of hydrated calcium sulphates in cement by DSC", *Thermochim. Acta*, **121**, 181 - 191.
- EIPELTAUER, E., GOTTSCHAMEL, G., MOLDAN, K. and PODEST, K. (1981), "Burning phosphogypsum in a carrier gas calcining plant in Austria", *Translation of ZKG* No. 2/81, **Jahrgang 134**, 94-102.
- ERDOGAN, Y., DEMIRBAS, A. and GENÇ, H. (1994), "Partly refined chemical by-product gypsums as cement additives", *Cem. Concr. Res.*, **24(4)**, 601-604.



- GADALLA, A., ROZGONYI, T. and SAYLAK, D. (1987), "Beneficiation of by-product phosphogypsum.", *Particulate and Multiphase Processes*, Vol 2, Edited by Ariman, T., and Veziroglu, T.N., Hemisphere, Washington, New York, London, pp 161-172.
- GADALLA, A.M., SAYLAK, D. and LINDNER, A.L. (1990), "Comparison of Strength Development in Waste Industrial Gypsum Produced by the Hemihydrate and Dihydrate Processes", *J. Am. Ceram. Soc.*, **73(8)**, 2255-2260.
- GEORGE, W.O. and MCINTYRE, P.S. (1987), "Infrared Spectroscopy", John Wiley & Sons, London, pp 1-201.
- GHAFOORI, N. and CHANG, W.F. (1993), "Investigation of Phosphate mining Waste for Construction Materials", *J. Mat. in Civ. Engrg.*, **5(2)**, 249-164.
- GREGG, S.J. and SING, K.S.W. (1982), "Adsorption, Surface Area and Porosity", Academic Press Inc., London, pp 1-110, 283-286.
- GRIFFITHS, P.R. (1975), "Chemical Infrared Fourier Transform Spectroscopy", John Wiley & Sons, New York, pp 1-80.
- GUTT, W. and SMITH, M.A. (1971), "The use of phosphogypsum as a raw material in the manufacture of Portland cement", *Cem. Tech.*, **Part I, March/April**, 41-50.
- HAINES, P.J. (1995), "Thermal Methods of Analysis", Chapman & Hall, London, pp 1-31.
- HAND, R.J. (1997), "Calcium sulphate hydrates: a review", *Br. Ceram. Trans. J.*, **96(3)**, 116-120.
- KREMPF, J. (1972), "Purification of phosphogypsum", French Patent FR 1972044.
- KRUGER, A. (1995), "The wet-process for phosphoric acid production". Ph.D. Thesis, University of Pretoria, Pretoria, South Africa, pp 1-75.

- HENDEY, Q.B. and DINGLE, R.V. (1989), "Onshore sedimentary phosphate deposits in south-western Africa", *Phosphate deposits of the world*, Notholt, A.J.G., Sheldon, R.P. and Davidson, D.F. (eds), Volume 2: Phosphate rock resources, Cambridge University Press, pp 200-206.
- HEWLETT, P.C. (ed.) (1998a), "Hydration, setting and hardening of Portland cement", *Lea's Chemistry of Cement and Concrete*, 4<sup>th</sup> Edition, Chapter 6, Odler, I. (Author), Arnold Publishers, London, pp 241 - 297.
- HEWLETT, P.C. (ed.) (1998b), "Portland cement: classification and manufacture", *Lea's Chemistry of Cement and Concrete*, 4<sup>th</sup> Edition, Chapter 2, Jackson, P. J. (Author), Arnold Publishers, London, pp 25 - 94.
- HEWLETT, P.C. (ed.) (1998c), "Physicochemical and mechanical properties of Portland cements", *Lea's Chemistry of Cement and Concrete*, 4<sup>th</sup> Edition, Chapter 8, Lawrence, C. D. (Author), Arnold Publishers, London, pp 343 - 419.
- JAROSIŃSKI, A., KOWALCZYK, J. and MAZANEK, Cz. (1993), "Development of the Polish wasteless technology of apatite phosphogypsum utilization with recovery of rare earths", *J. Alloys Comp.*, **200**, 147-150.
- JAROSIŃSKI, A. (1994), "Properties of anhydrite cement obtained from apatite phosphogypsum", *Cem. Concr. Res.*, **24**, 99-108.
- JENKINS, R., GOULD, R.W. and GEDCKE, D. (1981), "Quantitative X-ray spectrometry", Marcel Dekker Inc., New York, pp 1-6, 101-161, 363-394.
- KREMPFF, R., (1972), "Purification of phosphogypsum", French Patent FR 1972-34872, pp 1-4.
- KRUGER, A., (1998), "The wet-process for phosphoric acid production", Ph.D. Thesis, University of Pretoria, Pretoria, South Africa, pp 1-75.

- LAGER, G.A., ARMBRUSTER, Th., ROTELLA, F.J., JORGENSEN, J.D. and HINKS, D.G. (1984), "A crystallographic study of the low-temperature dehydration products of gypsum,  $\text{CaSO}_4 \cdot 2\text{H}_2\text{O}$ : hemihydrate  $\text{CaSO}_4 \cdot 0.5\text{H}_2\text{O}$  and  $\gamma\text{-CaSO}_4$ ", *Am. Mineral.*, **69**, 910-919.
- LUCKEVICH, L. (2000), "Gypsum Chemistry", *Gypsum 2000 Short Course*, Toronto, Canada, 16 May 2000, pp 1-16.
- MEHTA, P.K. and BRADY, J.R. (1977), "Utilization of phosphogypsum in Portland cement industry", *Cem. Concr. Res.*, **7(5)**, 537 - 543.
- MICROMERITICS INSTRUCTION MANUAL (1985), "Instruction manual, Flowsorb II 2300 for determining single point and multipoint surface area, Total pore volume and Pore area and volume distribution", Micromeritics Instrument Corporation, Norcross, Georgia, USA, pp 2.1 - 3.8, A1-A10.
- MORRIS, E.O. (1993), "Major environmental Improvements to an Existing Phosphate Fertilizer Manufacturing Facility", *AIChE Symp. Ser.*, **89(292)**, 142-148.
- MURAKAMI, K. (1968), "Utilization of Chemical Gypsum for Portland Cement", *Proceedings of the International Symposium on the Chemistry of Cement, Session 5, Part IV*, Tokyo, 457-510.
- NETZSCH-GERÄTEBAU, "Netzsch STA 409 EP Computer version, Operating Instructions", 1st edn., Netzsch-Gerätebau GmbH, Bayern, Germany, p 9.
- NOTHOLT, A.J.G., SHELDON, R.P. and DAVIDSON, D.F. (eds) (1989a), *Phosphate and deposits of the world, Volume 2: Phosphate rock resources*, Cambridge University Press, pp xxiii-xxv.
- SINGH, M. and GARG, M. (1989), "Gypsum binders and fibre-reinforced gypsum products" *Indian Concr. J.*, **63(6)**, 367-392.



- NOTHOLT, A.J.G., SHELDON, R.P. and DAVIDSON, D.F. (eds) (1989b), "Africa - Introduction", *Phosphate deposits of the world, Volume 2: Phosphate rock resources*, Cambridge University Press, pp164-170.
- ÖLMEZ, H. and ERDEM, E. (1989), "The effects of phosphogypsum on the setting and mechanical properties of Portland cement and trass cement", *Cem. Concr. Res.*, **19**, 377-384.
- ÖLMEZ, H. and YILMAZ, V.T. (1988), "Infrared study on the refinement of phosphogypsum for cements", *Cem. Concr. Res.*, **18(3)**, 449 - 454.
- ROODE, Q.I. (1996), "The crystallography of synthetic gypsum and rare-earth-doped gypsum", MSc Thesis, University of the Witwatersrand, Johannesburg, South Africa, pp 3,19-24.
- ROUX, E.H., DE JAGER, D.H., DU PLOOY J.H., NICOTRA, A., VAN DER LINDE, G.J. and DE WAAL, P. (1989), "Phosphate in South Africa.", *J. S. Afr. Inst. Min. Metall.*, **89(5)**, 129-139.
- SALZGITTER INDUSTRIEBAU GmbH (1979), "Chemical gypsum granulation plant - The by-pass method", pp 1-22.
- SALYAK, D., GADALLA, A.M. and YUNG, C.C. (1988), "Strength development in Waste Industrial Gypsum from the Dihydrate Wet Process.", *Ind. Eng. Chem. Res.*, **27**, 707-712.
- SINGH, M. (1987), "Influence of phosphogypsum impurities on two properties of Portland cement", *Indian Concr. J.*, **61**, 186-190.
- SINGH, M. and GARG, M. (1989), "Gypsum binders and fibre-reinforced gypsum products", *Indian Concr. J.*, **63(8)**, 387-392.

- SINGH, M., GARG, M. and Rehsi, S.S. (1993), "Purifying phosphogypsum for cement manufacture", *Constr. Build. Mater.*, **7(1)**, 3-7.
- SINGH, M., GARG, M., VERMA, C.L., HANDA, S.K. and KUMAR, R. (1996), "An improved process for the purification of phosphogypsum", *Constr. Build. Mater.*, **10(8)**, 597-600.
- SMADI, M.M., HADDAD, R.H. and AKOUR, A.M. (1999), "Potential use of phosphogypsum in concrete", *Cem. Concr. Res.*, **29 (9)**, 1419-1425.
- SMITH, B.C. (1996), "Fundamentals of Fourier transform infrared spectroscopy", CRC Press Inc., New York, pp 1-138.
- SOUTH AFRICAN BUREAU OF STANDARDS (1994), "Methods of testing of cement. Part 1. Determination of strength." Pretoria: SABS 1994 ; SABS EN 196-1.
- SOUTH AFRICAN BUREAU OF STANDARDS (1994), "Methods of testing of cement. Part 3. Determination of setting time and soundness." Pretoria : SABS 1994; SABS EN 196-3.
- STEWART, J.E. (1970), "Infrared Spectroscopy - Experimental Methods and Techniques", Marcel Dekker, Inc., New York, pp 1-26, 497-523.
- STRYDOM, C.A. and POTGIETER, J.H. (1999), "Dehydration behaviour of a natural gypsum and a phosphogypsum during milling", *Thermochim. Acta*, **332(1)**, 89-96.
- STUART, B. (1996), "Modern Infrared Spectroscopy", John Wiley & Sons, Chichester, pp 1-70.
- SVEHLA, G. (ed) (1976), "Wilson and Wilson's Comprehensive Analytical Chemistry", Volume VI, Elsevier Publishing company, Amsterdam, pp 1-220.

- TABIKH, A.A. and MILLER, F.M. (1971), "The nature of phosphogypsum impurities and their influence on cement hydration", *Cem. Concr. Res.*, **1(6)**, 663-678.
- TAYLOR, H.F.W., (1997), "Cement Chemistry", 2<sup>nd</sup> Edition, Thomas Telford Publishing, London, pp 84, 113-225.
- TODOROVSKY, D., TERZIEV, A. and MILANOVA, M. (1997), "Influence of mechanovation on rare earths leaching from phosphogypsum", *Hydrometallurgy*, **45**, 13-19.
- VAN DER MAAS, J.H., (1969), " Basic Infrared Spectroscopy", Heyden & Son Ltd., pp 48-64.
- VAN DER SLUIS, S., WITKAMP, G.J. and VAN ROSMALEN, G.M. (1986), "Crystallization of Calcium Sulphate in concentrated Phosphoric acid", *J. Cryst. Growth*, **79**, 620-629.
- WHISTON, C. (1987), "X-ray methods", John Wiley & Sons, London, pp 1-44, 166-305.
- WILSON, C.L. and WILSON, D.W. (eds) (1971), "Comprehensive Analytical Chemistry", Volume IIC, Elsevier Publishing company, Amsterdam, pp 318-399
- WIRSCHING, F. (1978), "Gypsum", *English translation of a contribution to Ullmanns Encyklopädie der technischen Chemie*, **12**, pp 1 - 28.
- WIRSCHING, F. (1982), "Residues from phosphoric acid production", *English Translation of a section of Müll- und Abfallbesitigung*, Erich Schmidt Verlag Berlin Bielefeld München, pp 3-15.
- WIRSCHING, F. (1983), "Gypsum", *Chemische Technologie*, Carl Hanser Verlag München Wien, **3(2)**, pp 1-18.



- WITKAMP, G.J. and VAN ROSMALEN, G.M. (1986), "Recrystallization of calcium sulphate modifications in phosphoric acid", *Proceedings of the Second International Symposium on Phosphogypsum, Miami, Florida, December, 1986*, Lloyd, G.M. (contract manager), **Vol.1**, 377-405.
- WITKAMP, G.J., and VAN ROSMALEN, G.M. (1990), "Continuous crystallisation of calcium sulphate phases from phosphoric acid solutions", *Crystallisation as a separation process*, ACS Symp. Ser., pp 381-394.
- WUNDERLICH, B. (1990), "Thermal Analysis", Academic Press Inc., London, pp 371-383.